UNIVERSIDADE FEDERAL DO ESPÍRITO SANTO
CENTRO DE CIÊNCIAS HUMANAS E NATURAIS
PROGRAMA DE PÓS-GRADUAÇÃO EM CIÊNCIAS BIOLÓGICAS

THE NECK OF FLYING ARCHOSAURS (AMNIOTA, REPTILIA): DESCRIPTION, RECONSTRUCTION AND BIOMECHANICS

Richard Santos Buchmann de Oliveira

Vitória, ES
Novembro, 2022

UNIVERSIDADE FEDERAL DO ESPÍRITO SANTO
CENTRO DE CIÊNCIAS HUMANAS E NATURAIS
PROGRAMA DE PÓS-GRADUAÇÃO EM CIÊNCIAS BIOLÓGICAS

THE NECK OF FLYING ARCHOSAURS (AMNIOTA, REPTILIA): DESCRIPTION, RECONSTRUCTION AND BIOMECHANICS

Richard Santos Buchmann de Oliveira

Orientadora: Profa. Dra. Taissa Rodrigues Marques da Silva

Tese submetida ao Programa de Pós-Graduação em Ciências Biológicas (Biologia Animal) da Universidade Federal do Espírito Santo como requisito parcial para a obtenção do título de Doutor em Biologia Animal.

Vitória, ES
Novembro, 2022

Ficha catalográfica disponibilizada pelo Sistema Integrado de Bibliotecas - SIBI/UFES e elaborada pelo autor

---

de Oliveira, Richard Santos Buchmann, 1991-
D278t The neck of flying archosaurs (Amniota, Reptilia): Description, reconstruction and biomechanics / Richard Santos Buchmann de Oliveira. - 2022.
152 f. : il.

Orientador: Taissa Rodrigues Marques da Silva.
Tese (Doutorado em Biologia Animal) - Universidade Federal do Espírito Santo, Centro de Ciências Humanas e Naturais.

1. Paleozoologia. 2. Anatomia. I. da Silva, Taissa Rodrigues Marques. II. Universidade Federal do Espírito Santo. Centro de Ciências Humanas e Naturais. III. Título.

CDU: 57

Programa de Pós-Graduação em Ciências Biológicas
UNIVERSIDADE FEDERAL DO ESPÍRITO SANTO

ATA DE DEFESA DE TESE DO CURSO DE DOUTORADO EM BIOLOGIA ANIMAL DO PROGRAMA DE PÓS-GRADUAÇÃO EM CIÊNCIAS BIOLÓGICAS DO CENTRO DE CIÊNCIAS HUMANAS E NATURAIS DA UNIVERSIDADE FEDERAL DO ESPÍRITO SANTO - ATA Nº 64 – 29/11/2022.

Em sessão pública ocorrida no dia 29 de novembro de 2022, através de webconferência, conforme previsto na Portaria Normativa nº 08, da Pró-Reitoria de Pesquisa e Pós-Graduação/UFES de 01 de julho de 2021, procedeu-se a avaliação da tese do aluno **Richard Santos Buchmann de Oliveira**. Às nove horas, a Profa. Dra. Taissa Rodrigues Marques da Silva, Presidente da Comissão Examinadora de Defesa de Tese, deu início aos trabalhos, convidando a tomar assento à mesa os examinadores externos, Profa. Dra. Fabiana Rodrigues Costa Nunes (UFABC), Prof. Dr. Felipe Chinaglia Montefeltro (UNESP), Prof. Dr. Alexandre Liparini Campos (UFMG) e Prof. Dr. Felipe Lima Pinheiro (UNIPAMPA). A seguir, a presidente solicitou ao doutorando que fizesse uma explanação de seu trabalho intitulado **"THE NECK OF FLYING ARCHOSAURS (AMNIOTA, REPTILIA): DESCRIPTION, RECONSTRUCTION AND BIOMECHANICS".** Finda a apresentação, a presidente passou a palavra aos examinadores, que procederam a arguição do candidato. Ao final, a Comissão, em sessão reservada, deliberou pela **APROVAÇÃO** da referida tese nos termos do Regimento Interno do Programa de Pós-Graduação em Ciências Biológicas e alertou que o aprovado somente terá direito ao título de Doutor após entrega da versão final de sua tese, em papel e meio digital, à Secretaria do Programa. Encerrada a sessão, eu, Profa. Dra. Taissa Rodrigues Marques da Silva, presidente da Comissão Examinadora, lavrei a presente ata que vai com as devidas assinaturas (De acordo com a Portaria citada acima, membros de banca externos à UFES que não atuam como docentes permanentes ou colaboradores nos Programas de Pós-Graduação da UFES estão dispensados da obrigatoriedade de assinatura digital da ata. Caso o membro externo não assine a ata e, sendo o Coordenador o responsável final pela realização da banca, a assinatura do Coordenador via Lepisma assegura a legitimidade necessária do documento).

Taissa Rodrigues

Profa. Dra. Taissa Rodrigues Marques da Silva (UFES)
Orientadora e Presidente da Comissão

Prof. Dr. Felipe Chinaglia Montefeltro (UNESP)
Examinador externo

Profa. Dra. Fabiana Rodrigues Costa Nunes (UFABC)
Examinadora externa

Prof. Dr. Alexandre Liparini Campos (UFMG)
Examinador externo

Prof. Dr. Felipe Lima Pinheiro (UNIPAMPA)
Examinador externo

Agradecimentos

Agradeço ao Programa de Pós-Graduação em Ciências Biológicas (PPGBAN) da Universidade Federal do Espírito Santo pela oportunidade do desenvolvimento do meu estudo e confecção da minha tese de doutorado. Em especial, agradeço à minha orientadora Profa. Dra. Taissa Rodrigues Marques da Silva, que me acompanha desde o início da minha vida acadêmica compartilhando conhecimento e esteve sempre presente e disponível durante todo desenvolvimento desta tese para eventuais dúvidas, revisões e discussões.

De modo geral, agradeço a todos os professores do PPGBAN/UFES, os quais sempre foram atenciosos, dedicados e contribuíram com discussões valiosas durante a confecção do projeto. Agradeço à Coordenação de Aperfeiçoamento de Pessoal de Nível Superior (CAPES) pelo fornecimento da bolsa durante meu doutorado. Além disso, agradeço ao Conselho Nacional de Desenvolvimento Científico e Tecnológico (CNPq) pelo financiamento do projeto "A evolução e biomecânica da coluna cervical de pterossauros (Reptilia: Archosauria)", que permitiu as análises e realização de tomografias dos materiais utilizados nesta tese.

Agradeço a todos os colegas do Instituto de Pesquisa e Reabilitação de Animais Marinhos, em especial ao coordenador científico Ralph Vanstreels, que aceitou colaborar com meu estudo fornecendo aves eutanasiadas para dissecção, e aos veterinários Leandro e Allan, pelas conversas e companhia no laboratório de necrópsia. Agradeço também aos colegas do Projeto Caiman, que me disponibilizaram um jacaré de papo amarelo eutanasiado para dissecção, e em especial ao Prof. Dr. Rodrigo Giesta Figueiredo e ao Phillipe Dangelo, que esteve presente comigo durante a dissecção e me hospedou no município de Alegre/ES, respectivamente.

Agradeço ao Dr. Takanobu Tsuihiji, Dr. Makoto Manabe e Chisako Sakata do National Museum of Nature and Science por permitirem minha análise da série vertebral do holótipo do *Anhanguera piscator* e por toda ajuda durante minha estadia no Japão. Agradeço ao Dr. Niels Bonde e Dra. Maria Eduarda de Castro Leal por fornecerem as tomografias do espécime MGUH 1891.738 e por me ajudarem e hospedarem em Copenhague. Agradeço ao Dr. Alexander Averianov por fornecer os modelos tridimensionais das vértebras de *Azhdarcho lancicollis*. Não poderia deixar de agradecer também à Profa. Dra. Fabiana Rodrigues Costa Nunes e ao Msc. Rodrigo Vargas Pêgas

pela companhia e conversas que tornaram as viagens ao Japão e Dinamarca muito melhores.

Gostaria de agradecer aos meus pais, Carlos Buchmann de Oliveira e Maria Aparecida Fundão Santos de Oliveira, aos meus tios Manoel Severino Freitas e Gilzete Fundão Santos Freitas, à minha avó materna Lizete Fundão Santos e ao meu avô paterno Carlos Gabriel de Oliveira por toda ajuda e apoio durante o curso e por sempre me estimularem nessa caminhada.

Agradeço pelo companheirismo de todos os amigos que passaram pelo Laboratório de Paleontologia da UFES enquanto eu estive realizando esta tese, em especial ao Augusto Barros e Arianny Storari, que sempre estiveram comigo nos melhores e piores momentos durante esses quatro anos. Gostaria de realizar um agradecimento póstumo à amiga Paula Heloísa Resende pela amizade e companhia durante as dissecções das aves realizadas nesse estudo.

Agradeço aos velhos e novos amigos que dividem apartamento comigo Christofe Klippel, Luiz Fernando Vieira, João Marcos Costa, Renato Kunz, Kalil Boechat e Felipe Luther pela convivência agradável e divertida que tornam os dias leves e tranquilos. Agradeço à Clara Júlio Freitas e Júlia Faria Stofel, pelas conversas e amizade nos últimos anos. Por fim, mas não menos importante, agradeço a todos os companheiros que conheci através do Grêmio Recreativo e Escola de Samba Seleção Natural pelo compromisso de ao menos uma pelada e reunião no bar do Pedro semanalmente, o que tornou por várias vezes as segundas-feiras o dia mais aguardado da semana, sendo sem dúvidas o melhor jeito de começar a semana ao longo dos últimos anos.

Sumário

Introduction 14

Objectives 17

Specific objectives 17

Chapter I – Neck osteology, arthrology, and myology of the Aequorlitornithes (Neoaves) 18

Introduction 19

Material and methods 20

Anatomical abbreviations 23

Osteology 23

Vertebrae of the first segment 27

Vertebrae of the second segment 28

Vertebrae of the third segment 30

Arthrology 31

Atlas and Axis 31

Articulatio intercorporalis and ligaments associated with the centrum in post-axial cervical vertebrae 31

Articulatio zygapophysialis and ligaments associated with the neural arch in post-axial cervical vertebrae 34

Myology 35

Epaxial muscles 43

Transversospinalis group 43

Longissimus group 48

Iliocostalis group 49

Hypaxial muscles 51

Discussion 52

Conclusions 58

References 59

Chapter II - Reconstruction of the soft tissues of the pterosaur neck and their implications for the cervical neutral position 65

Introduction 66

Material and methods 66

Anatomical abbreviations 71

Reconstruction of the pterosaur neck 71
Discussion 84
Conclusions 91
References 92
Chapter III - Flesh and bone? The musculature and cervical movements of pterosaurs from osteological correlates 100
Introduction 101
Material and methods 102
Anatomical abbreviations 103
Identification of osteological correlates 103
Cervical musculature reconstruction 107
Epaxial muscles 108
Transversospinalis group 108
Longissimus and *Iliocostalis* group 112
Hypaxial muscles 117
Maximum possible force production (F_{pmax}) by the cervical muscles 120
Discussion 124
Conclusion 131
References 132
Final Remarks 139
References 141

Lista de Figuras

Figure 1 Bird cervical vertebrae and muscles in transverse section. Brackets show the orientations in which muscle thicknesses were measure 23

Figure 2 Photographs and interpretative drawings of the articulated cervical vertebrae. (A, B) Complete cervical series belonging to *Haematopus palliatus* in dorsal view; (C, D) cervical series from atlas to seventh vertebra belonging to *Procellaria aequinoctialis* in left lateral view; (E, F) cervical series from the ninth to the fourteenth vertebra belonging to *Procellaria aequinoctialis* in left lateral view. Scale bar: 10 mm..... 24

Figure 3 Photographs and interpretative drawings of the cervical vertebrae. (A, B) fifth vertebra belonging to *Sula leucogaster* in cranial view; (C, D) eighth vertebra belonging to *Procellaria aequinoctialis* in caudolateral view; (E, F) eighth vertebra belonging to *Procellaria aequinoctialis* in dorsal view; (G, H) eleventh vertebra belonging to *Thalassarche chlororhynchos* in ventral view. Scale bar: 10 mm 25

Figure 4 Photographs and interpretative drawings of the articulated cervical vertebrae in ventral view. (A, B). Cervical series from ninth to fourteenth vertebra belonging to *Procellaria aequinoctialis*; (C, D) cervical series from tenth to thirteenth vertebra belonging to *Thalasseus acuflavidus*. Scale bar: 10 mm 29

Figure 5 Photographs and interpretative drawings of the articular capsules associated with the *facies articular caudalis* of the cervical vertebrae. (A, B) tenth vertebra belonging to *Thalassarche melanophris* in caudal view; (C, D) ninth vertebra belonging to *Thalassarche melanophris* in left lateral view; (E, F) ninth vertebra belonging to *Thalassarche chlororhynchos* in left lateral view. Scale bar: 10 mm 32

Figure 6 Interpretative drawings of the arrangement of the superficial musculature (A), deep musculature (B) and the deeper *rectus capitis* (C) of *Sula leucogaster* in left lateral view. Scale bar: 50 mm 35

Figure 7 Cross-section showing the ninth vertebra in *Haematopus palliatus* (A) and *Procellaria aequinoctialis* (B) in cranial view, and in *Thalasseus acuflavidus* (C) and *Phaethon aethereus* (D) in caudal view. The ruler on the left side and below each cross section shows that the width and height are equivalent. The metric marked in yellow indicates that the lateral musculature represents approximately 25% of the width of the cervical vertebra. Scale bar: 10 mm 43

Figure 8 Photographs of the superficial muscles of the neck of *Sterna hirundo* (A) and *Nannopterum brasilianus* (B) in dorsal view. 44

Figure 9 Photographs and interpretation of the superficial muscles of the neck of *Phaethon aethereus* (A, B), *Sula leucogaster* (C, D) and *Ardea alba* in left lateral view. 45

Figure 10 Interpretative drawings indicating muscle attachment sites on the vertebrae. (A) Cervical series from the atlas to seventh vertebra belonging to *Procellaria aequinoctialis* in left lateral view; (B) cervical series from the ninth to the fourteenth vertebra belonging to *Procellaria aequinoctialis* in left lateral view; (C) fifth vertebra belonging to *Sula leucogaster* in cranial view; (D) sixteenth vertebra belonging to *Sula leucogaster* in ventral view. Scale bar: 10 mm 46

Figure 11 Photographs of the deep long muscles of the neck in *Thalassarche chlororhynchos* (A, B) and *Calonectris diomedea* (C, D) in dorsal view 47

Figure 12 Photographs of the superficial muscles of the neck of *Puffinus puffinus* (A) and *Phaeton aethereus* (B) in ventral view 51

Figure 13 Photographs and interpretation of the superficial muscles of the neck (A, B) and interpretative drawings of the arrangement of the superficial musculature (C), deep musculature (D), origin of the *complexus* muscle (E) and origin of the *splenius capitis* and *rectus capitis dorsalis* and *lateralis* muscles (F) of *Cariama cristata* in left lateral view. Scale bar: 50 mm 56

Figure 14 Photograph (A) CT scan (B) and interpretative drawing (C) of the series of cervical vertebrae belonging to the specimen MGUH 1891.738, attributed to *Rhamphorhynchus muensteri*, in ventral view. Scale bar: 10 mm 69

Figure 15 Drawings showing the method of measuring the angles (A) and distance (B) between the analyzed vertebrae. The continuous red line represents the axis of the vertebral condyle and the dashed red line represents the axis of the condyle of the next vertebra. Abbreviations: ce, distance between condyle and cotyle in the central portion of the joint; pe, distance between condyle and cotyle in the peripheral portion of the joint 71

Figure 16 CT scans and interpretative drawings of the seventh vertebra (A, B) in left lateral view and the eighth vertebra (C, D) in left dorsolateral view of *Azhdarcho*

lancicollis (ZIN PH 138/44 and ZIN PH 137/44, respectively). Dashed line indicates reconstructed regions 72

Figure 17 Photographs and interpretative drawings of the fourth vertebra (A, B) in caudal view, fifth vertebra (C, D) in cranial view and eighth vertebra (E, F) in caudal view of *Anhanguera piscator* (NSM-PV 19892) and the articulated seventh and eighth vertebrae (G, H) in ventrolateral view of *Rhamphorhynchus muensteri* (MGUH 1891.738). Dashed line indicates reconstructed regions. Dotted regions indicate greater surface roughness. Scale bar: 10 mm 74

Figure 18 Reconstruction of the position at rest of the cervical vertebral column of *Anhanguera piscator* (A), *Azhdarcho lancicollis* (B) and *Rhamphorhynchus muensteri* (C) in left lateral view. Inset on the upper right corner shows a reconstructed *Anhanguera piscator* skull and neck. The intervertebral cartilage and cartilage of the zygapophyseal joints are shown in light brown. Scale bars: 10 mm. 78

Figure 19 Detail of the reconstruction of the neck at rest position of *Anhanguera piscator* (A), *Azhdarcho lancicollis* (B) and *Rhamphorhynchus muensteri* (C), showing the reconstructed articular capsule and cervical ligaments 80

Figure 20 Reconstruction of the neck at rest position of *Anhanguera piscator* (A), *Azhdarcho lancicollis* (B) and *Rhamphorhynchus muensteri* (C) in ventral view, with the anterior and posterior portions of the neck in detail (middle and right-side columns, respectively)..... 82

Figure 21 Reconstruction of the neck at rest position of *Anhanguera piscator* (A), *Azhdarcho lancicollis* (B) and *Rhamphorhynchus muensteri* (C) in dorsal view, with the anterior and posterior portions of the neck in detail (middle and right-side columns, respectively)..... 84

Figure 22 Photographs/3D models and interpretative drawings of the atlas and axis of *Procellaria aequinoctiallis* (A, B), *Anhanguera piscator* (C, D) and *Azhdarcho lancicollis* (E, F) in cranial (CV) and left lateral view (LLF). Dotted regions indicate greater surface roughness. Scale bar: 10 mm 105

Figure 23 Photographs and interpretative drawings of the fifth (A, B), eighth (C, D) and ninth (E, F) cervical vertebrae of *Anhanguera piscator* in right lateral view and the articulated cervical series of *Rhamphorhynchus muensteri* in ventral view. Dotted regions indicate greater surface roughness. Scale bar: 10 mm..... 107

Figure 24 Cervical muscle reconstruction showing the superficial musculature of *Anhanguera piscator* (A), *Azhdarcho lancicollis* (B) and *Rhamphorynchus muensteri* (C) in left lateral view. Scale bar: 10 mm 109

Figure 25 Photography (A) and interpretative drawing with locations of muscular attachments (B) of the occipital region of the skull of *Anhanguera piscator*. Scale bar: 10 mm 111

Figure 26 Locations of muscular attachments in the cervical vertebral column of *Anhanguera piscator*. Scale bar: 10 mm 113

Figure 27 Muscular reconstruction of the neck of *Anhanguera piscator* (A), *Azhdarcho lancicollis* (B) and *Rhamphorynchus muensteri* (C), without the *transversospinalis capitis*, *complexus* and *longissimus capitis superficialis*, in left lateral view. Scale bar: 10 mm 117

Figure 28 Muscular reconstruction of the neck of *Anhanguera piscator* (A), *Azhdarcho lancicollis* (B) and *Rhamphorynchus muensteri* (C) without the *transversospinalis capitis*, *complexus*, *transversospinalis cervicis*, *longissimus capitis superficialis*, *longissimus capitis profundus*, *flexor colli*, *rectus capitis ventralis* and *rectus capitis lateralis* in left lateral view. Scale bar: 10 mm..... 119

Figure 29 Cross-section showing the fourth (A) and seventh (B) cervical vertebra of *Anhanguera piscator*, the fourth (C) and sixth (D) cervical vertebra of *Azhdarcho lancicollis* and the fourth (E) and sixth (F) cervical vertebra of *Rhamphorhynchus muensteri* in cranial view. The ruler on the left and below each cross-section shows the height and the width of the neck, respectively. The red marks on the ruler below the cross-section indicate that the width of the lateral musculature, which together represents approximately one third of the total width of the neck and 50% of the width of the vertebra. Ruler measurements shown in millimeters 121

Lista de Tabelas

Table 1 Taxonomic identification, sex and dry body weight at the time of death or euthanasia of the dissected birds 20

Table 2 Proportional length and number of birds vertebrae per neck segment. Abbreviations: v, vertebrae 26

Table 3 Proportion of cartilage to the neck length of birds. Abbreviations: CV, sum of the centrum lengths of the cervical vertebrae; TOTAL, total neck length; CART, percentage of cartilage to neck length 33

Table 4 Area of origins and thickness of the *transversospinalis* muscles of birds. Muscle thickness was measured at their thickest point 36

Table 5 Area of origins and thickness of the *longuissimus, iliocostalis* and hypaxial muscles of birds. Muscle thickness was measured at their thickest point 39

Table 6 Length and thickness (in mm) of the "short muscles" of each analyzed bird .. 49

Table 7 Voxel sizes for different scans of the *Anhanguera piscator* holotype..... 67

Table 8 Angles of inclination and distance (from the central and peripheral region) of the condyle and cotyle between a vertebra and its succeeding one on the neck of pterosaurs in neutral pose. (+) above and (-) below the axis of succeeding vertebra. Abbreviations: ATAX, atlas and axis; CV, cervical vertebra; DV, dorsal vertebra. Roman algarisms indicate each vertebra's position 75

Table 9 Proportion of total cartilage in the neck length. Abbreviations: CV, sum of the centrum lengths of the cervical vertebrae; TOTAL, total neck length; CART, percentage of synovial cartilage on the neck centra 81

Table 10 Established area of muscle origins and maximum suggested thickness of each inferred cervical muscle. This table disregards the bilateral arrangement 113

Table 11 Area established for the locations of maximum thickness of each inferred cervical muscle and Maximum possible force production (F_{pmax}) of each muscle. The cross-sectional areas were multiplied by two for muscles arranged bilaterally 122

Resumo

Pterossauros e aves são arcossauros alados que se originaram no Mesozóico. O voo permitiu que representantes de ambos os clados explorassem nichos anteriormente vagos, e a diferenciação dos membros anteriores em asas tornou o pescoço desses animais um membro ativo e funcional usado durante o forrageamento. Atualmente, as aves se diversificaram e possuem pescoços de comprimentos variados, adaptados a diferentes hábitos de vida. No entanto, a falta de descendentes existentes de pterossauros cria lacunas no conhecimento sobre a biologia desse grupo, incluindo sua anatomia cervical e biomecânica. Aqui, identificamos e descrevemos a disposição vertebral e a influência dos tecidos moles cervicais na posição do pescoço em repouso de aves viventes. Em seguida, aplicamos esses dados para estabelecer e inferir a posição do pescoço em repouso, reconstruir os tecidos moles cervicais e quantificar os prováveis movimentos realizados pela musculatura do pescoço dos pterossauros. Para tanto, dissecamos os pescoços de espécimes representando dezesseis espécies de aves viventes e utilizamos tomografias computadorizadas da série cervical dos pterossauros *Anhanguera piscator*, *Azhdarcho lancicollis* e *Rhamphorhynchus muensteri* com preservação tridimensional do maior número de elementos vertebrais. Inferimos as forças dos músculos cervicais de pterossauros multiplicando a espessura do ponto mais largo do músculo e seu valor de tensão. Descobrimos que a espessura da cartilagem intervertebral de aves viventes varia ao longo do pescoço e que a excluir pode distorcer as reconstruções do pescoço de animais extintos. Também reconhecemos dezesseis músculos associados ao pescoço de aves viventes. As vértebras de arcossauros viventes e pterossauros mostraram convergências evolutivas que nos permitiram reconstruir cartilagens sinoviais nas articulações e ligamentos neste último. De acordo com a angulação das vértebras cervicais, o pescoço dos pterossauros provavelmente tinha uma forma levemente sinuosa quando em posição de repouso. Além disso, inferimos treze músculos cervicais em pterossauros. Concluímos que em pterossauros a musculatura responsável pelos movimentos dorsoventrais do crânio e pescoço era provavelmente mais robusta e forte, como nas aves viventes, e que os músculos menos robustos estavam associados à estabilização do pescoço ou à realização de força adicional para os movimentos cervicais.

Palavras-chave: Vértebras cervicais, Pterosauria, Aves, Aequorlitornithes, Músculos cervicais, Ligamentos cervicais.

Abstract

Pterosaurs and birds are winged archosaurs that originated in the Mesozoic. Flight allowed representatives of both clades to explore previously vacant niches, and the differentiation of forelimbs into wings made the neck of these animals an active, functional limb used during foraging. Presently, birds have diversified and have necks of varying lengths, which are adapted to different life habits. However, the lack of extant descendants of pterosaurs creates gaps in the knowledge regarding the biology of this group, including its cervical anatomy and biomechanics. Here, we identify and describe the vertebral arrangement and influence of cervical soft tissues on the neck position at rest of extant birds. We then apply this data to establish and infer the neck position at rest and associated cervical soft tissues, and quantify the likely movements performed by the neck musculature of pterosaurs. For that end, we dissected the necks of specimens representing sixteen species of extant birds and used computed tomography scans of the cervical series of the pterosaurs *Anhanguera piscator*, *Azhdarcho lancicollis* and *Rhamphorhynchus muensteri* with three-dimensional preservation of the largest number of vertebral elements. We inferred the cervical muscles forces for pterosaurs by multiplying the thickness of the widest point of the muscle and its stress value. We found that the thickness of the intervertebral cartilage of extant birds varies along the neck and that excluding it can distort reconstructions of the neck of extinct animals. We also recognized sixteen muscles associated with the neck of extant birds. The vertebrae of extant archosaurs and pterosaurs showed evolutionary convergences that allowed us to reconstruct synovial cartilages in joints and ligaments in the latter. According to the angulation of the cervical vertebrae, the pterosaur neck probably had a slightly sinuous shape when in a rest position. Furthermore, we inferred thirteen cervical muscles in pterosaurs. We conclude that in pterosaurs the musculature responsible for the dorsoventral movements of the skull and neck was probably more robust and stronger, as in extant birds, and that less robust muscles were associated with stabilizing the neck or performing additional force for cervical movements.

Key words: Cervical vertebrae, Pterosauria, Birds, Aequolitornithes, Cervical muscles, Cervical ligaments.

Introduction

Archosauria is a monophyletic group of Diapsida reptiles, currently represented only by Crocodylia and Aves (Nesbitt, 2011). The clade is supported by several synapomorphies, such as the presence of the anterorbital fenestra in the skull and the fourth trochanter in the femur (Nesbitt, 2011). The diversified morphological features of extant and extinct archosaurs allowed the representatives of this clade to explore varied niches (Kellner, 1994; Sick & Pacheco, 1997; Molnar et al., 2015).

One of the least studied topics on archosaur anatomy is neck function, despite its implications for understanding their posture during locomotion and foraging (Witton & Naish, 2008; Averianov 2013; Snively et al., 2013; Naish & Witton, 2017). In birds, because the forelimbs are adapted for flight and the mouth for capturing food, the presence of a mobile neck is important (Marek et al., 2021). Their neck is divided into three functional segments, in which the cranial and the middle segments have greater flexibility in all axes (Boas, 1929; Zusi, 1962). There are differences between its functional modules, which are reflected on the anatomical variation presented by the cervical vertebrae along the length of the neck (Terray et al., 2020). These differences indicate that each neck region requires different levels of resistance and that there are distinct associations of soft tissues along the neck (Tambussi et al., 2012; Cobley et al., 2013). Lastly, despite bird neck anatomy being currently well known, descriptions are often based on an isolated specimen of a species (Kuroda, 1962; Zusi & Storer, 1969; Landolt and Zweers, 1984; Zusi & Bentz, 1984).

The bird clade Aequortlitornithes has representatives distributed in environments in tropical, temperate, and polar areas (Kuroda, 1991; Prince et al., 1992; Guinard et al., 2010; Anchudia et al., 2017). They have adaptations that allow for aquatic foraging, such as hook-shaped beaks to capture and hold prey, keel-shaped bodies that favor diving, flat feet for swimming, and black and white coloration (Sick and Pacheco, 1997; Schreiber & Burger, 2001; Yuri et al., 2013; Prum et al., 2015). Their necks vary between extremely elongate as in flamingos to short as in terns, and neck length is relevant for the proper positioning of the head of birds with different foraging habits (Zweers et al., 1994; Wendeln & Becker, 1996; Barbraud et al., 2003). Birds with long necks have more robust cervical muscles and ligaments, due to the load required to perform cervical movements (Tambussi et al., 2012; Marek et al., 2021). The comparative analysis of the neck of birds

that present great morphological diversity within the same order could allow the identification of anatomical differences related to the varied foraging habits.

Furthermore, the osteological, arthrological and myological anatomical description of the neck of Aequorlitornithes is also useful to support inferences on the cervical soft tissues of extinct archosaurs phylogenetically close to birds (Witmer, 1995). The recognition of osteological correlates in Aequolitornithes can be useful to support this type of inference in pterosaurs, as both represent clades of generally long-necked winged archosaurs (Sick and Pacheco, 1997; Kellner, 2003). Furthermore, piscivorous habits with different foraging strategies, as present in the Aequorlitornithes, has also been inferred for many pterosaurs (Sick and Pacheco, 1997; Bennett, 2001; Kellner and Campos, 2002).

Pterosaurs are extinct Mesozoic archosaurs that also had their forelimbs specialized for flight (Kellner, 1994; Butler et al., 2009). Due to their flight capabilities, pterosaurs and birds share several convergent characteristics, such as the presence of a developed sternum and bone fusions, allowing to use extant birds as analogs for pterosaur biology (Bennett, 2001; Kellner & Campos, 2002; O'Connor, 2006; Butler et al., 2012).

The cervical vertebrae of pterosaurs vary in morphology between species and along the neck of a single individual, as in birds (Wellnhofer, 1991; Kellner & Tomida, 2000; Bennett, 2001; Veldmeijer, 2009; Eck et al., 2011; Vila Nova et al., 2015, Buchmann et al., 2018; Andres & Langston Jr., 2021). Similarly to birds, the pterosaur neck is also classically divided into anatomical segments: the atlas and axis as specialized vertebrae for articulation with the skull, the mid-cervical vertebrae, which occupy the middle of the neck, and the posterior cervical vertebrae, at the caudal end (Bennett, 2001; Vila Nova et al., 2015).

The presence of cervical anatomical segments indicates that some regions of the neck could be more flexible and resistant than others (Bennett, 2001; Kellner & Tomida, 2000; Averianov, 2003; Vila Nova et al., 2015). However, there is still a shortage of research into the flexibility, strength and elasticity of vertebral elements (Williams, 2021). In addition, cervical arthrology has been still little discussed, despite the influence that the intervertebral cartilage can exert on the angulation between the vertebrae and on the range of neck movements in archosaurs (Tsuihiji, 2004; Tambussi et al., 2012; Taylor & Wedel, 2013).

The anatomical differences present among the cervical vertebrae of pterosaurs imply changes in the shape and extent of the soft tissue attachment sites, which probably reflects on the volume and efficiency of muscles and ligaments (Tambussi et al., 2012; Cobley et al., 2013). Currently, few inferences regarding the presence of pterosaur cervical muscles according to the recognition of osteological correlates have been made (Bennett, 2003; Witmer et al., 2003; Habib & Godfrey, 2010, Bennett, 2003; Elgin & Frey, 201; Naish & Witon, 2016). Furthermore, the foraging and locomotion habits of pterosaurs are often presented disregarding the influence and activity of ligaments and cervical muscles (Nesov, 1984; Kellner & Langston Jr., 1996; Prieto, 1998; Kellner & Tomida, 2000; Kellner & Campos, 2002; Humphries, 2007; Averianov, 2013; Padian et al., 2021; Williams et al., 2021). Thus, the identification of osteological correlates from extant archosaurs has the potential to support inferences regarding the neutral position of the neck and the presence and volume of soft tissues, allowing analyses about the execution of the cervical movement of pterosaurs.

Objectives

The main objective of this thesis is to reconstruct and/or describe the osteological, arthrological and myological anatomy of the neck of pterosaurs and Aequolitornithes (Reptilia, Archosauria) and to make inferences on the possible neck movements performed by pterosaurs.

Specific objectives

• To describe how the osteological, arthrological and myological differences in the neck of different Aequorlitornithes birds relate to the cervical position at rest;

• To identify whether pterosaur vertebrae had osteological correlates compatible with the soft tissue attachment sites of extant archosaurs;

• To analyze whether there would be differences in the angulation of the segments of the articulated cervical series of pterosaurs;

• To investigate how the thickness of muscles can be inferred according to the proportion observed at the sites of soft tissue attachments;

• To analyse whether the probable movements indicated by the inferred muscles are in accordance with suggested habits for pterosaurs.

Chapter I

Neck osteology, arthrology, and myology of the Aequorlitornithes (Neoaves)

Richard Buchmann[1] and Taissa Rodrigues[1]

[1]Departamento de Ciências Biológicas, Centro de Ciências Humanas e Naturais, Universidade Federal do Espírito Santo, Vitória, ES, Brazil

Correspondence

Richard Buchmann, Departamento de Ciências Biológicas, Centro de Ciências Humanas e Naturais, Universidade Federal do Espírito Santo, Vitória, ES, Brazil.
Email: richardbuchmann@gmail.com

Abstract

Birds have extremely flexible necks, which help their foraging. However, studies on the variation of osteological anatomy and soft tissue comparing bird necks are rare, despite the large variation seen between species. Here, we analyze and compare the morphology of the neck of the Aequolitornithes, a clade known for the use of several strategies in aquatic foraging, noting the differences responsible for their varied cervical morphologies. We dissected specimens representing fifteen species of the Aequorlitornithes and two specimens belonging to the Inopinaves for comparison. The cervical vertebrae differ morphologically along the neck in all birds analyzed but in all they are organized in only three functional segments that respond to neck movement. The synovial cartilage present in the *articulatio intercorporalis* affects the angulation between the vertebrae and also represents a small proportion in the length of the avian neck. However, this proportion is not greater than that seen in animals that have intervertebral discs. The presence of articular capsules ensures that the zygapophyses are extremely mobile in the analyzed birds, presenting an overlap between consecutive zygapophyses that varies between > 50% and < 50% during the resting position and neck movement, respectively. The shorter cervical muscles, commonly restricted to the first segment, showed variation in origin sites between species, mainly in Pelecaniformes. The muscle attachment site in the vertebrae was frequently associated with rough surfaces, but not exclusively. The cervical flexor and extensor muscles are six times thicker than the area

of muscular origin, while in the other muscles the value of this proportion is reduced by half. Furthermore, the width of the musculature lying lateral to the vertebra represents one third of the total width of any cervical cross-section, which is useful for estimating the volume of soft tissue when only osteological material is available. Furthermore, the zygapophyses disposition and slippage and soft tissues thickness we observed may support cervical reconstructions and kinetic models for extinct animals. Our analysis points to morphological differences of vertebrae and soft tissues along all segments of the neck and between species, which we hypothesize may reflect different biomechanical requirements.

Key-words: Birds, cervical vertebrae, musculature, synovial cartilage, joint, anatomy.

Introduction

Wings are one of the most outstanding features present in birds. They have allowed birds to explore important ecological niches, enabling their evolutionary radiation and diversification. However, they also brought some constraints. Due to their highly specialized forelimbs, birds need to use their mouths to capture food, thus having a mobile neck is an important asset (Marek et al., 2021).

The avian neck is classically divided into three segments, according to the movements performed by each portion (Boas, 1929). Historically, neck anatomy has been well described, although studies have been frequently based on individual species (Kuroda, 1962; Zusi and Storer, 1969; Landolt and Zweers, 1984; Zusi and Bentz, 1984). Comparative anatomy, including osteological, arthrological, and myological descriptions, have rarely focused on variation between species of the same clade.

Aequorlitornithes are distributed worldwide, including tropical, temperate, and glacial environments (Kuroda, 1991; Prince *et al*., 1992; Guinard *et al*., 2010; Anchundia *et al*., 2017). They have morphological adaptations that allow aquatic foraging, such as hook-shaped beaks to capture and hold prey, keel-shaped body to favor diving, flat feet for swimming, and black and white coloration (Sick and Pacheco, 1997; Schreiber and Burger, 2001; Yuri *et al*., 2013; Prum *et al*., 2015). The length of the neck is relevant for positioning the head properly during the different habits of birds in this clade (Zweers *et al*., 1994). Their necks usually range from small to large, as seen in terns and flamingos, respectively (Wendeln and Becker, 1996; Barbraud *et al*., 2003). In addition, birds with

longer necks have stronger cervical muscles and ligaments due to the forces required to perform the movements (Tambussi *et al*., 2021; Marek *et al*., 2021).

The analysis of the morphological and size variations present in the cervical vertebrae, cartilages and musculature of the Aequorlitornithes also is useful to understand how such variations occurred in the neck of extinct archosaurs through the Extant Phylogenetic Bracket (EPB) method, which establishes criteria to support inferences about the probable soft tissues in fossil species (Witmer, 1995). Aequorlitornithes species are also useful to support this sort of inference in pterosaurs, as they represent a clade with different foraging strategies for piscivorous habits, such as most pterosaurs (Sick and Pacheco, 1997; Bennett, 2001; Kellner and Campos, 2002).

Material and Methods

Here, we describe specimens belonging to 15 species of Aequorlitornithes with aquatic foraging, representing five orders. We also analyzed two individuals of Inopinaves for comparison (Table 1).

The specimens were dissected on the premises of the Institute for the Research and Rehabilitation of Marine Animals (Instituto de Pesquisa e Reabilitação de Animais Marinhos - IPRAM), in Cariacica, Espírito Santo, Brazil. IPRAM is responsible for the rehabilitation of birds and other aquatic tetrapods (under the following authorizations: SISFAUNA IEMA 001/2014, process 68077610; IEMA 001/2014, process 67277780; and SISBIO 34510 and 26896). The dissected birds died or were euthanized after veterinary monitoring.

Table 1. Taxonomic identification, sex and dry body weight at the time of death or euthanasia of the dissected specimens.

Aequorlitornithes	Species	Sex	Weight (kg)
Charadriiformes	*Haematopus palliatus* Temminck,1820	Male	0.37
	Larus dominicanus Lichtenstein, 1823	Female	0.73
	Sterna hirundo Linnaeus, 1758	Male	0.07

	Thalasseus acuflavidus (Cabot, 1847)	Female	0.16
Pelecaniformes	*Ardea alba* Linnaeus, 1758	Male	1.09
	Ixobrychus exilis (Gmelin, 1789)	Undetm.	0.09
Phaethontiformes	*Phaethon aethereus* Linnaeus, 1758	Male	0.62
Procellariiformes	*Calonectris diomedea* (Scopoli, 1769)	Female	0.55
	Procellaria aequinoctialis Linnaeus, 1758	Female	0.66
	Puffinus puffinus (Brünnich, 1764)	Female	0.24
	Thalassarche chlororhynchos (Gmelin, 1789)	Male	1.50
	Thalassarche melanophris (Temminck,1820)	Male	2.23
Suliformes	*Fregata magnificens* Mathews, 1914	Male	1.46
	Nannopterum brasiliensis (Gmelin, 1789)	Female	0.75
	Sula leucogaster (Boddaert, 1783)	Female	1.19
Inopinaves			
Accipitriformes	*Coragyps atratus* (Bechstein, 1793)	Undetm.	1.52
Cariamiformes	*Cariama cristata* (Linnaeus, 1766)	Undetm.	2.30

We identified the cervical series following Zusi (1962), who considers cervical vertebrae as those that do not have ribs or those in which they are fused to the centrum. For the description of vertebral, arthrological and myological anatomy, we followed the

nomenclature presented by Baumel and Witmer (1993). Dissections were made with a scalpel, scissors, and forceps to access the superficial and deep muscles and ligaments of the neck.

Total neck length was measured using a measuring tape. We used a caliper to measure the length, height, and width of the *lacuna interzygapophysialis* in each vertebra, following Tambussi *et al*. (2012). The measurement of thickness of the synovial cartilage present in the *articulatio intercorporalis* was taken on the ventral surface, using a caliper. The complexity of the heterocoelous *facies articularis* made it difficult to accurately establish a single value for joint thickness, so we separated the values in <0.5, =0.5, and >0.5 mm. For a more precise quantification of the additional length of synovial cartilage in the *articulatio intercorporalis* relative to the length of the cervical series, we calculated the difference between the total length of the articulated cervical series and the sum of the centrum length of all disjointed cervical vertebrae, as proposed by Taylor and Wedel (2013).

The measurements of the overlapping of *articulatio zygapophysialis* were taken with a caliper. The measurements were taken with the vertebrae in articulation, so that one could observe the influence of articular capsules in their range of motion, although it precluded a more precise measurement.

We refer to the muscles that extend only in the cranial third as "short muscles of the neck". Muscle length was measured with a measuring tape. "Thickness" was determined as the distance between the edge of the muscle closest to the vertebra to the most superficial opposite edge (Figure 1). The thickness was measured with a caliper at the mid-length of short muscles and the mid-length of the first, second, and third segments of long muscles. In muscle descriptions, “branches” are defined as bundles that extend cranially and are bilaterally arranged, and “portions” as bundles that overlap and may or may not be arranged bilaterally.

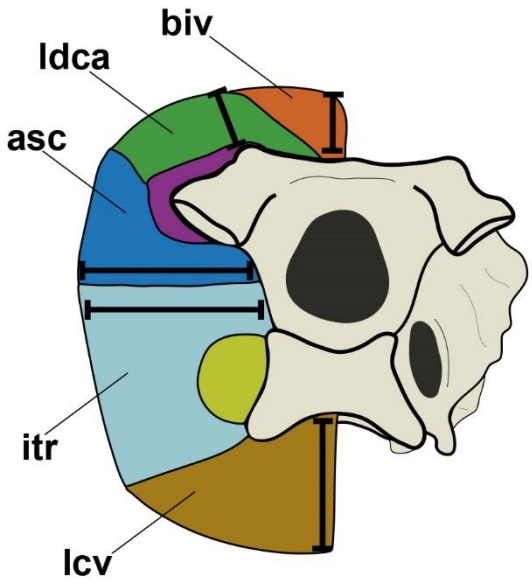

Figure 1. Bird Cervical vertebrae and muscles in transverse section. Brackets show the orientations in which muscle thicknesses were measured.

Anatomical abbreviations

ac, *ansa costotransversaria*; arc, articular capsule; asc, *ascendens cervicales*; biv, *biventer cervicis*; cap, carotid process; com, *complexus*; cop, costal process; faca, *facies articularis caudalis*; facr, *facies articularis cranialis*; fcl, *flexor colli lateralis*; fopn, pneumatic foramen; ftr, *foramen transversarium*; fvcr, *fovea cranioventralis*; hyp, hypapophysis; ica; *articulatio intercorporalis*; icr, *intercristales*; isp, *interspinalis*; itr, *intertransversarii*; inc, *inclusi*; lc, lateral crest; lco, *ligamentum collaterale*; lcv, *longus colli ventralis*; ldca, *longus colli dorsalis pars caudalis*; ldcr, *longus colli dorsalis pars cranialis*; lis, *ligamentum interspinalis*; linz, *lacuna interzygapophysealis*; ms, muscle scar; nc, neural canal; ns, neural spine; poz, postzygapophysis; prz, prezygapophysis; rcd, *rectus capitis dorsalis*; rcl, *rectus capitis lateralis*; rcv, *rectus capitis ventralis*; spc, *splenius capitis*; ta, *tuberculum ansae*; td, *torus dorsalis*; toc, transverse oblique crest; tpr, transverse process.

1. Osteology

The total length of the cervical series and the number of vertebrae varied in the analyzed species (Table 2). All analyzed Pelecaniformes had 17 cervical vertebrae, and all other species of Aequorlitornithes, except one of Procellariiformes and of Suliformes, had 13 or14 cervicals (Table 2).

The cervical vertebrae vary in length between segments. The longest vertebrae are mainly located in the transitional region between the first and second segments, usually the fifth, sixth or seventh vertebra. The shortest vertebrae are at the cranial and caudal ends of the neck: the atlas and axis, cranially, and the most caudal cervical. In all analyzed specimens, the prezygapophyses are craniodorsally oriented, and the postzygapophyses, caudoventrally. This allows for a total overlap between consecutive articular surfaces (Figure 2).

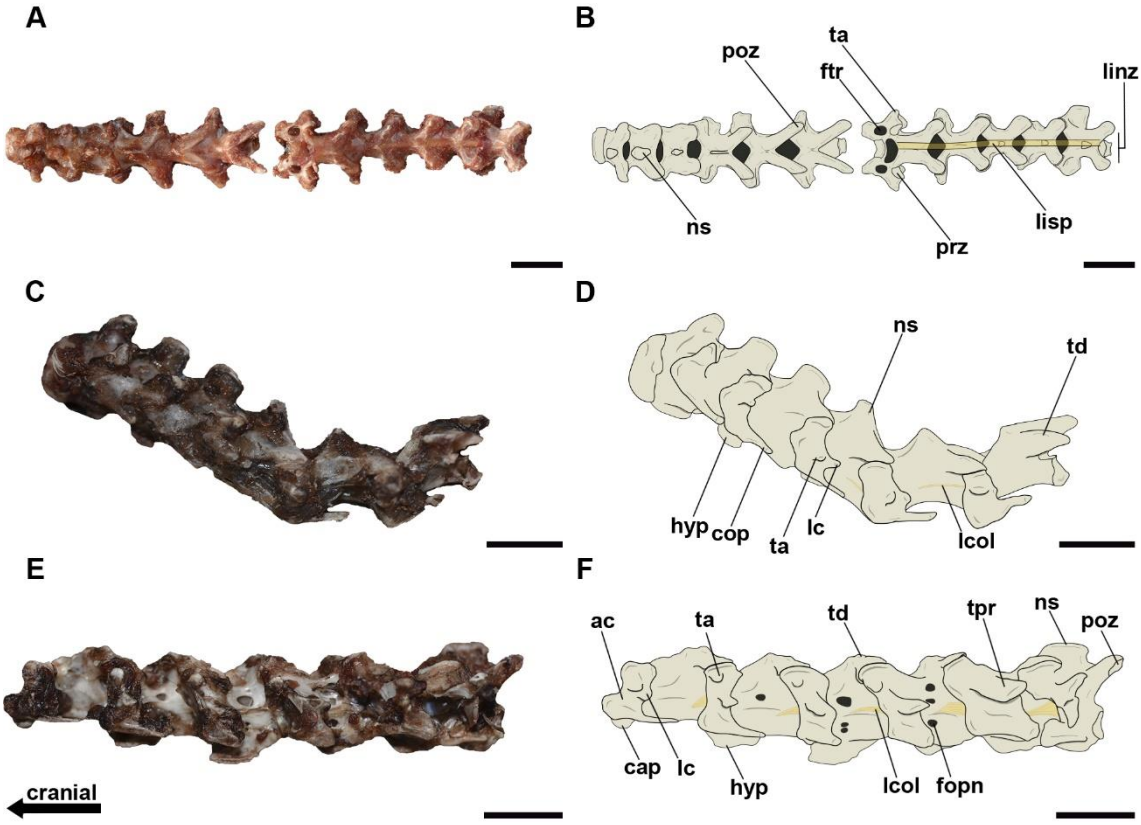

Figure 2. Photographs and interpretative drawings of the articulated cervical vertebrae. (A, B) Complete cervical series belonging to *Haematopus palliatus* in dorsal view; (C, D) cervical series from atlas to seventh vertebra belonging to *Procellaria aequinoctialis* in left lateral view; (E, F) cervical series from the ninth to the fourteenth vertebra belonging to *Procellaria aequinoctialis* in left lateral view. Scale bar: 10 mm.

Throughout the cervical series, the width of the *lacuna interzygapophysealis* of the prezygapophyses is always wider than that of the postzygapophyses (Figure 2). The transverse oblique crest extends from the base of the postzygapophyses to the dorsomedial portion of the neural arch in all cervical vertebrae (Figure 3).

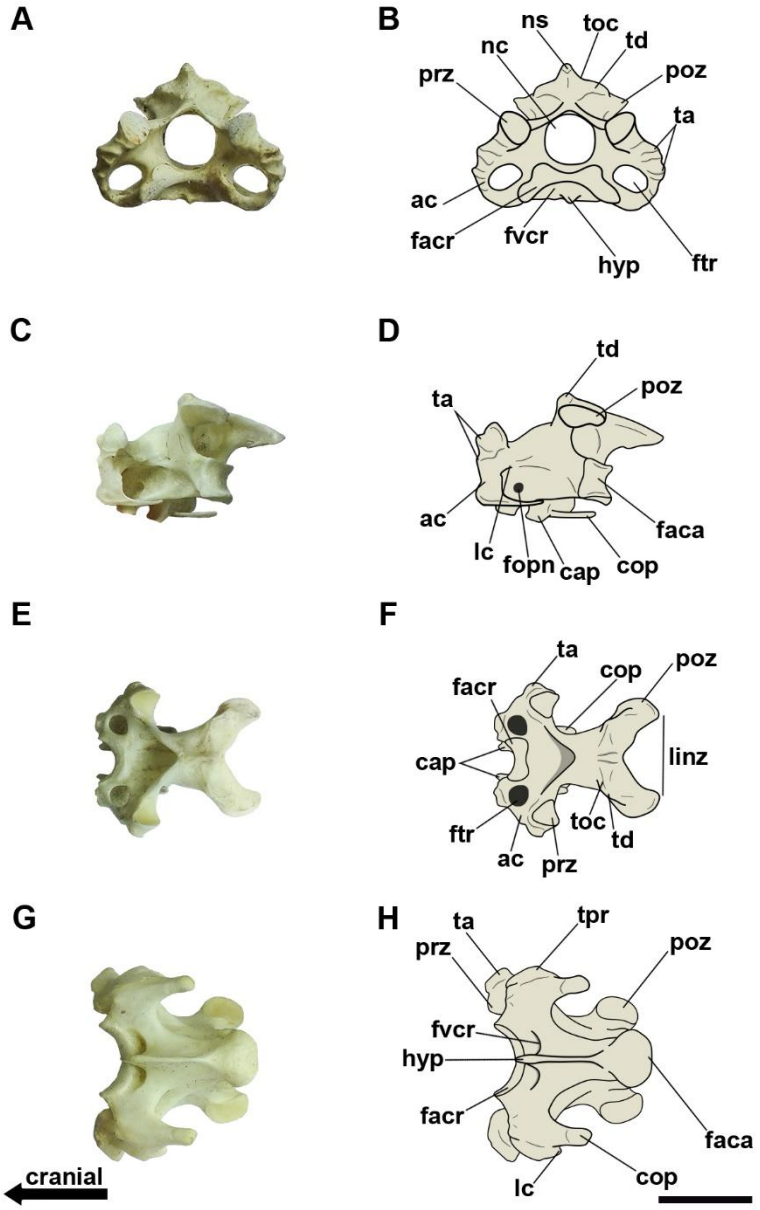

Figure 3. Photographs and interpretative drawings of the cervical vertebrae. (A, B) fifth vertebra belonging to *Sula leucogaster* in cranial view; (C, D) eighth vertebra belonging to *Procellaria aequinoctialis* in caudolateral view; (E, F) eighth vertebra belonging to *Procellaria aequinoctialis* in dorsal view; (G, H) eleventh vertebra belonging to *Thalassarche chlororhynchos* in ventral view. Scale bar: 10 mm.

All vertebrae have heterocoelous *facies articularis* in the centrum, with the *facies articularis cranialis* wider than the *caudalis*. The *ansa costotransversaria* is developed and forms the *foramen transversarium* along the cervical column (Figure 2). The articular surfaces, processes ends, and lateral surface of the *ansa costotransversaria* are rough compared to the other surfaces in cervical vertebrae. Laminar surfaces are slightly smooth (Figure 3).

In almost all species, the vertebrae of the first two segments of the neck have pneumatic foramina on the laterocranial portion of the centrum (Figure 3). Besides having these foramina in the same location, the vertebrae of the third segment also present foramina lateromedially on the centrum and neural arch, except in the analyzed Pelecaniformes (Figure 2). *Nannopterum brasilianus* was the only species that did not present any pneumatic foramen in cervical vertebrae.

Table 2. Proportional length and number of birds vertebrae per neck segment. Abbreviations: v, vertebrae.

Species	Seg. I (%)	Seg. II (%)	Seg. III (%)	Total neck length (mm)
Aequorlitornithes				
Charadriiformes				
Haematopus palliatus	**35.7**	**38.1**	**26.1**	**126**
	5 v	4 v	3 v	12 v
Larus dominicanus	**26.6**	**48.9**	**24.5**	**167**
	5 v	5 v	3 v	13 v
Sterna hirundo	**36.6**	**38.6**	**25.6**	**83**
	5 v	5 v	4 v	14 v
Thalasseus acuflavidus	**32.4**	**39.4**	**28.0**	**114**
	5 v	5 v	4 v	14 v
Pelecaniformes				
Ardea alba	**27.5**	**47.0**	**26.3**	**554**
	5 v	7 v	5 v	17 v
Ixobrychus exilis	**23.5**	**53.5**	**22.9**	**186**
	5 v	7 v	5 v	17 v
Phaethontiformes				
Phaethon aethereus	**28.5**	**38.9**	**32.4**	**154**
	4 v	5 v	5 v	14 v
Procellariiformes				
Calonectris diomedea	**33.9**	**42.0**	**24.0**	**183**
	5 v	5 v	3 v	13 v
Procellaria aequinoctialis	**32.2**	**40.3**	**27.3**	**161**
	5 v	5 v	4 v	14 v
Puffinus puffinus	**35.3**	**34.0**	**29.9**	**106**
	5 v	4 v	4 v	13 v
Thalassarche chlororhynchos	**32.2**	**36.2**	**31.5**	**302**
	5 v	4 v	4 v	13 v
Thalassarche melanophris	**33.5**	**35.1**	**31.2**	**310**
	5 v	4 v	4 v	13 v
Suliformes				
Fregata magnificens	**35.1**	**45.2**	**19.6**	**269**
	5 v	5 v	4 v	14 v
Nannopterum brasiliensis	**37.9**	**36.4**	**25.5**	**258**
	5 v	5 v	4 v	14 v
Sula leucogaster	**30.0**	**40.0**	**30.0**	**303**

	5 v	6 v	5 v	16 v
Inopinaves				
Accipitriformes				
Coragyps atratus	**34.8**	**38.1**	**26.9**	**215**
	5 v	5 v	4 v	14 v
Cariamiformes				
Cariama cristata	**36.4**	**37.5**	**26.0**	**280**
	5 v	6 v	4 v	15 v

1.1. Vertebrae of the first segment

The analyzed birds often have five vertebrae in this segment (Table 2), increasing in length caudally (Figure 2). Atlas and axis, even when articulated, do not exceed the length of the third vertebra, in any species. The atlas intercentrum is laterally compressed. Cranially, the condyloid fossa is concave and oval, and articulates with the occipital condyle in the skull. Caudally, the *facies articularis axialis* of the atlas is concave and laterally expanded. The neural arch is dorsally flat and the pedicles are laterally expanded. The neural spine is absent.

The axis is dorsoventrally expanded (Figure 2). Cranially, in the centrum, the *facies articularis atlantica* is concave and laterally expanded. Ventrally, there is a well-developed hypapophysis, which stands out as a site for muscular attachment (Figure 2). The *facies articularis caudalis* is heterocoelic. The neural arch presents an odontoid process that extends cranially, to articulate with the atlas. The neural spine is high and dorsocaudally expanded (Figure 2), and its cranial face has a well-developed muscle scar. Postzygapophyses are dorsocaudally expanded, but do not reach the height of the neural spine. The *lacuna interzygapophysealis* of the postzygapophyses of the axis is always smaller than the height of this vertebra; hence, in all analyzed species the axis is higher than wide.

The subsequent vertebrae have a dorsolaterally expanded neural arch, while the centrum is dorsoventrally reduced and craniocaudally elongated. The third and fourth vertebrae often present well-developed hypapophyses (Figure 2). The *tuberculum ansae* and lateral crest in the *ansa costotransversaria* are frequently laterally developed (Figure 3). Very marked muscle scars are seen on the edges of the *tuberculum ansae* (Figure 3). The *sulcus caroticus* is open on the last vertebra of the segment. Costal processes are fused to the *ansa costotransversaria* and are arranged ventrally to the centrum, extending

caudally. The *torus dorsalis* is often shallower in the third and fourth vertebrae than in the axis; they are, however, well developed in the fifth (Figures 2 and 3). The neural spine is dorsally extended and usually has a cranial orientation (Figure 2).

Comments. This segment is shorter in the Pelecaniformes than in the other analyzed clades. *Phaethon aethereus* is the only analyzed bird that does not have five vertebrae composing the segment. In Suliformes and *Thalassarche*, the last vertebra of this segment is the longest of the cervical series. Apparently, there is a direct relationship between the increased width of the condyloid fossa of the atlas and the length of this vertebra, which is longer in *Ardea alba* and shorter in *Sterna hirundo*. The width of the *lacuna interzygapophysealis* of the postzygapophyses of the axis also reflects the height of the axis. *Thalassarche melanophris* had the highest axis and the widest *facies articularis caudalis*, while *Sterna hirundo* had the lowest axis and the narrower *facies articularis caudalis*.

In Pelecaniformes, the hypapophyses extend craniocaudally in the vertebrae of this segment, whereas in other birds they are limited to the cranioventral portion. The length of the costal processes in the first segment frequently reaches the mid-length level of the centrum, although in *Phaethon aethereus* and *Thalassarche melanophris* they extend to near the end, and in the Pelecaniformes they do not reach the mid-length. This could be explained by the longer vertebrae in the latter. Pelecaniformes are the only of the analyzed birds that do not present a laterally developed *ansa costotransversaria*. This is reflected in the diameter of the *foramen transversarium*, which is smaller than in the others. *Phaethon aethereus* is the only analyzed bird that does not have an open *sulcus caroticus* in the last vertebra of this segment.

The widths of the *lacuna interzygapophysealis* in the post-axial vertebrae exceed their heights in the analyzed Charadriiformes and Pelecaniformes. The neural spine is lower and longer in the Pelecaniformes and *Sula leucogaster*. The third cervical vertebra is the highest in the neck only in *Calonectris diomedea*, *Phaethon aethereus*, and *Puffinus puffinus*. Only in *Phaethon aethereus*, *Sterna hirundo*, and *Thalasseus acuflavidus* the neural spines are not cranially oriented.

1.2. Vertebrae of the second segment

This segment was often the longest of the analyzed birds. The vertebrae are distinguished from those of the other segments by the more dorsoventrally compact neural arches (Figures 2 and 3). The centra are craniocaudally expanded, similar to the more caudal vertebrae of the first segment (Figures 2 and 3). The longest vertebrae of the segment are in the cranial portion, which are frequently also the longest of the whole neck. However, unlike the first segment, not all birds have a caudal increase in the length of this segment's vertebrae.

The *facies articularis cranialis* are usually wider than in the vertebrae of the first segment. The vertebrae have no hypapophysis (Figure 3). The *sulcus caroticus* is open and concave, located below the *facies articularis cranialis* (Figure 3). Laterally, the carotid processes are bilaterally arranged and ventromedially oriented (Figure 3). The *tuberculum ansae* is more laterally expanded and the costal processes are longer in this segment (Figures 2 and 3). Muscle scars are present around the tubercles, although not as deep as in the first segment (Figures 3).

The most cranial vertebrae in the segment frequently have the longest postzygapophyses and the widest *lacunae interzygapophysialis* of the whole neck. The *torus dorsalis* are most prominent in this segment (Figures 3 and 4), and neural spines are extremely low and dorsocranially oriented (Figures 2 and 3).

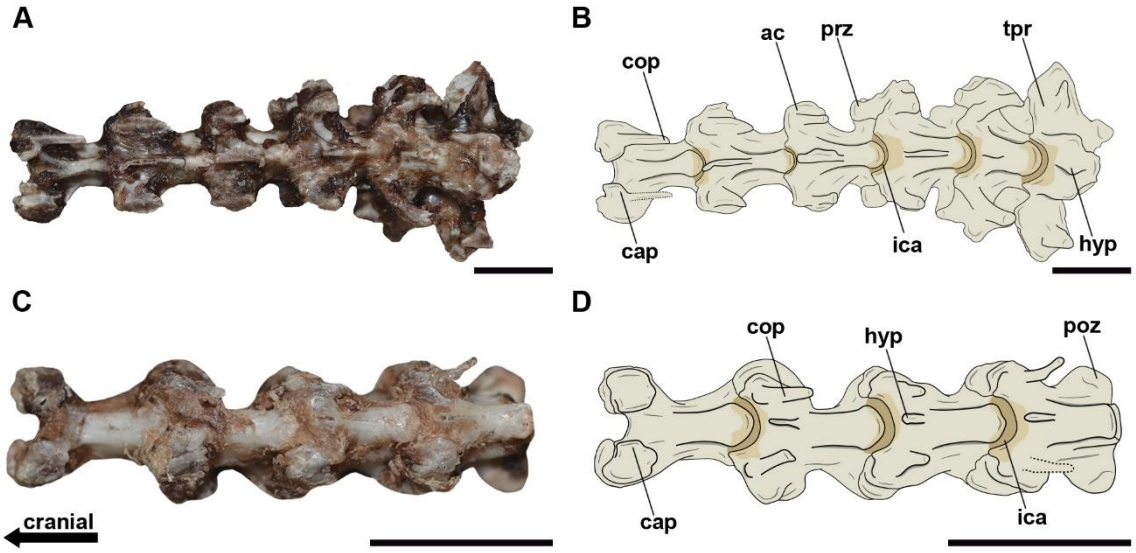

Figure 4. Photographs and interpretative drawings of the articulated cervical vertebrae in ventral view. (A, B). Cervical series from ninth to fourteenth vertebra belonging to *Procellaria aequinoctialis*; (C, D) cervical series from tenth to thirteenth vertebra belonging to *Thalasseus acuflavidus*. Scale bar: 10 mm.

Comments. Only *Thalassarche* and the Suliformes did not present the longest vertebra of the neck in this segment. The width between the carotid processes is narrower in the Pelecaniformes and wider in the Procellariiformes, Suliformes and *Phaethon aethereus*. The costal processes in Charadriiformes and Pelecaniformes are not as long as in other Aequorlitornithes. The *torus dorsalis* is more developed in Pelecaniformes than in other Aequorlitornithes, but these birds also have very low neural spines.

1.3. Vertebrae of the third segment

The vertebrae have a craniocaudally compressed centrum and a dorsoventrally expanded neural arch, making them more similar to the thoracics (Figures 2 and 3). The vertebrae are usually taller than those of other segments, due to their tall neural arch and to the presence of hypapophysis (Figure 2).

Ventrally to the *facies articularis cranialis*, the *fovea cranioventralis* is well developed and presents an hypapophysis that extends cranioventrally and that is larger in height and length in more caudal vertebrae (Figure 2 and 3). The *ansa costotransversaria* extends craniodorsally and laterally (Figure 2). The more caudal vertebrae have laterally developed transverse processes (Figure 2). Costal processes fused to the *ansa costotransversaria* are ventrocaudally oriented and are smaller than the vertebrae in other segments (Figure 3).

The *lacuna interzygapophysealis* of the prezygapophysis is wider than in other segments, due to the lateral extension of the *ansa costotransversaria*. The craniodorsal increase of the *ansa costotransversaria* also contributes to the elevation of the prezygapophyses in relation to the neural arch, reaching a taller level than the neural spine (Figure 2). The more caudal ones have extremely tall neural spines, frequently short in length (Figure 2).

Comments. The third segment of the neck is the shortest of the analyzed species, except *Phaethon aethereus*. The analyzed Pelecaniformes present the hypapophysis in a more caudal position. Although frequently reduced, the *tuberculum ansae* is still considerably prominent in the Procellariiformes, Suliformes, and *Phaethon aethereus*. The height of the zygapophyses allows for these articulations to be more dorsal than in the previous segments (Figure 2). The analyzed Pelecaniformes have a long neural spine, extending from the cranial to the caudal portion of the neural arch.

2. Arthrology

2.1. Atlas and axis

The *articulatio atlanto-occipitalis* has a fibrous cartilage covering all margins of the *fossa condyloidea*. The *ligamentum apicis dentis* is present inside the *fossa condyloidea*. It is thin and short, extending from the connection with the occipital condyle to the cranial end of the *incisura fossae*.

The *articulatio atlanto-axialis* joint in the intervertebral space between the *facies articularis axialis* and *atlantis* is usually <0.5 mm thick. The *processus articularis caudalis* of the atlas articulates with the base of the odontoid process and the dorsocranial surface of the axis, also through synovial cartilage. Two ligaments are associated with the *articulatio atlanto-axialis*: the *ligamentum medianum atlantoaxiale* is a single bundle that extends from the ventral base of the odontoid process to the dorsal surface of the atlantical centrum, and the *ligamentum collaterale atlantoaxiale* extends laterally from the odontoid process to both sides of the *facies articularis caudalis* of the atlas.

Comments. In *Phaethon aethereus*, the cranial surface of the odontoid process is enveloped by synovial cartilage next to the *incisura fossae* of the atlas. In the analyzed Pelecaniformes and *Nannopterum brasilianus*, both ligaments restricted to the *atlanto-axialis* joint are ossified.

2.2. *Articulatio intercorporalis* and ligaments associated with the centrum in post-axial cervical vertebrae

The *articulatio intercorporalis* is composed by a thin layer of synovial cartilage over the heterocoelous *facies articularis* of both vertebrae involved (Figure 4). The intervertebral meniscus is immersed in the synovial fluid. The *articulatio intercorporalis* is limited by the articular capsule, a thin layer that lines mediolaterally and dorsoventrally the synovial cartilage (Figure 5).

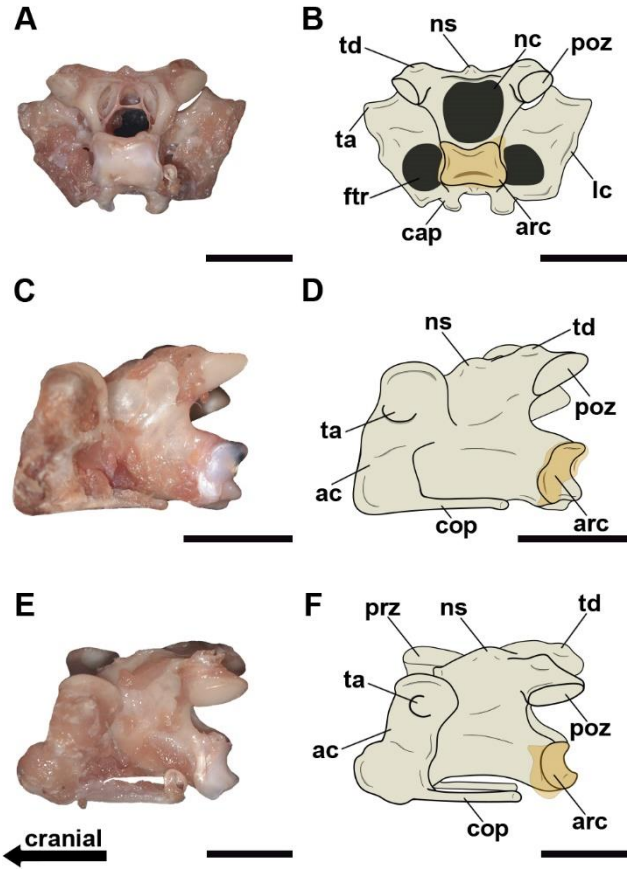

Figure 5. Photographs and interpretative drawings of the articular capsules associated with the *facies articular caudalis* of the cervical vertebrae. (A, B) tenth vertebra belonging to *Thalassarche melanophris* in caudal view; (C, D) ninth vertebra belonging to *Thalassarche melanophris* in left lateral view; (E, F) ninth vertebra belonging to *Thalassarche chlororhynchos* in left lateral view. Scale bar: 10 mm.

In the segments I and II of the neck, the thickness of the synovial cartilage in the *articulatio intercorporalis* is often <0.5 mm. Caudally, there is a continuous increase in their thickness in the third segment vertebrae, in which this value is usually >0.5 mm (Figure 4). In Suliformes and Procellariformes, except *Puffinus puffinus*, the thickness of the *articulatio intercorporalis* between the last two vertebrae of the cervical series is >1 mm. Even when each joint is apparently not that thick, some birds show a significant difference in the length of the cervical series with and after removing the cartilaginous tissue from the *facies articularis*, as it frequently ranges from 3.5 to 5.6% of the total length of the neck (Table 3).

The *ligamentum collaterale* is located laterally to the centrum, bordering the lateral surface of the articular capsules. It originates on the laterocaudal surface of all cervical vertebrae, except the atlas, and attaches to the *ansa costotransversaria* of the next vertebra (Figure 2).

We observed two ligaments ventrally to the centrum in different regions of the cervical series. The *ligamentum ventrolaterale* attaches to both carotid processes and extends to the ventrolateral surface of the subsequent cranial vertebra, between the fifth and the caudalmost vertebra of the second segment. The *ligamentum intercristale ventrale* is present only in the third segment, where it attaches to the hypapophysis. It usually extends from the cranialmost cervical vertebra that has an hypapophysis to the last cervical.

Table 3. Proportion of cartilage to the neck length of birds. Abbreviations: CV, sum of the centrum lengths of the cervical vertebrae; TOTAL, total neck length; CART, percentage of cartilage to neck length.

	CV (mm)	**TOTAL (mm)**	**CART (%)**
Aequorlitornithes			
Charadriiformes			
Haematopus palliatus	118	125	5.6
Larus dominicanus	157	165	4.8
Sterna hirundo	79	82	3.6
Thalasseus acuflavidus	109	113	3.5
Pelecaniformes			
Ardea alba	551	553	0.3
Ixobrychus exilis	183	185	1.1
Phaethontiformes			
Phaethon aethereus	145	153	5.2
Procellariiformes			
Calonectris diomedea	172	182	5.5
Procellaria aequinoctialis	153	160	4.3
Puffinus puffinus	99	104	4.8
Thalassarche chlororhynchos	286	299	4.3
Thalassarche melanophris	294	307	4.2
Suliformes			
Fregata magnificens	258	268	3.7
Nannopterum brasiliensis	245	256	4.2
Sula leucogaster	290	302	4.0

Inopinaves			
Accipitriformes			
Coragyps atratus	209	215	1.9
Cariamiformes			
Cariama cristata	267	280	4.6

Comments. The presence of synovial fluid in the *articulatio intercorporalis* indicates that this is the most flexible neck joint. *Fregata magnificens, Sula leucogaster, Thalassarche chlororhynchos* and *Thalassarche melanophris* present a >0.5 mm thickness in each *articulatio intercorporalis* of the third segment. Pelecaniformes differed from the others regarding the thickness of the cartilage to the total neck length, having considerably less cartilage filling the *articulatio intercorporalis* (Table 3). In the analyzed Pelecaniformes, Suliformes, and *Thalassarche*, the *ligamentum collaterale* was ossified, conferring lateral stiffness.

2.3. *Articulatio zygapophysialis* and ligaments associated with the neural arch in post-axial cervical vertebrae

The zygapophyses also present synovial cartilage, limited by articular capsules and with extremely thin menisci between the articular facets. They show an overlap that varies between =50% and >50% along the cervicals at rest position. Pelecaniformes, Suliformes, and *Thalassarche* presented overlap varying between <50% and =50% in the first and second segments, although in the third segment the values were similar to those seen in the other Aequorlitornithes.

Due to the presence of synovial fluid and menisci, the *articulatio zygapophysialis* has a malleability that allows one zygapophysis to slide over the other. The total flexion of the neck requires minimal overlapping of the zygapophyses in the first and second segments. In the third segment, flexion is more limited and the zygapophyses overlap varies between <50% and =50%.

Dorsally to the neural spine, we observe the *ligamentum elasticum interspinale* and *ligamentum elasticum interlaminare*. Both are easily recognizable from the more caudal vertebrae of the second neck segment to the end of the neck, with the *ligamentum elasticum interspinale* being the more robust (Figure 2). Although less robust, both

ligaments extend to the cranialmost vertebrae in the second segment in *Thalassarche* and in Suliformes, except *Nannopterum brasilianus*.

Comments. Due to the thickness of the cartilage and the anatomy of the zygapophyses, the *articulatio zygapophysialis* does not contribute to the length of the cervical series. Pelecaniformes and *Nannopterum brasilianus* stand out for presenting less overlapping of the zygapophyses with the neck at rest. The third segment presents greater overlapping of the zygapophyses in relation to the first and second segments during rest or flexion of the neck.

3. Myology

Sixteen cervical muscles are recognized in most analyzed birds (Figure 6). The muscles are arranged bilaterally, except for the *splenius capitis* and *interspinales*, which are median. All muscle attachments to the *ansa costotransversaria* are aponeurotic. However, muscles also show aponeuroses attached to other surfaces, such as the hypapophysis, making it difficult to determine the type of muscle attachment based on the fixation site alone.

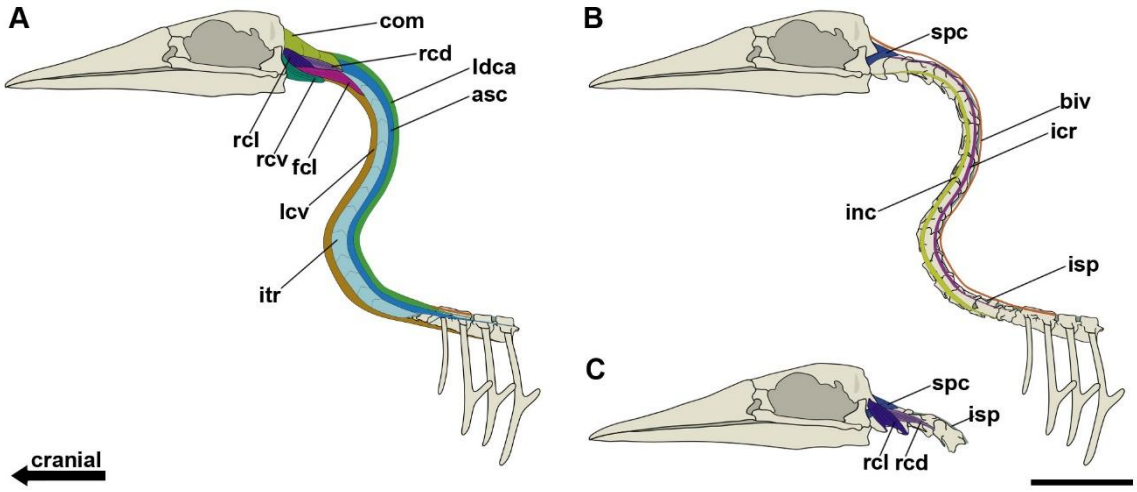

Figure 6. Interpretative drawings of the arrangement of the superficial musculature (A), deep musculature (B) and the deeper *rectus capitis* (C) of *Sula leucogaster* in left lateral view. Scale bar: 50 mm.

Muscles that do not extend to at least the second segment of the neck are thicker. Variations in the thickness of muscles that extend to the entire length of the neck occur due to contact with the vertebral surface. The presence of the *ansa costotransversaria* and of processes in the neural arch make the vertebral surfaces irregular, which shifts the depth of the inner surface of the muscles in relation to the vertebral cortex. Therefore, the

thickness of the cervical muscles varies along the neck, being thickest in the third segment. The thickness of *biventer cervicis*, *complexus*, *splenius capitis*, *longus colli dorsalis pars. cranialis* and *caudalis*, *rectus capitis ventralis*, *flexor colli medialis* and *longus colli ventralis* is approximately six times the area of origin of the muscles, while in the other muscles the thickness is only about three times wider (Table 4 and 5).

Table 4. Area of origins and thickness of the *transversospinalis* muscles of birds. Muscle thickness was measured at their thickest point.

	biv	***com***	***spc***	***ldcr***	***ldca***	***asc***	***icr***	***isp***
Aequorlitornithes								
Charadriiformes								
Haematopus palliatus								
Origin area	0.32	1.46	1.04	0.52	0.53	1.0	0.67	0.39
Muscle thickness	1.9	9.4	5.9	2.9	2.9	3.1	2.3	1.1
Larus dominicanus								
Origin area	0.34	1.62	1.01	0.50	0.53	1.45	1.28	0.45
Muscle thickness	2.3	9.4	6.2	2.7	2.8	3.9	3.0	1.6
Sterna hirundo								
Origin area	0.17	1.0	0.55	0.27	0.28	0.70	0.48	0.14
Muscle thickness	1.1	5.3	3.1	1.4	1.6	2.4	1.9	0.5
Thalasseus acuflavidus								
Origin area	0.17	0.95	0.52	0.31	0.32	0.65	0.53	0.18
Muscle thickness	1.2	6.1	3.1	1.5	1.5	2.4	1.9	0.6

Pelecaniformes								
Ardea alba								
Origin area	-	1.01	1.15	0.66	0.68	1.12	0.90	0.42
Muscle thickness	-	6.2	7.7	3.6	3.7	3.5	2.8	1.2
Ixobrychus exilis								
Origin area	-	0.83	0.54	0.21	0.20	0.70	0.57	0.16
Muscle thickness	-	5.1	2.8	1.3	1.3	2.2	1.6	0.5
Phaethontiformes								
Phaethon aethereus								
Origin area	0.45	1.61	1.06	0.59	0.59	1.27	1.02	0.22
Muscle thickness	2.3	10.0	6.5	3.2	3.3	3.8	3.1	1.5
Procellariiformes								
Calonectris diomedea								
Origin area	0.47	1.89	1.18	0.51	0.53	1.45	1.02	0.41
Muscle thickness	2.4	11.1	6.6	3.2	3.4	4.2	3.1	1.5
Procellaria aequinoctialis								
Origin area	0.42	1.62	1.11	0.56	0.57	1.37	1.10	0.56
Muscle thickness	2.5	8.9	6.8	3.3	3.3	4.0	3.4	1.8
Puffinus puffinus								
Origin area	0.43	1.43	1.15	0.59	0.62	1.34	0.98	0.52

Muscle thickness	2.3	8.0	6.7	3.4	3.5	4.0	3.1	1.7
Thalassarche chlororhynchos								
Origin area	0.42	1.71	1.10	0.60	0.64	1.36	1.53	0.71
Muscle thickness	2.9	10.1	6.7	3.3	3.4	4.5	3.8	2.0
Thalassarche melanophris								
Origin area	0.43	1.65	1.10	0.61	0.67	1.35	1.52	0.71
Muscle thickness	3.0	10.0	6.5	3.2	3.4	4.4	3.6	2.2
Suliformes								
Fregata magnificens								
Origin area	0.52	2.02	1.01	0.52	0.53	1.45	1.21	0.69
Muscle thickness	2.7	11.9	6.2	3.2	3.4	4.4	3.5	2.0
Nannopterum brasiliensis								
Origin area	-	2.00	1.14	0.55	0.57	1.8	1.10	0.44
Muscle thickness	-	11.1	6.7	3.3	3.3	4.2	3.2	1.8
Sula leucogaster								
Origin area	0.50	2.23	1.20	0.64	0.64	1.67	1.48	0.80
Muscle thickness	3.2	13.0	7.0	3.6	3.7	4.8	3.9	2.5
Inopinaves								
Accipitriformes								
Coragyps atratus								

Origin area	0.43	2.0	1.13	0.60	0.63	1.7	1.22	0.68
Muscle thickness	2.7	12.3	7.0	3.4	3.4	4.5	3.4	2.0
Cariamiformes								
Cariama cristata								
Origin area	0.56	2.01	1.18	0.59	0.62	1.56	1.34	0.70
Muscle thickness	3.1	12.4	7.1	3.8	3.8	4.4	3.8	2.2

Table 5. Area of origins and thickness of the *longuissimus*, *iliocostalis* and hypaxial muscles of birds. Muscle thickness was measured at their thickest point.

	rcd	***int***	***rcl***	***fcl***	***rcv***	***fcm***	***inc***	***lcv***
Aequorlitornithes								
Charadriiformes								
Haematopus palliatus								
Origin area	2.53	1.18	2.58	1.90	1.09	0.90	0.89	0.57
Muscle thickness	7.4	3.4	7.9	6.6	6.9	5.2	2.5	3.0
Larus dominicanus								
Origin area	2.25	1.45	2.08	2.09	1.05	0.92	0.97	0.64
Muscle thickness	7.1	4.3	6.1	6.5	6.0	5.2	3.1	3.3
Sterna hirundo								
Origin area	1.15	1.06	1.02	1.13	0.66	0.55	0.67	0.36
Muscle thickness	3.7	3.1	2.9	3.7	3.6	3.0	2.3	1.9

Thalasseus acuflavidus								
Origin area	1.31	0.97	1.08	1.24	0.71	0.67	0.75	0.41
Muscle thickness	4.1	3.0	3.5	4.2	3.9	3.5	2.3	2.0
Pelecaniformes								
Ardea alba								
Origin area	1.41	1.37	1.67	1.35	0.59	0.60	0.87	0.72
Muscle thickness	4.3	4.2	5.1	4.2	3.1	3.4	2.8	3.9
Ixobrychus exilis								
Origin area	1.05	0.81	0.96	0.74	0.34	0.39	0.47	0.40
Muscle thickness	3.1	2.4	3.0	2.4	1.7	2.0	1.6	2.0
Phaethontiformes								
Phaethon aethereus								
Origin area	2.53	1.36	2.22	2.09	1.38	0.99	1.11	0.68
Muscle thickness	8.2	4.3	7.1	6.4	7.8	5.4	3.5	3.7
Procellariiformes								
Calonectris diomedea								
Origin area	2.52	1.41	1.95	2.57	1.37	1.16	1.01	0.67
Muscle thickness	8.2	4.3	6.2	7.9	7.9	7.0	3.2	3.6
Procellaria aequinoctialis								
Origin area	2.01	1.35	1.69	2.18	1.12	0.99	1.17	0.67

Muscle thickness	6.2	4.5	5.3	6.7	6.0	5.7	3.6	3.8
Puffinus puffinus								
Origin area	1.97	1.33	1.42	1.98	0.97	0.95	1.17	0.66
Muscle thickness	5.9	4.3	4.5	6.2	5.3	5.2	3.3	3.6
Thalassarche chlororhynchos								
Origin area	2.43	1.54	2.06	2.46	1.31	1.19	1.32	0.78
Muscle thickness	7.3	4.9	6.4	7.8	7.2	6.6	4.0	4.3
Thalassarche melanophris								
Origin area	2.44	1.50	2.02	2.31	1.40	1.24	1.19	0.74
Muscle thickness	7.8	5.0	6.4	7.3	7.6	6.7	3.8	4.1
Suliformes								
Fregata magnificens								
Origin area	2.55	1.49	2.35	2.44	1.33	1.19	1.20	0.68
Muscle thickness	8.1	4.7	7.6	7.7	7.9	7.0	3.7	4.0
Nannopterum brasiliensis								
Origin area	3.02	1.59	2.66	3.10	1.81	1.56	1.14	0.65
Muscle thickness	9.4	4.6	8.4	9.9	9.6	9.0	3.5	3.8
Sula leucogaster								
Origin area	3.21	1.71	3.67	3.11	1.67	1.65	1.33	0.78
Muscle thickness	10.0	5.1	11.7	9.7	8.7	8.9	4.0	4.3

Inopinaves

Accipitriformes								
Coragyps atratus								
Origin area	3.04	1.43	2.49	2.40	1.34	1.15	1.43	0.63
Muscle thickness	9.5	4.7	8.1	7.4	7.3	6.8	3.7	4.0
Cariamiformes								
Cariama cristata								
Origin area	3.0	1.55	2.79	2.51	1.47	1.23	1.37	0.70
Muscle thickness	9.1	4.7	8.5	7.9	7.7	7.0	4.0	4.3

The neck cross section does not represent an exact circumference at any point on the birds' neck, however, the height and width in cross-sectional view are approximately equivalent (Figure 7). The musculature disposed laterally to the vertebra represents approximately one third of the width of the cross section in any part of the neck of birds, being therefore about half of the vertebral width (Figure 7).

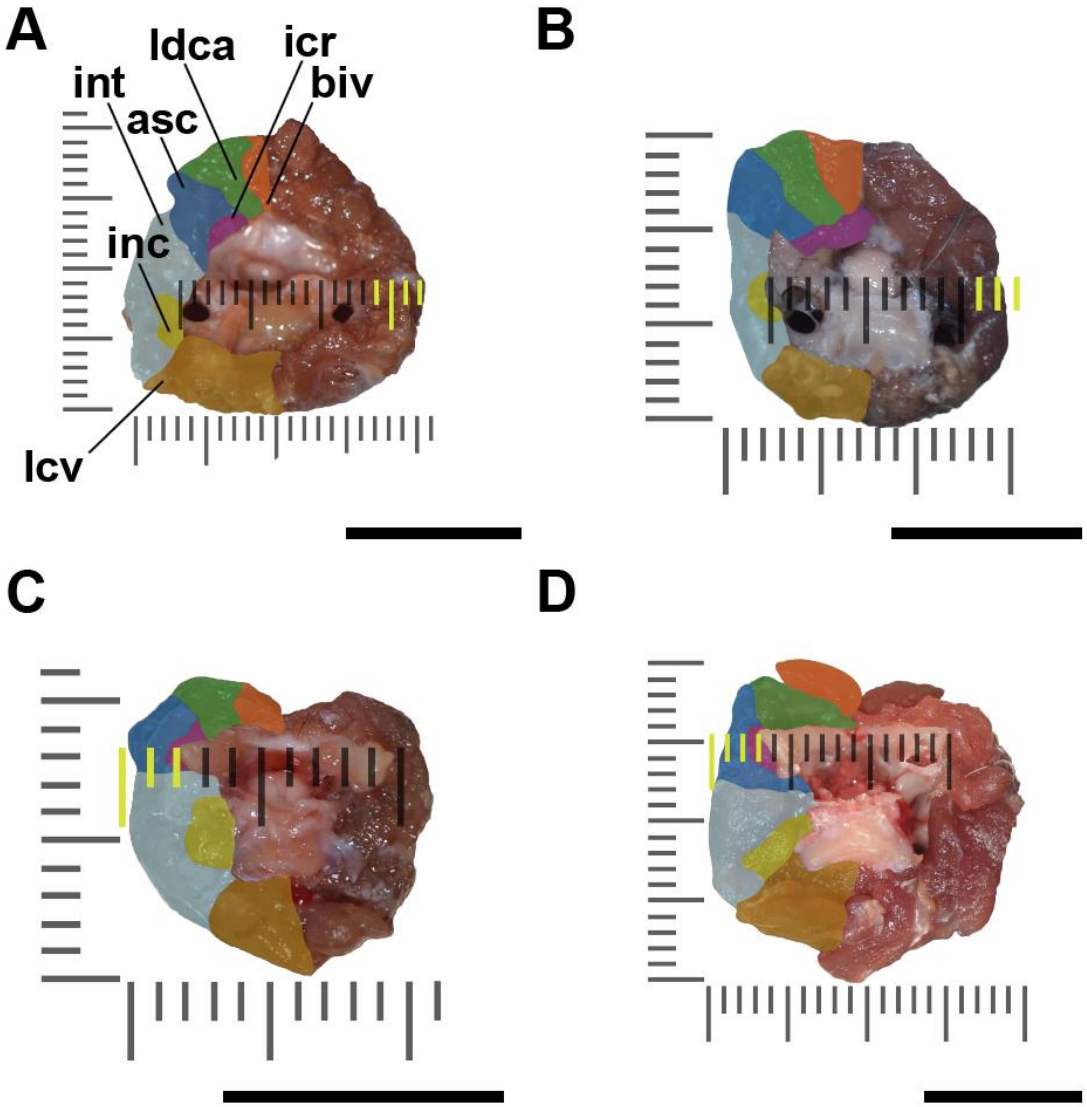

Figure 7. Cross-section showing the ninth vertebra in *Haematopus palliatus* (A) and *Procellaria aequinoctialis* (B) in cranial view, and in *Thalasseus acuflavidus* (C) and *Phaethon aethereus* (D) in caudal view. The ruler on the left side and below each cross section shows that the width and height are equivalent. The metric marked in yellow indicates that the lateral musculature represents approximately 25% of the width of the cervical vertebra. Scale bar: 10 mm.

3.1. Epaxial muscles

3.1.1 *Transversospinalis* group

Biventer cervicis

It is the narrower among the muscles that extend throughout the entire neck. It is located dorsally to the *longus colli dorsallis pars caudalis* and between the *complexus* muscles (Figure 8). The origin is located on the caudal face of the neural spines of the *notarium* (when present) or *cervicodorsales* vertebrae (Figure 6). The insertion of the muscle is at the dorsomedial end of the *crista nuchalis transversa* (Figure 6).

Comments. This is the only muscle that does not have attachments in the cervical vertebrae in any of the analyzed birds. It is absent in *Ardea alba*, *Ixobrychus exilis*, and *Nannopterum brasilianus*, which had the *longus colli dorsalis pars caudalis* as the dorsalmost neck muscle (Figure 8).

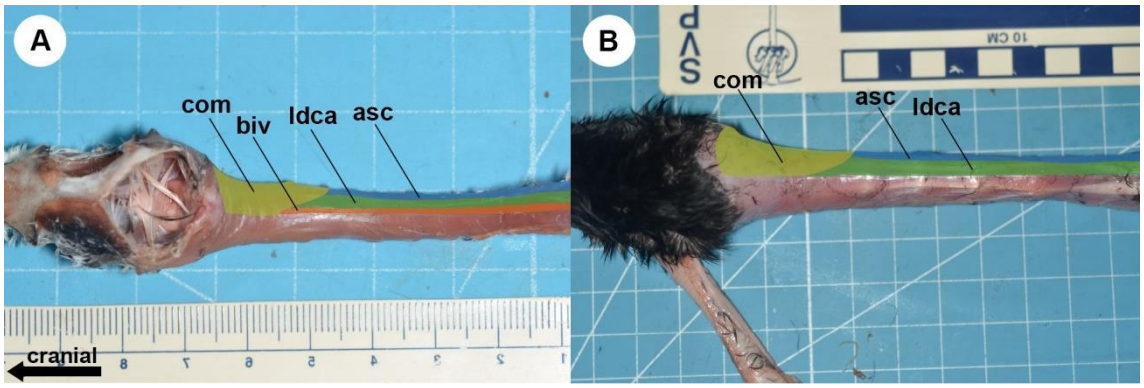

Figure 8. Photographs of the superficial muscles of the neck of *Sterna hirundo* (A) and *Nannopterum brasilianus* (B) in dorsal view.

Complexus

This is a superficial muscle that occupies the laterodorsal portion of the first neck segment (Figures 6 and 9). Laterally, it has folds that divide it into bellies, whose number varies between species (Figures 6 and 9). This is the thickest neck muscle of all analyzed species (Table 4).

The origins of the *complexus* usually attach to the *torus dorsalis* and the lateral crest of the fourth or fifth cervical vertebra, through transverse aponeuroses (Figure 10). The cranialmost portion of the muscle extends craniodorsally and inserts on the margins of the *crista nuchalis transversa*.

Comments. The number of bellies varied between two in the analyzed Pelecaniformes and three in the other Aequorlitornithes (Figure 9). Pelecaniformes also differ in the muscular origin, which is more caudally located on the lateral crest of the fourth cervical vertebra, while in other birds the aponeurosis extends to the fifth cervical vertebra. Only in *Phaethon aethereus* the more caudal muscular origins are on the fifth and sixth vertebrae, culminating in a proportionally longer *complexus* (Figure 9).

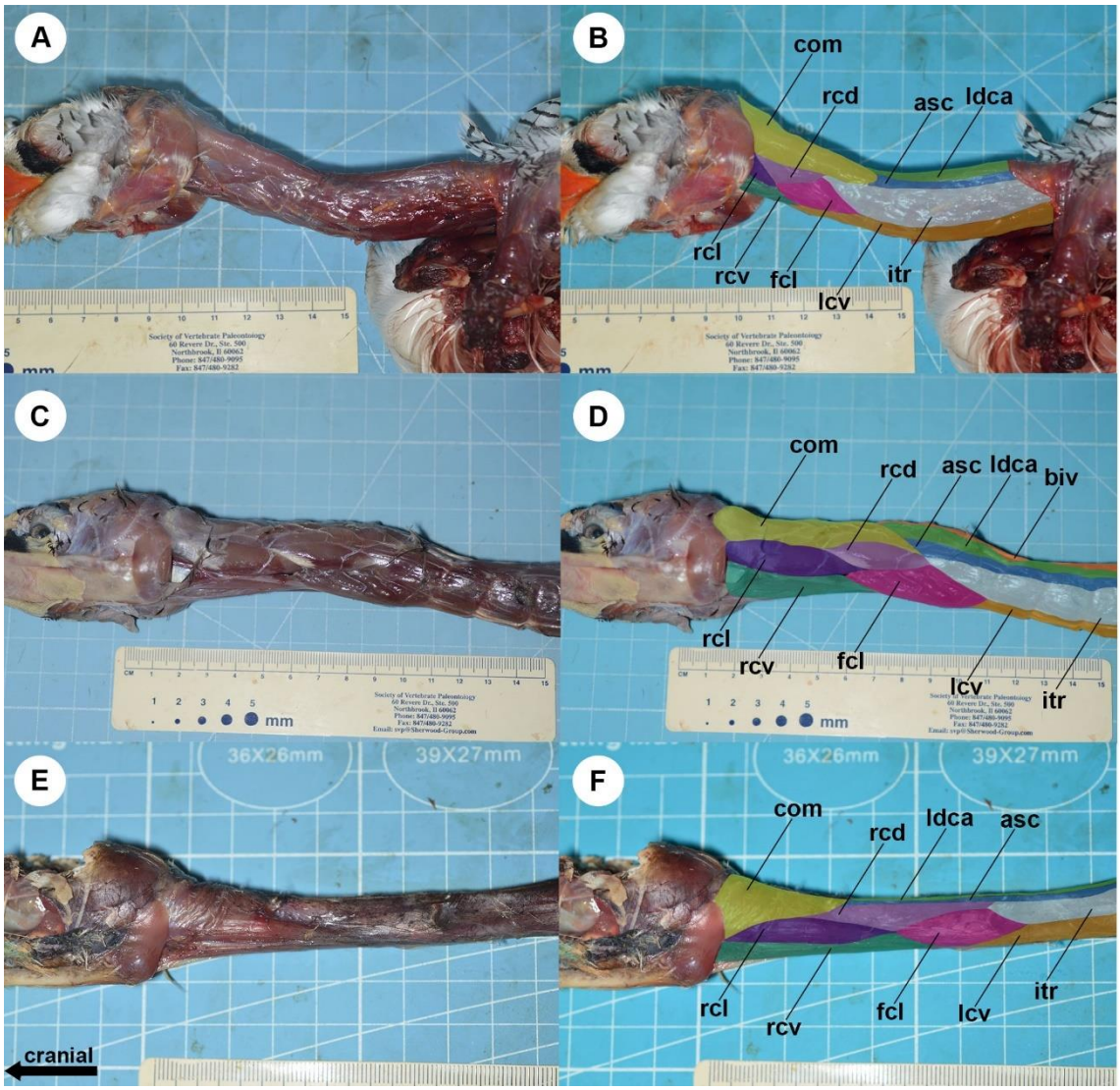

Figure 4. Photographs and interpretation of the superficial muscles of the neck of *Phaethon aethereus* (A, B), *Sula leucogaster* (C, D) and *Ardea alba* in left lateral view.

Splenius capitis

This muscle has two bellies, with the shorter under the longer one. Both have a triangular shape with broad cranially oriented bases, and are superimposed by the *complexus* (Figure 6). The origins of the shorter belly attach on the cranial face of the neural spine of the axis by an aponeurosis, while those of the longer belly connect to the cranial face of the top of the neural spine of the third vertebra (Figures 10). The insertions attach on the *crista nuchalis transversa*, deeper than the insertion of the *complexus*, and extend to the paraoccipitals.

Comments. The analyzed Pelecaniformes had the origins of both bellies only on the axis.

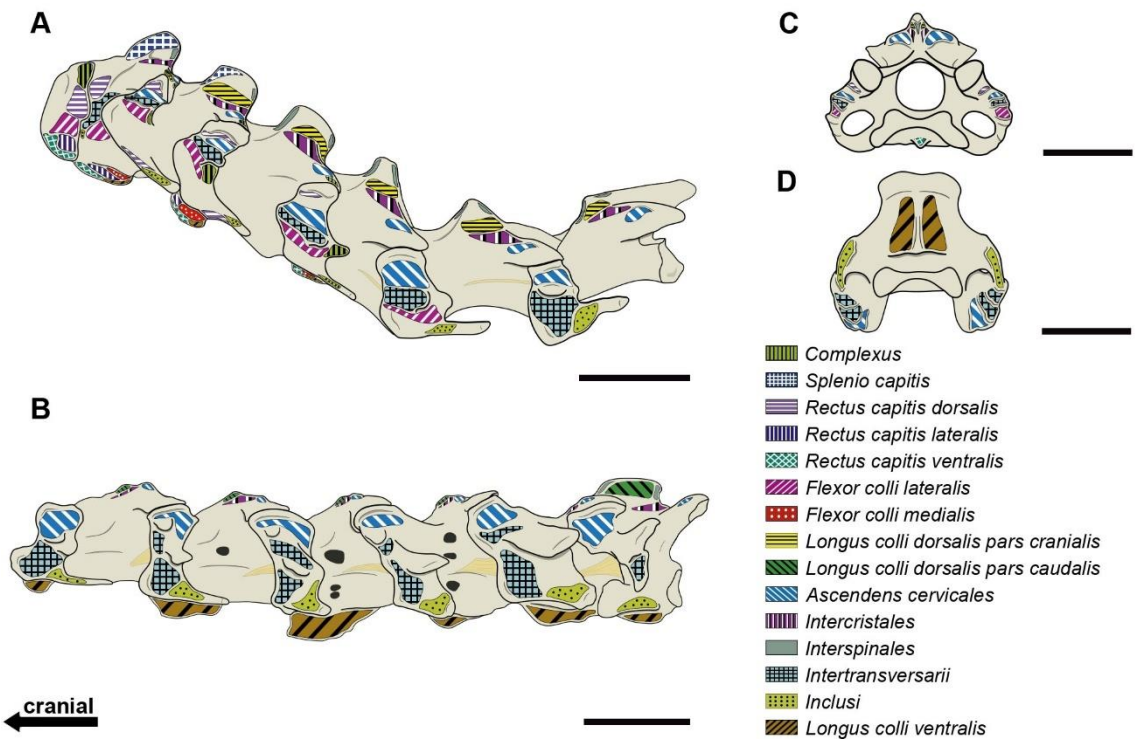

Figure 10. Interpretative drawings indicating muscle attachment sites on the vertebrae. (A) Cervical series from the atlas to seventh vertebra belonging to *Procellaria aequinoctialis* in left lateral view; (B) cervical series from the ninth to the fourteenth vertebra belonging to *Procellaria aequinoctialis* in left lateral view; (C) fifth vertebra belonging to *Sula leucogaster* in cranial view; (D) sixteenth vertebra belonging to *Sula leucogaster* in ventral view. Scale bar: 10 mm.

Longus colli dorsalis (*pars cranialis* and *caudalis*)

These muscles are apparently continuous, showing similarities in their origins and insertions; however, they are separated by faciae. The *pars caudalis* is longer and more superficial (Figure 6, 8 and 9), and entirely overlaps the *pars cranialis* (Figure 11).

The more caudal origins of the *pars cranialis* are on the caudal face of the base of the neural spine, varying between the eighth, ninth, and tenth cervical vertebrae, by an aponeurosis (Figure 10). The *pars caudalis* had its most caudal origins placed caudally to the cervical series, on the caudal surface of the base of the neural spine of the *notarium* and/or more cranial free thoracic vertebrae, by an aponeurosis (Figure 6).

The insertions of the *pars caudalis* are in the most caudal cervical vertebrae, on the *torus dorsalis* of vertebrae of the second and third segments of the neck in all the analyzed birds (Figure 10). A single filament of the *pars caudalis* extends along the first segment of the neck and converges with the more cranial filaments of the *pars cranialis*, forming a single tendon that inserts on the *torus dorsalis* of the axis (Figure 10).

Comments. In birds that lack the *biventer cervicis*, the left and right *longus colli dorsalis pars caudalis* are arranged side by side, being the most dorsal muscles of the neck (Figure 8). A proportionally longer *longus colli dorsalis pars cranialis* was observed in *Sula leucogaster* and in both Pelecaniformes analyzed.

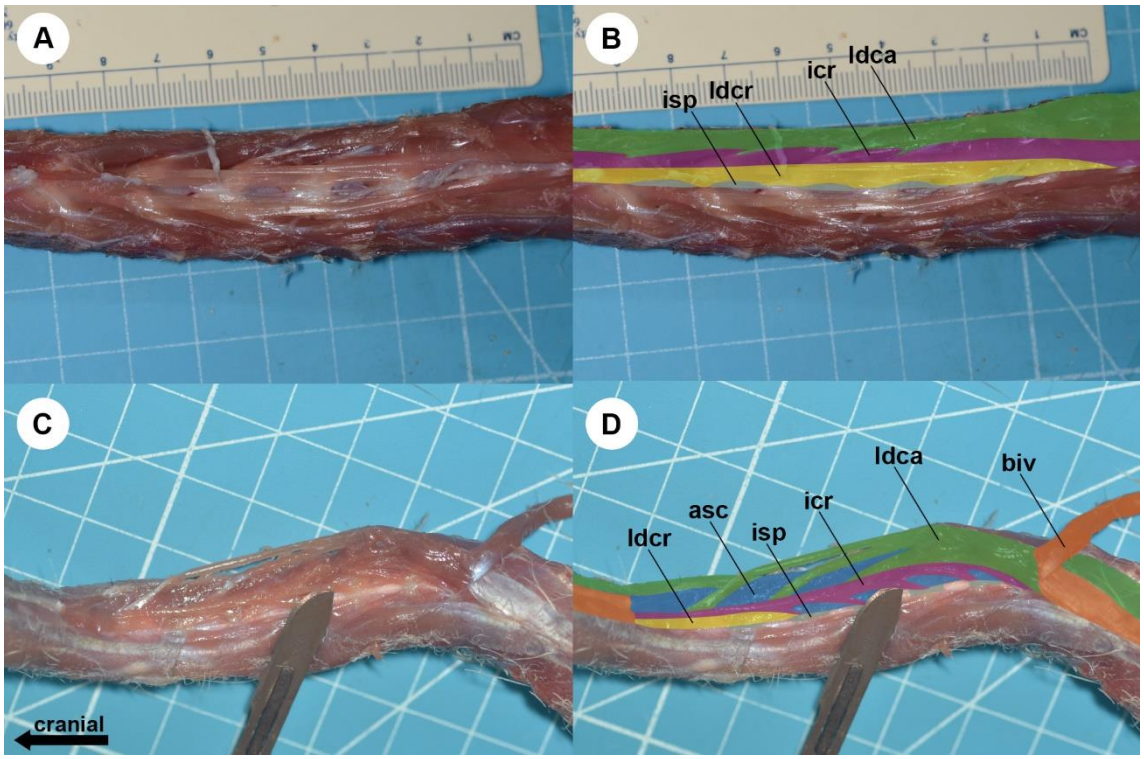

Figure 11. Photographs of the deep long muscles of the neck in *Thalassarche chlororhynchos* (A, B) and *Calonectris diomedea* (C, D) in dorsal view.

Ascendens cervicalis

This muscle is arranged bilaterally to the cervical series and has complex attachments with each cervical vertebra along its length. They are located next to the prezygapophyses' bases, laterally the *ansa costotransversaria*, and on the *torus dorsalis* (Figure 10). The same sites harbor the most caudal and cranial origins and insertions, respectively, of this muscle. The most caudal origins are located laterally on the centrum, bordering the parapophyses of the *notarium* or more cranial free thoracic vertebrae (Figure 6). Cranially, the insertion is established via a transverse aponeurosis, attached to the *torus dorsalis* of the axis (Figure 10).

Comments. Among the muscles whose length is longer than or equal to that of the neck, the *ascendens cervicalis* is the thickest in the first segment of the analyzed birds, except in *Ardea alba*, *Sterna hirundo*, and *Thalasseus acuflavidus* (Table 4). Along the

second segment, its less thick than the *intertransversarii* (Table 4). This makes the *ascendens cervicalis* the only long muscle that does not show an increase in thickness from the cranial to the caudal direction in the analyzed birds.

Intercristales

These are segmented and deep muscles, placed bilaterally to the neural arch of the cervical series (Figures 6, 7 and 11). Their origins are on the last cervical vertebra and the insertions, on the atlas and axis (Figure 10). The attachment sites, from the base of the neck to the axis, are on the transverse oblique crest of each vertebra (Figures 8 and 10). In the atlas, they are dorsolateral, on the neural arch. All attachments are by aponeuroses (Figure 11).

Interspinales

These are segmented and deep muscles, whose fleshy portions are arranged between the neural spines of the cervical vertebrae (Figures 6 and 11). Their attachment sites are located on the cranial and caudal surfaces of the neural spines, extending dorsoventrally in these structures (Figures 10 and 11).

3.1.2. *Longissimus* group

Rectus capitis dorsalis

This superficial muscle is arranged craniocaudally, dorsally to the other *rectus capitis* (Figures 6 and 9). Its origins are established via a transverse aponeurosis, usually in the more caudal vertebrae of the first segment of the cervical series (Figures 6 and 10). The aponeurosis lies laterally on the prezygapophyses and close to the bases of the costal processes. The insertions are arranged ventrolaterally to the occipital condyle, on the basioccipital.

Comments. There is variation in the vertebra where the muscle originates. Most frequently, muscles originate laterally to prezygapophyses of the fifth vertebra (Figures 6 and 10). Pelecaniformes presents the most caudal origin in the same location, but on the sixth vertebra, and terns (*Sterna hirundo* and *Thalasseus acuflavidus*) usually present the origin laterally to the neural arch of the fourth vertebra.

Intertransversarii

These muscles are superficial and arranged bilaterally on the cervical series (Figures 6 and 9). Unlike others, they are composed of intersegments, which have a complex system of filaments that attach to each vertebra in the neck, making them visually easy to distinguish from others (Figure 9). They extend from the axis to the last cervical vertebra. All attachments, including origins and insertions, are located on the *tuberculum ansae* and the lateral crest through aponeuroses (Figure 10).

Comments. These are usually the thickest of the long muscles in the second and third segments. Their thickness is wider especially in the Procellariiformes and Suliformes (Table 4).

3.1.3. *Iliocostalis* group

Rectus capitis lateralis

This muscle is more superficial and lateral than the other *rectus capitis* (Figures 6 and 9). It originates through an aponeurosis, generally on the lateral face of the hypapophysis of the third vertebra (Figure 6). The muscle also attaches laterally to the hypapophysis of the axis, and ventrolaterally to the intercentrum of the atlas (Figure 10). The insertions are present on both ventral ends of the paraoccipital processes.

Comments. This is typically the shortest neck muscle, except in birds that have an extremely short *complexus* (Table 6). Although its origin is usually on the third vertebra, the Procellariiformes and *Ardea alba* present a more caudal origin, extending through a thin aponeurosis to the fourth vertebra (Figure 12). Among the short neck muscles, this is the thinnest in the Procellariiformes, Suliformes (except *Sula leucogaster*) and in both terns analyzed (*Sterna hirundo* and *Thalasseus acuflavidus*) (Table 5).

Table 6. Length and thickness (in mm) of the "short muscles" of each analyzed species.

	com	***rcd***	***rcl***	***rcv***	***fcl***
Aequorlitornithes					
Charadriiformes					
Haematopus palliatus					
length	34.7	37.1	22.2	31.2	42.8
Larus dominicanus					
length	32.2	41.8	26.3	29.6	56.4
Sterna hirundo					
length	22.4	21.7	17.8	19.2	26.1
Thalasseus acuflavidus					
length	25.3	19.7	13.0	18.8	22.4

Pelecaniformes					
Ardea alba					
length	32.5	64.1	40.6	56.3	72.3
Ixobrychus exilis					
length	10.9	21.1	11.0	19.4	21.4
Phaethontiformes					
Phaethon aethereus					
length	54.8	29.3	16.7	27.5	45.5
Procellariiformes					
Calonectris diomedea					
length	38.3	41.5	25.6	34.3	50.8
Procellaria aequinoctialis					
length	33.5	42.8	29.4	37.8	56.6
Puffinus puffinus					
length	31.1	36.4	28.7	34.9	42.0
Thalassarche chlororhynchos					
length	59.4	55.3	32.5	49.4	67.9
Thalassarche melanophris					
length	53.8	54.7	36.0	48.9	69.1
Suliformes					
Fregata magnificens					
length	47.2	50.3	35.5	40.1	58.0
Nannopterum brasiliensis					
length	43.2	56.2	36.4	51.9	78.1
Sula leucogaster					
length	76.3	78.6	55.9	61.5	99.3
Inopinaves					
Accipitriformes					
Coragyps atratus					
length	41.3	43.3	38.5	42.8	63.5
Cariamiformes					
Cariama cristata					
length	51.1	59.8	47.5	59.4	73.4

Flexor colli lateralis

These are the longest "short muscles" (Table 6), exceeding the caudal limit of the first segment in all analyzed birds (Figures 6 and 9). Although they are superficial, their first third is arranged deeper than the *rectus capitis* muscles (Figures 6 and 9). Their more caudal origins attach laterally to the *tuberculum ansae* and on the lateral crest of the sixth or seventh vertebra (Figure 10). Such attachments, in the same locations, are also present on the fifth and fourth vertebrae (Figure 10). The insertions extend along the costal process of the third vertebra and laterally to the axis and to the atlas centrum and intercentrum (Figure 10).

Comments. Only the more cranial insertion is by a tendon, and the other attachments are made by aponeuroses. These are frequently the longest among the superficial "short muscles", except in *Phaethon aethereus*.

3.2. Hypaxial muscles

Rectus capitis ventralis

This superficial muscle is arranged craniocaudally, ventrally to the other *rectus capitis* (Figures 6, 9 and 12). Unlike those others, the filaments form two distinct bellies, one medial and one lateral, which are easily identified (Figure 12). The origins occur through aponeuroses on the hypapophysis of the more cranial vertebrae of the first segment (Figure 10). Additional attachments are observed ventrolaterally on the axis and atlas, beneath the attachment site of the *rectus capitis lateralis* (Figure 10). Insertions are present on the basioccipital, ventrally to those of the *rectus capitis dorsalis*.

Comments. In Pelecaniformes, Procellariiformes, *Haematopus palliatus*, *Nannopterum brasilianus*, and *Phaethon aethereus*, the more caudal origin of the medial belly is on the fifth vertebra (Figure 10), while in other taxa it is on the fourth vertebra.

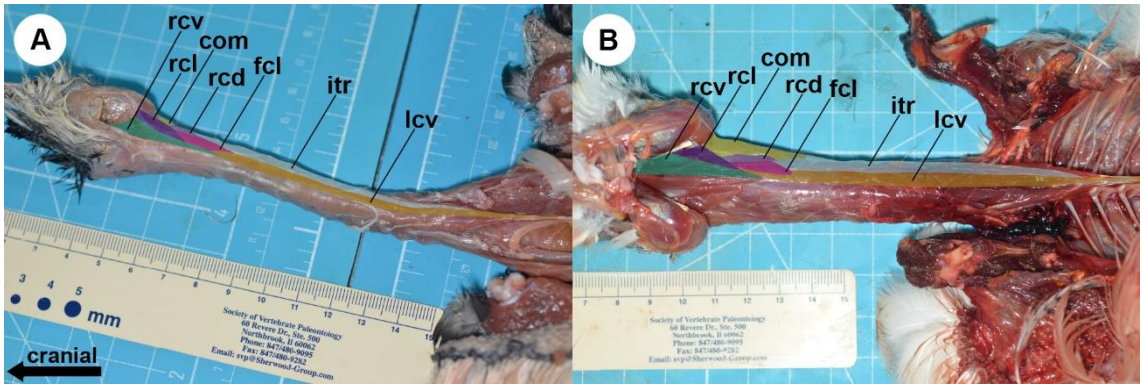

Figure 12. Photographs of the superficial muscles of the neck of *Puffinus puffinus* (A) and *Phaeton aethereus* (B) in ventral view.

Flexor colli medialis

This muscle is arranged deeper and ventrally to the *flexor colli lateralis*, although both have very similar muscle filaments. Its more caudal origins are found on the carotid and costal processes of the cranial vertebrae of the second segment. Along its length, the filaments connect to costal processes and ventrolateral surfaces of the centrum of the first segment vertebrae (Figure 10). The insertions extend on the laterocaudal surface of the long hypapophysis, often of the third vertebra and axis (Figure 10).

Comments. This muscle is as long as the *flexor colli lateralis*, which is usually attached to the same vertebrae, albeit more caudally. The type of attachments varies: as the *flexor colli lateralis*, only the more cranial insertion is by a tendon, and the rest by aponeuroses.

Inclusi

These are narrower and deep muscles, arranged bilaterally to the centrum of the vertebrae (Figures 6 and 7) and totally overlapped by the *intertransversarii* (Figure 7). They originate on the last cervical vertebra, attaching to the middle portion of the costal processes and laterally to the centrum (Figure 10). Attachments such as those are also present in each vertebra of the cervical series (Figure 10). Their insertion is lateral to the centrum of the axis (Figure 10). All attachments are performed by aponeuroses.

Comments. The filaments of these muscles are similar to the deeper portion of the *intertransversarii*, making their identification difficult, especially in Pelecaniformes.

Longus colli ventralis

This is the superficial muscle arranged more ventrally on the cervical series (Figures 6, 9 and 12). Its most caudal origin attaches, through tendons, on the laterocaudal surface of the ventral process of the *notarium*, or of the third or fourth free thoracic vertebrae (Figure 6 and 12). Throughout the cervical series, it presents a complex system of muscular attachments on each vertebra, located laterally to the hypapophysis (commonly in the first and third segment vertebrae) and/or the carotid process (commonly in the second segment vertebrae) (Figure 10). The insertions are established by a thin and long tendon, attached to the axis, ventrally to the insertion of the *flexor colli medialis* (Figure 10).

Comments. Although both cranial and caudal attachments have developed tendons, apparently all other attachments in each vertebra are performed by aponeuroses.

Discussion

Differences in the morphology of the vertebrae between the segments of the cervical series of birds were already expected, as necks are adapted to different types of stress caused by diverse selective pressures (Muller *et al*., 2010). Although we have followed previous works and considered three segments in the neck of Aequorlitornithes,

if we had evaluated them on the basis of vertebral shape or range of motion, there would be more modules (Guinard *et al*., 2010; Terray *et al*., 2020). The inclusion of atlas, axis, and the anterior post-axial cervical vertebrae in a single segment does not exclude the fact that atlas and axis make up an additional functional partition (Dzemski and Christian, 2007; Guinard *et al*., 2010). Vertebrae on the cranial part of the second segment are also different from the subsequent ones by their elongate shape, and were also previously recognized as representing a separate module in birds (Terray *et al*., 2020).

The fifth and ninth cervicals have been recognized as transitional vertebrae between the first and second, and second and third segments, respectively, of the Phorusrhacidae *Andalgalornis steulleti* (Tambussi *et al*., 2012). However, their classification in different modules is not supported in any of the Aequorlitornithes and Inopinaves we studied, based on the vertebral anatomy and/or movement restriction, even in *Cariama cristata*, which, as *Andalgalornis*, also belongs to the Cariamiformes (Alvarenga and Höfling, 2003).

The third segment presents the widest vertebrae we observed, which reflects the predominance of lateral incursions in the range of motion of this part (Dzemski and Christian, 2007). Although the vertebrae are wide, the segment is short, which may be related to the lower need for absorbing tensions generated by dorsoventral flexions (Zusi, 1962).

The heterocoelous *facies articularis* and the orientation of the zygapophyses confer high flexibility in the vertebral joints even without the presence of vertebral discs, as in other Amniota (Taylor and Wedel, 2013). Although most birds analyzed have a significant difference in neck length with or without synovial cartilage between the vertebrae, the proportion of cartilage to bone do not exceed 5.6%, which is fewer than the additional length of cartilage in the neck of mammals, alligators and ostriches (Cobley *et al*., 2013; Taylor and Wedel, 2013). This difference possibly occurs due to the heterocoely of the *facies articularis*, which limits intervertebral space (Baumel and Witmer, 1993; Taylor and Wedel, 2013), and due to the delicacy of the synovial cartilages in the birds we analyzed, which differ from the robust intervertebral discs seen, for instance, in ostriches (Cobley *et al*., 2013).

The thicker synovial cartilage in the *articulatio intercorporalis* than in the *zygapophysialis* is probably related to the greater resistance required by the centrum,

which needs to absorb mechanical shocks between the *facies articularis* during movement (Humphries *et al*., 2007; Liu and El-Rich, 2020). The variation in the thickness of the synovial cartilage present in the *articulatio intercorporalis*, especially between the more caudal cervical vertebrae, affects the center of rotation of the vertebrae and, consequently, analyzes of the range of motion of the neck widely used in fossil species (Jones *et al*., 2021).

The short neural arch, the thinness of the cartilage between the *articulatio intercorporalis*, and the reduced overlapping of zygapophyses indicates a high dorsal flexibility in the second segment of the neck of the birds analyzed (Cobley *et al*., 2013). This allows this segment to be the most vertical of the three, reducing tensions in the third segment, which is the base of the neck (Dzemski and Christian, 2007). The maximum dorsal and ventral flexions of the second and first segments in the Aequorlithornithes, respectively, agree with the usual tensegrity patterns of bird necks, in which the opposite forces complement each other (Furet *et al*., 2018; Fasquelle *et al*., 2019). However, the maximum and minimum flexions discussed here represent the limits of flexibility of the intervertebral joint for each segment, which does not mean that it represents the maximum and minimum mobility performed by a bird in a given movement in life (Jones *et al*., 2021).

The morphology of the muscles we observed agrees with previous descriptions (Kuroda, 1962; Zusi and Storer, 1969; Landolt and Zweers, 1984; Zusi and Bentz, 1984; Vanden-Berge and Zweers, 1993; Tsuihiji, 2005, 2007; Snively and Russel, 2007). The medial and lateral bellies of the *rectus capitis ventralis* have been seen in other Aequorlitornithes and in non-Aequorlitornithes birds (Kuroda, 1962, Zusi and Storer, 1969; Landolt and Zweers, 1984; Vanden-Berge and Zweers, 1993). The *biventer cervicis* muscle arranged bilaterally in the analyzed Aequorlitornithes birds may vary for a single bundle, as seen in *Pygoscelis*, which also belongs to that clade (Kuroda, 1962). The *biventer cervicis* was the only muscle we observed attached to the *notarium* and skull, a characteristic already recognized in the literature for birds (Landolt and Zweers, 1984; Zweers *et al*., 1987; Vanden-Berge and Zweers, 1993), although we also observed it in birds that do not have a *notarium*.

The variation we observed regarding the vertebra where a muscle has its origin has also been reported in other descriptions of the avian neck musculature (Kuroda, 1962;

Zusi and Storer, 1969; Landolt and Zweers, 1984; Tsuihiji, 2005, 2007; Snively and Russel, 2007). It seems to be frequent that muscles with the same length as the neck originate more caudally when more cervicals are present (Zusi and Storer, 1969; Tsuihiji, 2005, 2007; Snively and Russel, 2007). Although this also happens for some short muscles, there are exceptions, such as a more caudal origin of the *rectus capitis ventralis* muscle in *Haematopus palliatus*, a short-necked bird, and more cranial origins of the *complexus* and *splenius capitis* in Pelecaniformes, which are long-necked birds.

Pelecaniformes also stood out for their thinner short muscles, even in *Ardea alba*, which has the longest neck of all analyzed birds. The reduced thickness in the most cranial region of the long muscles contributes to weight reduction in first segment of the neck, which already supports the accumulation of short muscles and the skull (Vanden-Berge and Zweers, 1993; Dzemski and Christian, 2007).

We observed some similarities between Pelecaniformes and *Nannopterum brasilianus*: in both, the ligaments associated to the atlas and axis are ossified; they have a small overlap of the zygapophyses, and lack the *biventer cervicis* muscle. *Anhinga anhinga*, which is phylogenetically close to *Nannopterum brasilianus* (Yuri *et al*., 2013; Prum *et al*., 2015), also lacks the *biventer cervicis* (Boas, 1929). However, this may also be related to similar foraging habits, such as diving and swimming in deeper water (Vidal *et al*., 1986; Sick and Pacheco, 1997; Dzemski and Christian, 2007; Taylor *et al*., 2009; Muller *et al*., 2010), although movements during feeding are probably confined to two or only one segment (Dzemski and Christian, 2007).

The main difference observed between the myology of most Aequorlitornithes and of the two species of Inopinaves we analyzed regards the vertebra in which some muscles originate. In *Cariama cristata*, the *complexus* originates in the fourth vertebra and apparently is also divided into two portions, as in the analyzed Pelecaniformes (Figure 13). *Cariama cristata* is also similar to the Pelecaniformes by the more caudal origin of the *splenius capitis*, which is attached only to the cranial surface of the neural spine of the axis (Figure 13). In contrast, the *complexus* of *Coragyps atratus* has its attachments and morphology similar to that observed in the most Aequorlitornithes. However, its *rectus capitis lateralis* originates in the fourth vertebra, as in Procellariiformes and Pelecaniformes, while that of *Cariama cristata* originates in the third vertebra, as often seen in the Aequorlitornithes (Figure 13).

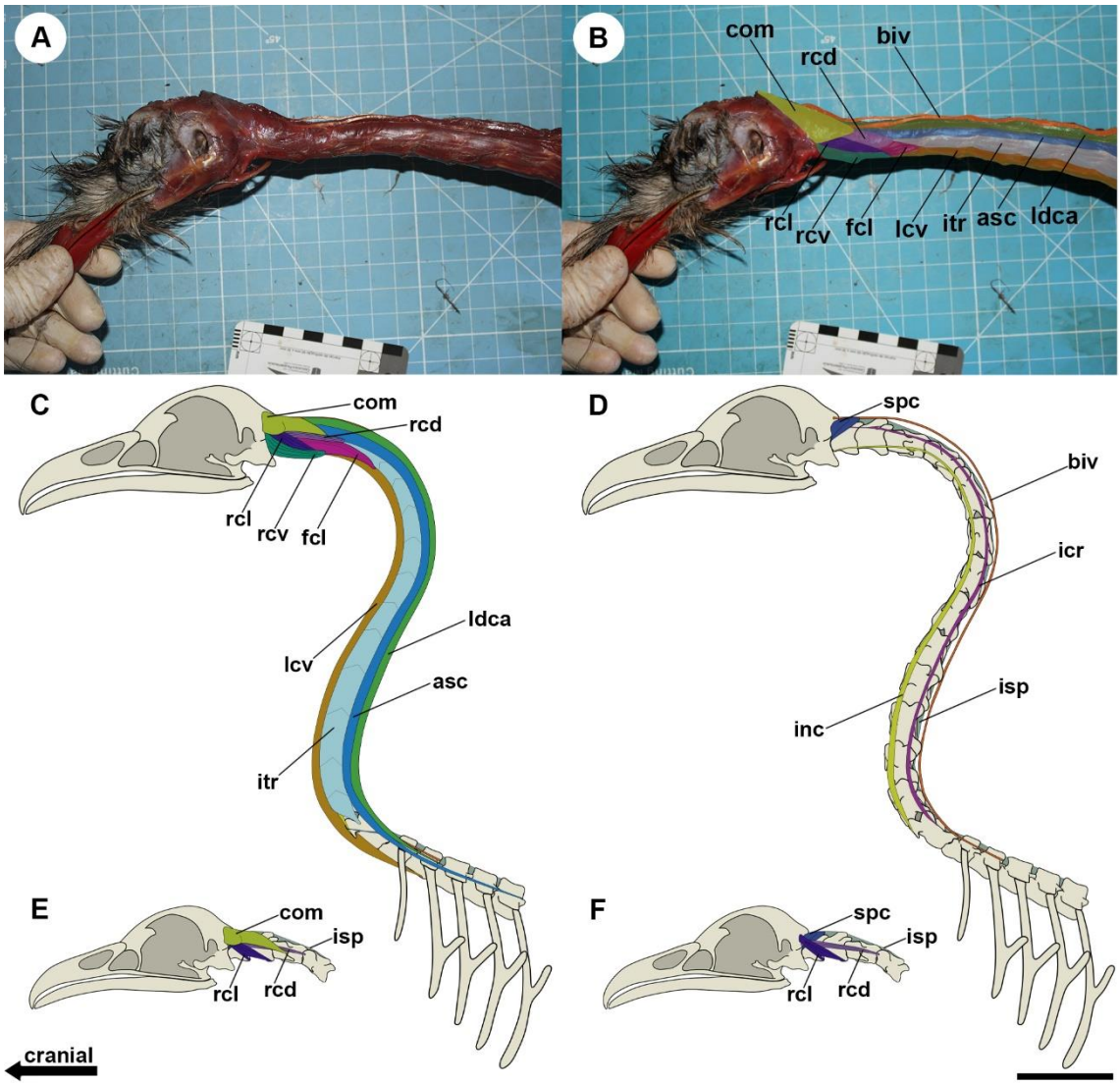

Figure 13. Photographs and interpretation of the superficial muscles of the neck (A, B) and interpretative drawings of the arrangement of the superficial musculature (C), deep musculature (D), origin of the *complexus* muscle (E) and origin of the *splenius capitis* and *rectus capitis dorsalis* and *lateralis* muscles (F) of *Cariama cristata* in left lateral view. Scale bar: 50 mm.

Considering that the cervical anatomy of the Aequorlitornithes may be useful for reconstructing soft tissues of extinct, long-necked piscivorous archosaurs, some considerations are relevant. First, the number of neck vertebrae in the birds dissected varies, unlike what is observed in crocodilians, its phylogenetically closest extant clade (Nesbitt, 2011), which usually have only nine vertebrae (Chamero *et al*., 2014; Iijima & Kubo, 2019). Variation in the number of vertebrae contributes to the establishment of long necks in some birds, although the increase in vertebral length is the main variable in neck length (Marek et al., 2021). Also, variations in muscle thickness along the entire length of the three segments do not reflect a thicker neck in them, but the latter seems to be more directly related to the width of vertebrae in the analyzed birds. The proportion of

thickness equivalent to six times the area of origin of the cervical flexor and extensor muscles and half of this value for the other muscles proved to be reliable to determine the cervical muscle volume of extinct archosaurs, whose reconstructions are limited to the establishment of origin and muscle insertion (Snively and Russell, 2007; Snively et al., 2013). Furthermore, the formula that relates the width of the musculature disposed laterally to the vertebra being equivalent to one third of the total width of any cross-section of the neck has the potential to confirm the full thickness of the cervical arrangement. Lastly, the relationship between the vertebral surface roughness and the presence of an aponeurosis is frequent for mammalian muscle attachment sites (Bryant and Seymour, 1990). However, aponeurotic attachments have also been observed on some smooth surfaces, precluding more precise inferences regarding this relationship in soft tissue reconstructions based on osteology alone (McGowan, 1979, 1986).

The third neck segment of the analyzed birds has synovial cartilage, ligaments and muscles that are thicker than the previous ones. The thickness of the ligaments and musculature in this segment indicates a high mechanical demand, which is supplied by a greater storage of elastic energy in response to ventral flexion by the pronounced *ligamentum elasticum interspinale* and *interlaminare* and the greater muscular force to execute the movement by the volume of the muscles (Gál, 1993; Dzemski and Christian, 2007). The frequent increase in the thickness of the synovial cartilage between the *facies articularis* of the more caudal vertebrae challenges the recognized concept of "neutral position" used in reconstructions of extinct animals, which minimizes the size of the space between the vertebrae by predicting that the cervical soft tissues would be in relaxation with complete pairing of the *facies articularis* and zygapophyses (Stevens and Parrish, 1999). Besides, due to the increase in the thickness of synovial cartilage in the intervertebral joints in the posterior cervical vertebrae, we agree that the partial overlap between the zygapophyses ensures a more accurate reconstruction of the neck (Vidal, 2020).

The partial overlap of the zygapophyses seen when the neck is at relaxed is different from what was established for the neutral position by Stevens and Parrish (1999). However, an overlap <50% during movement has been suggested before for other amniotes (Vidal *et al*., 1986; Stevens and Parrish, 2005; Taylor *et al*., 2009). The presence of a synovial capsule wrapped around the zygapophyses, observed here and in other birds (Baumel & Raikow, 1993), allows them to present very low overlap during the maximum

range of motion. However, we observe that the anatomy of the zygapophyses itself sets a limit for the sliding of facets, as observed for the limit of sagittal flexion for other amniotes (Jones *et al*., 2021). Therefore, predictions made using only disarticulated vertebrae can underestimate the overlap of zygapophyses (Vidal *et al*., 2020). The variation in the overlap of the zygapophyses along the cervical series and the thickness of the synovial joint observed here reflect on the angulation displayed by the vertebrae in different neck segments.

Conclusions

The cervical vertebrae vary anatomically within the three classically established segments and relates to the flexibility of the neck of the birds, which justifies the proposition of more neck modules supported by the vertebral anatomy. The synovial cartilage present between the Aequorlitornithes vertebrae does not represent an increase in the neck length as observed in animals that have intervertebral discs. Although minimally reflected in the length of the neck, the thickness of the intervertebral spaces and the level of overlap of the zygapophyses impact the angulation between vertebrae, due to the position of the center of rotation in the *articulatio intercorporalis*. Such vertebral spaces, as well as the ligaments and muscles of Aequorlitornithes, are thickest in the third segment of the neck, which we hypothesize may be an evolutionary response to biomechanical requirements. Among all the Aequorlitornithes analyzed, Pelecaniformes is the clade that most differs from the others, due to the level of overlap of the zygapophyses, thickness of the intervertebral and muscle spaces and muscle insertion sites.

Aequorlitornithes birds showed well-marked rough areas and scars on the vertebrae that relate to their muscular insertions and joints, which facilitates the recognition of osteological correlates in fossil species. The roughness presented on the surfaces of the vertebrae was mainly, but not exclusively, associated with aponeurotic muscle insertions. The longer intervertebral spaces in the most caudal cervical vertebrae and the partial overlap of zygapophyses while the neck of Aequorlitornithes is relaxed is different from what was established for neutral pose of extinct animals (Stevens & Parrish, 1999). We assumed that the thickness of the cervical muscles is approximately three to six times the area of the muscle origins, which has proved to be a reliable formula to estimate the volume of the neck muscles of Aequorlitornithes birds. Furthermore, the

height and width of the neck are approximately equivalent, and the muscles arranged laterally to the vertebra represent one-third of the width of the cross section, which could confirm cervical thickness in reconstructions of fossil archosaurs that have anatomically similar cervical.

Acknowledgements

We would like to thank the employees of Ipram for providing specimens, place and proper material for dissection, especially scientific supervisor Ralph Vanstreels and veterinarians Allan Santos and Leandro Egert. We would like to make a posthumous acknowledgement to Paula Heloísa Santana Resende, a former masters' student and friend, who accompanied some dissections and photographed some specimens that appear in this manuscript. This study was financed in part by the Coordenação de Aperfeiçoamento de Pessoal de Nível Superior – Brasil (CAPES) – Finance Code 001 (to RB) and by the Conselho Nacional de Desenvolvimento Científico e Tecnológico (CNPq) (grant 421412/2018-6 to TR).

Author contributions

RB – Conceptualization, Investigation, Visualization, Writing – original draft, Writing – review & editing.

TR - Funding acquisition, Project administration, Writing – review & editing

References

Alvarenga, H.M.F and Höfling, E. (2003) Systematic revision of the Phorusrhacidae (Aves: Ralliformes). *Papéis Avulsos de Zoologia, Museu de Zoologia da Universidade de São Paulo*, 43(4), 55–91.

Anchundia, D.J., Anderson, J.F. and Anderson, D.J. (2017) Overland flight by seabirds at Isla Isabela, Galápagos. *Marine Ornithology* 45, 139–141.

Barbraud, C., Johnson, A.R., Bertault, G. (2003) Phenotypic correlates of post-fledging dispersal in a population of greater flamingos: the importance of body condition. *Journal of Animal Ecology* 72, 246–257.

Baumel, J.J. and Raikow, R.J. (1993) Arthrologia. In: Baumel, J.J., King, A.S., Breazile, J.C., Evans, H.E. and Vanden-Berge, J.C. (Eds.) *Handbook of avian anatomy:*

nomina anatomica avium. Cambridge, MA: Cambridge Univertisty Press, pp. 133–187.

Baumel, J.J. and Witmer, L.M. (1993) Osteologia. In: Baumel, J.J., King, A.S., Breazile, J.C., Evans, H.E. and Vanden-Berge, J.C. (Eds.) *Handbook of avian anatomy: nomina anatomica avium*. Cambridge, MA: Cambridge Univertisty Press, pp. 45–132.

Bennett, S.C. (2001). The osteology and functional morphology of the Late Cretaceous pterosaur *Pteranodon* Part I. General description of osteology. *Palaeontographica Abteilung A*, 260, 1–112.

Boas, J.E.V. (1929) Biologisch-anatomische Studien über den Hals der Vögel. Kongl. Danske Vidensk. Selsk. Skrifter, Naturvidensk. *Math*, (Ser. 9) 1, 105–222.

Bryant, H.N. and Seymour, K.L. (1990) Observations and comments on the reliability of muscle reconstruction in fossil vertebrates. *Journal of Morphology*, 206, 109–117.

Chamero, B., Buscalioni, Á.D., Marugan-Lobón, J. and Sarris, I. (2014) 3D geometry and quantitative variation of the cervico-thoracic region in Crocodylia. *Anatomical Record*, 297, 1278–1291.

Cobley, M.J., Rayfield, E.J. and Barrett, P.M. (2013) Inter-Vertebral Flexibility of the Ostrich Neck: Implications for Estimating Sauropod Neck Flexibility. *Plos One*, 8(8), e72187.

Dzemski, G. and Christian, A. (2007) Flexibility along the neck of the ostrich (*Struthio camelus*) and consequences for the reconstruction of dinosaurs with extreme neck length. *Journal of Morphology*, 268, 701–714.

Fasquelle, B., Furet, M., Chevallereau, C. and Wenger, P. (2019) Dynamic modeling and control of a tensegrity manipulator mimicking a bird neck. *Mechanisms and Machine Science*, 73, 2087–2097.

Furet, M., van Riesen, A., Chevallereau, C. and Wenger, P. (2018) Optimal design of tensegrity mechanisms used in a bird neck model. *Mechanisms and Machine Science*, 59, 365–375.

Gál, J.M. (1993) Mammalian spinal biomechanics 2: intervertebral lesion experiments and mechanisms of bending resistance. *Journal of Experimental Biology*, 174, 281–297.

Guinard, G., Marchand, D., Courant, F., Gauthier-Clerc, M. and Le Bohec, C. (2010) Morphology, ontogenesis and mechanics of cervical vertebrae in four species of penguins (Aves: Sphenicidae). *Polar Biology*, 33, 807–822.

Humphries, S., Bosner, R.H.C., Witton, M.P. and Martill, D.M. (2007) "Did pterosaurs feed by skimming? Physical modelling and anatomical evaluation of an unsual feeding method". *Plos Biology*, 5, 1647–1655.

Iijima, M. and Kubo, T. (2019) Comparative morphology of presacral vertebrae in extant crocodylians: taxonomic, functional and ecological implications. *Zoological Journal of the Linnean Society*, 186, 1006–1025.

Jones, K.E., Brocklehurst, R.J. and Pierce S.E. (2021) AutoBend: An automated approach for estimating intervertebral joint function from bone-only digital models. *Integrative Organismal Biology*, 3, obab026.

Kellner, A.W.A. and Campos, D.A. (2002) The function of the cranial crest and jaw of a unique pterosaur from the Early Cretaceous of Brazil. *Science*, 297, 389–392.

Kuroda, N. (1962) On the cervical muscles of birds. *Journal of the Yamashina Institute for Ornithology*, 3, 189–211.

Kuroda, N. (1991) Distributional Patterns and seasonal movements of Procellariiformes in the North Pacific. *Journal Yamashina Institute for Ornithology*, 23, 23–84.

Landolt, R. and Zweers, G.A. (1984). Anatomy of the muscle-bone apparatus of the cervical system in the Mallard (*Anas platyrhynchus* L.). *Netherlands Journal of Zoology*, 35, 611–670.

Liu, T. and El-Rich, M. (2020) Effects of nucleus pulposus location on spinal loads and joint centers of rotation and reaction during forward flexion: a combined finite element and musculoskeletal study. *Journal of Biomechanics*, 104, 109740.

Marek, R.D., Falkingham, P.L., Benson, R.B.J, et al. (2021) Evolutionary versatility of the avian neck. *Proceedings Royale Society B*, 288, 20203150.

McGowan, C. (1979) The hind limb musculature of the Brown kiwi, *Apteryx australis mantelli*. *Journal of Morphology*, 160, 33–74.

McGowan, C. (1986) The wing musculature of the Weka (*Gallirallus australis*), a flightless rail endemic to New Zealand. *Journal of Zoological Society of London*, 210, 305–346.

Muller, J., Scheyer, T.M., Head, J.J., et al. (2010) Homeotic effects, somitogenesis and the evolution of vertebral numbers in recent and fossil amniotes. *Proceedings of the National Academy of Sciences*, 107(5), 2118–2123.

Nesbitt, S.J. (2011) The early evolution of archosaurs: relationships and the origins of major clades. *Bulletin of the American Museum of Natural History*, 352, 1–292.

Prince, P.A., Wood, A.G., Barton, T., Croxall, J.P. (1992) Satellite tracking of wandering albatrosses (Diomedea exulans) in the South Atlantic. *Antarctic Science*, 4(1), 31–36.

Prum, R.O., Berv, J.S., Dornburg, A., et al. (2015) A comprehensive phylogeny of birds (Aves) using targeted next-generation DNA sequencing. *Nature*, 526, 569–573.

Schreiber, E.A. and Burger, J. (2001) *Biology of Marine Birds*. Boca Raton, FL: CRC Press, pp. 722.

Sick, H. and Pacheco, J.F. (1997) *Ornitologia Brasileira* vol 1. Rio de janeiro, RJ: Editora Nova Fronteira.

Snively, E. and Russell, A.P. (2007) Functional morphology of neck musculature in the Tyrannosauridae (Dinosauria, Theropoda) as determined via a hierarchical inferential approach. *Zoological Journal of the Linnean Society*, 151, 759–808.

Snively, E., Cotton, J.R., Ridgely, R., Witmer L.M. (2013). Multibody dynamics model of head and neck function in Allosaurs (Dinosauria, Theropoda). Palaeontologia Electronica, 16, 11A, 29p.

Stevens, K.A. and Parrish, J.M. (1999) Neck posture and feeding habits of two Jurassic sauropod dinosaurs. *Science*, 284, 798–800.

Stevens, K.A. and Parrish, J.M. (2005) Digital reconstructions of sauropod dinosaurs and implications for feeding. In: Curry Rogers K.A. and Wilson J.A. (Eds.) *The Sauropods: Evolution and Paleobiology*. Berkeley, CA: University of California Press, pp. 178–200.

Tambussi, C.P., de Mendoza, R., Degrange, F.J. and Picasso, M.B. (2012) Flexibility along the Neck of the Neogene Terror Bird *Andalgalornis steulleti* (Aves Phorusrhacidae). *Plos One*, 7(5), e37701.

Taylor, M.P., Wedel, M.J. and Naish, D. (2009) Head and neck posture in sauropod dinosaurs inferred from extant animals. *Acta Palaeontologica Polonica*, 54(2), 213–220.

Taylor, M.P. and Wedel, M.J. (2013) The Effect of Intervertebral Cartilage on Neutral Posture and Range of Motion in the Necks of Sauropod Dinosaurs. *Plos One*, 8(10), e78214.

Terray, L., Plateau, O., Abourachid, A., et al. (2020) Modularity of the neck in birds (Aves). *Evolutionary Biology*, Doi: 10.1007/s11692-020-09495-w.

Tsuihiji, T. (2005) Homologies of the *transversospinalis* muscles in the anterior presacral region of Sauria (crown Diapsida). *Journal of Morphology*, 263, 151–178.

Tsuihiji, T. (2007) Homologies of the *longissimus*, *iliocostalis*, and hypaxial muscles in the anterior presacral region of extant diapsida. *Journal of Morphology*, 268, 986–1020.

Vanden-Berge, J.C. and Zweers, G.A. (1993) Myologia In: Baumel, J.J., King, A.S., Breazile, J.C., Evans, H.E. and Vanden-Berge, J.C. (Eds.) *Handbook of avian anatomy: nomina anatomica avium*. Cambridge, MA: Cambridge Univertisty Press, pp. 189–247.

Vidal, D., Mocho, P., Páramo, A., Sanz, J.L. and Ortega, F. (2020) Ontogenetic similarities between giraffe and sauropod neck osteological mobility. *Plos One*, 15(1), e0227537.

Vidal, P.P., Graf, W. and Berthoz, A. (1986) The orientation of the cervical vertebral column in unrestrained awake animals. *Experimental Brain Research*, 61, 549–559.

Wendeln, H. and Becker, P.H. (1996) Body mass change in breeding common terns *Sterna hirundo*. *Bird Study*, 43, 85–95.

Witmer, L.M. (1995) The Extant Phylogenetic Bracket and the importance of reconstructing soft tissues in fossils. In: Thomason J.J. (Ed) *Functional morphology in vertebrate palaeontology*. Cambridge: Cambridge University Press, pp. 19–33

Yuri T, Kimball RT, Harshman J, et al. (2013) Parsimony and model-based analyses of indels in avian nuclear genes reveal congruent and incongruent phylogenetic signals. *Biology*, 2, 419–444.

Zusi, R.L. (1962) Structural adaptations of the head and neck in the Black Skimmer, *Rynchops nigra* Linnaeus. *Publications of the Nuttal Ornithological Club*, 3, 1–153.

Zusi, R.L. and Bentz, G.D. (1984) Myology of the purple-throated carib (*Eulampis jugularis*) and other hummingbirds (Aves: Trochilidae). *Smithsonian Contributions to Zoology*, 385, 1–70.

Zusi, R.L. and Storer, R.W. (1969) Osteology and myology of the head and neck of the pied-billed grebes (*Podilymbus*). In: *Publications of the Museum of Zoology* vol 139: University of Michigan, 49 pp.

Zweers, G.A., Vanden-Berge, J.C. and Koppendraier, R. (1987) Avian cranio-cervical systems. Part I: Anatomy of the cervical column in the chicken (*Gallus gallus* L.). *Acta Morphologica Neerlando-scandinavica*, 25, 131–155.

Zweers, G.A., Bout, R., Heidweiller J. (1994) Motor organization of avian head-neck system. In: David, M., Green, P. (Eds.) *Perception and motor control in birds*. Berlin: Springer-Verlag, pp. 201–221.

Chapter II

Reconstruction of the soft tissues of the pterosaur neck and their implications for the cervical position at rest

Richard Buchmann[1], Taissa Rodrigues[1]

[1] Laboratório de Paleontologia, Departamento de Ciências Biológicas, Centro de Ciências Humanas e Naturais, Universidade Federal do Espírito Santo, Vitória, ES, 29075-910, Brazil.

Abstract

The lack of any pterosaur living descendants creates gaps in the knowledge of the biology of this group, including its biomechanics, which makes it difficult to understand their posture and life habits. To mitigate part of this issue, we aimed to reconstruct the cervical osteology and arthrology of three pterosaur genera, which allowed us to make more assertive inferences about the position of the neck of these animals at rest. We used CT scans of the cervical series of the pterosaurs *Anhanguera piscator*, *Azhdarcho lancicollis* and *Rhamphorhynchus muensteri* for the reconstructions, species representative of different pterosaur clades and for which there are known three-dimensionally preserved cervical series. For the recognition of ligaments, cartilages in joints, and levels of overlapping of the zygapophyses, we used the Extant Phylogenetic Bracket method, based on extant birds and *Caiman latirostris*. We infer that the pterosaur intervertebral joint was probably covered by a thin layer of synovial cartilage whose thickness possibly varied along the neck, being thicker in the posterior region. Ignoring this cartilage can distort the reconstructions of pterosaur necks. According to the angulation of the cervical vertebrae, the pterosaur neck could be slightly sinuous when in rest position. Most of the ligaments extended along the neck and were likely more robust in the base, near the shoulder.

Key words: cervical biomechanics, cervical vertebrae, cervical ligaments, Pterosauria, Archosauria.

Introduction

Pterosaurs and birds have several converging characteristics, such as the presence of pneumatic bones, a well-developed sternum and the fusion of some bones, which allows extrapolating functions from avian structures to those of pterosaurs (Bennett, 2001; Kellner & Campos, 2002; O'Connor, 2006; Butler et al., 2012). These hypothetical extrapolations can be tested through biomechanical studies (Rayfield, 2007; Lautenschlager, 2017). An understudied topic in pterosaur biology is the functional anatomy of the neck, despite the importance of cervical position in their biology and behavior (Witton & Naish, 2008; Averianov 2013; Naish & Witton, 2017).

In birds, the neck is divided into three functional segments, in which the first and second more cranial ones present greater freedom of movement in all axes (Boas, 1929; Zusi, 1962). The distinct vertebral morphology also allows the pterosaur neck to be classified into three anatomical segments, of which the atlas and axis represent the more cranial segment, with specialized vertebrae for articulation with the skull, mid-cervical vertebrae (i.e., from the third to the seventh cervical vertebrae) constitute the second segment and occupy the middle of the neck, and two posterior cervical vertebrae at the caudal end are the third segment.

However, so far, little has been investigated about the biomechanics of the pterosaur neck segments, despite the reasonably common preservation of vertebral elements (Bennett, 2001; Kellner & Tomida, 2000; Averianov, 2010; Vila Nova et al., 2015). Furthermore, little is known about neck arthrology, even though it influences the cervical angulation and degree of freedom of movement of the neck in archosaurs (Tsuihiji, 2004; Tambussi et al., 2012; Taylor & Wedel, 2013). Thus, the present study aims to reconstruct the cervical arthrology and to infer the position of the pterosaur neck at rest, which could support more assertive proposals regarding cervical movements during locomotion and foraging.

Material and methods

We analyzed the cervical vertebral column of the holotype of *Anhanguera piscator* (NSM-PV 19892) (Kellner & Tomida, 2000), which comes from the Lower Cretaceous Romualdo Formation in the Santana Group (Araripe Basin, Brazil) and is housed in the collection of the National Museum of Nature and Science, in Tsukuba, Japan; of specimens attributed to *Azhdarcho lancicollis* (ZIN PH, several specimens; and

CCMGE 1/11915) (Averianov, 2010), from the Upper Cretaceous Bissekty Formation at Dzharakuduk, Uzbekistan and housed in the Paleoherpetological collection of the Zoological Institute of the Russian Academy of Sciences (ZIN PH) and Chernyshev's Central Museum of Geological Exploration (CCMGE), both in Saint Petersburg, Russia; and a specimen attributed to *Rhamphorhynchus muensteri* (MGUH 1891.738) (Bonde & Christiansen, 2003) from the Upper Jurassic Solnhofen limestones of southern Germany and housed in the Geological Museum/Natural History Museum of Denmark, Copenhagen, Denmark. The choice of the specimens is justified by the excellent three-dimensional preservation of almost all cervical vertebrae.

Computed tomography (CT) scans of the *Anhanguera piscator* holotype were scanned at 300 to 310 kV and 200 μA, with different voxel sizes for different scans (listed in Table 1). The complete plate containing *Rhamphorhynchus muensteri* (MGUH 1891.738) was scanned at 120 kV and 280 μA, and the voxel sizes were 0.2 mm. The CT scans of the cervical vertebrae and *notarium* of *Azhdarcho lancicollis* (ZIN PH; several specimens) were given to this research but the scan data were unavailable.

Table 7. Voxel sizes for different scans of the *Anhanguera piscator* holotype.

Element	Voxel size (mm)
Skull	0.198
Atlas + axis and cervical III	0.065
Cervical IV	0.075
Cervical V	0.175
Cervical VII	0.166
Cervical VIII	0.166
Cervical IX	0.166
Dorsal I	0.166

The osteological reconstructions of the damaged parts of the vertebrae and the inclusion of the soft tissues were performed using the Blender 3D software, version 2.91 (Blender Development Team, 2019). The vertebrae of *Rhamphorhynchus muensteri* are attached to a slab that displays the cervical series in ventral view on the main surface of the slab and the neural spines on the opposite surface (Figure 1). The vertebrae were digitally isolated from the matrix and reconstructed based on previously published photographs and drawings of the cervical vertebrae of other specimens of this species (Wellnhofer, 1975). The cervical vertebrae of *Anhanguera piscator* were already extracted from the rock before scanning, but as its sixth vertebra was not preserved, we reconstructed it using as a basis the dimensions of the sixth vertebra of AMNH 22555, belonging to *Anhanguera* sp. (Wellnhofer, 1991; Pinheiro & Rodrigues, 2017), due to the similarity of their other preserved vertebrae. We had to make more inferences for the osteological reconstruction of the cervical vertebral series of *Azhdarcho lancicollis*, due to the lack of completely preserved specimens. The well-defined regionalization in the cervical vertebrae of *Anhanguera piscator*, *Rhamphorhynchus muensteri* and other pterosaurs, including other azhdarchids (Bennett, 2001; Pereda-Suberbiola et al. 2003; Kellner, 2010), indicates that *Azhdarcho lancicollis* probably also had mid-cervical and posterior cervical vertebrae with distinct morphologies. The differences are noticeable in their lengths, which are very long in mid-cervical vertebrae.

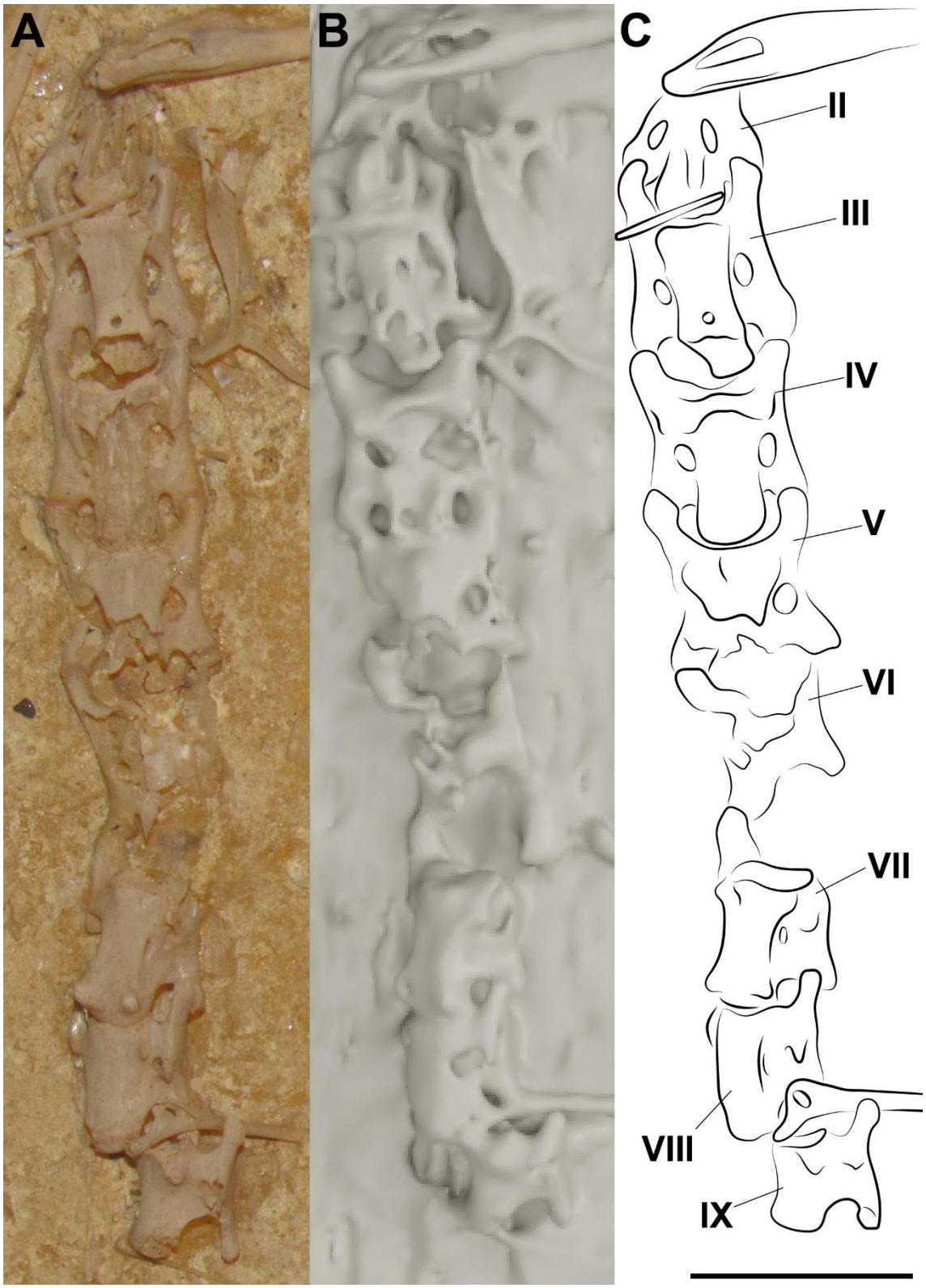

Figure 14. Photograph (A), CT scan (B), and interpretative drawing (C) of the cervical series of the specimen MGUH 1891.738, attributed to *Rhamphorhynchus muensteri*, in ventral view. Scale bar: 10 mm.

The measures of length, height and width of the vertebrae of *Anhanguera piscator* and *Rhamphorhynchus muensteri* were taken first-hand with a caliper. The same measurements for *Azharcho lancicollis* were taken from Averianov (2010) or measured in the MeshLab software, version 2021.10 (Cignoni et al., 2008). We used the nomenclature by Baumel & Witmer (1993) for the osteological and arthrological description.

The inferences regarding cervical arthrology and the level of overlapping of the zygapophyses made here were supported by the criteria of the Extant Phylogenetic Bracket (EPB) (Witmer, 1995). To support the EPB we used data obtained first-hand, by dissecting several extant birds (species listed in the previous chapter) and an alligator (*Caiman latirostris*). The dissected avian specimens died or were euthanized at the Institute for the Research and Rehabilitation of Marine Animals (IPRAM), in Cariacica/ES, Brazil, which is responsible for the rehabilitation of marine animals under the following authorizations: SISFAUNA IEMA 001/2014, process 68077610; IEMA 001/2014, process 67277780; and SISBIO 34510 and 26896. The alligator was euthanized at the Caiman Project headquarters (under the coordination of the Marcos Daniel Institute, a non-profit organization), in Vitória/ES, Brazil (under the authorization: SISBIO 92997549)., and dissected at the Universidade Federal do Espírito Santo's Veterinary Hospital, in Alegre/ES, Brazil. The angles between the vertebrae were also measured in Blender 3D software, version 2.91 (Blender Development Team, 2019), and were obtained by the position of the vertebral axis in relation to the axis of its anterior vertebra (Figure 2). The distance between the condyle and the cotyle of the next vertebra was measured in the central and peripheral regions of this joint (Figure 2). The area of the zygapophyses was measured only in the vertebrae belonging to *Anhanguera piscator* and *Azhdarcho lancicollis*, due to the vertebrae of *Rhamphorhynchus muensteri* being preserved articulated. Both these measurements were obtained using the ImageJ software (Schneider et al., 2012).

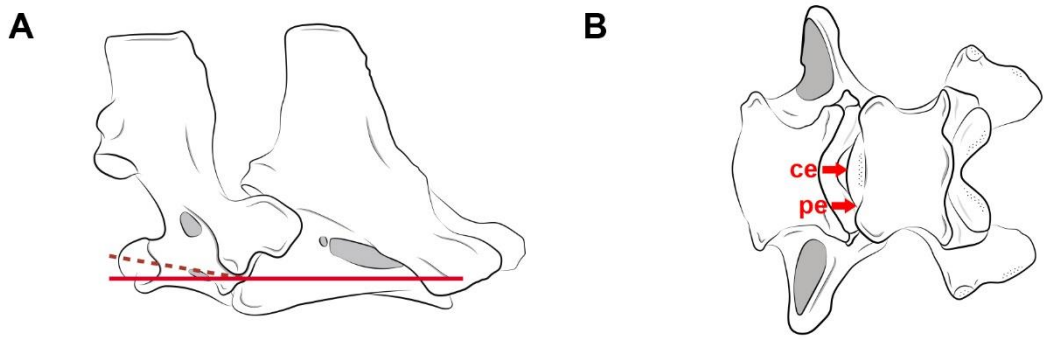

Figure 15. Drawings showing the method of measuring the angles (A) and distance (B) between the analyzed vertebrae. The continuous red line represents the axis of the vertebral condyle and the dashed red line represents the axis of the condyle of the next vertebra. Abbreviations: ce, distance between condyle and cotyle in the central portion of the joint; pe, distance between condyle and cotyle in the peripheral portion of the joint.

The partial articulation between the zygapophyses indicates the presence of gaps between the condyle and the cotyle of the adjacent cervical vertebra, which would be filled by synovial cartilage, annular ligaments and fluid (Baumel & Raikow, 1993; Taylor & Wedel, 2013). The increase in cervical length due to the presence of vertebral cartilage was calculated by subtracting the total length of the articulated vertebrae with partial overlapping zygapophyses and the sum of the lengths of all cervical vertebrae and per neck segment (Taylor & Wedel, 2013).

Although the atlas and axis of *Rhamphorhynchus muensteri* are not fused as in the other analyzed pterosaurs, we disregarded the span length in this joint because, due to the absence of zygapophyses and restriction of movement between these vertebrae, the addition of cartilage would be irrelevant for the neutral pose analysis and to the degree of freedom to which the neck would be subject.

Anatomical abbreviations

ac, *ansa costotransversaria*; arc, articular capsule; co, cotyle; con, condyle; ep, epipophysis; fopn, pneumatic foramen; fov, fovea; hyp, hypapophysis; lcol, *ligamentum collaterale*; lilm, *ligamentum elasticum interlaminare*; lisp, *ligamentum elasticum interspinale*; lnuc, *ligamentum nuchae*; nc, neural canal; ns, neural spine; poex, postexapophysis; poz, postzygapophysis; prex, preexapophysis; prz, prezygapophysis; ro, roughness; syn, synovial cartilage; tpr, transverse process.

Reconstruction of the pterosaur neck

All analyzed vertebrae of *Azhdarcho lancicollis* have prominent hypapophysis and postexapophyses preserved, with the exception of the seventh, which does not have a well-preserved centrum. The neural spines of the mid-cervical vertebrae of this species are known by fragmented parts, mainly from the third and seventh vertebrae (ZIN PH 131/44; ZIN PH 138/44). We observed that these neural spines are highest at the cranial and caudal ends of the fourth, fifth, and sixth vertebrae (ZIN PH 144/44; CCMGE 1/11915, ZIN PH 139/44; ZIN PH 147/44), with the middle part of these vertebrae having a low spine and thus a cylindrical appearance. The seventh vertebra (ZIN PH 138/44) does not have a preserved neural spine but the latero-dorsal laminae of the neural arch are directed towards the mid-dorsal surface along the entire vertebral length, giving the neural arch a triangular cross-section, different from the more cranial vertebrae. This architecture indicates the presence of a neural spine of uniform height along the seventh vertebra of this pterosaur (Figure 3), but the dimensions presented by the neural arch are not consistent with the presence of a tall neural spine, and it apparently does not exceed the maximum height of the neural spine of the sixth vertebra (ZIN PH 147/44).

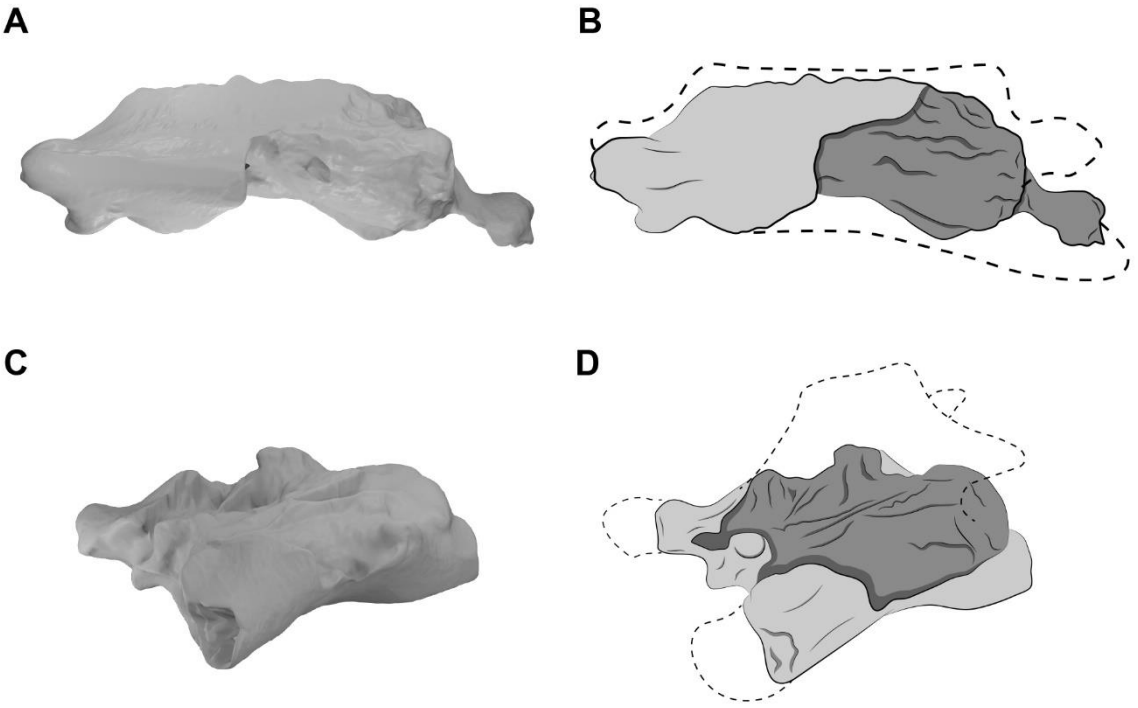

Figure 16. CT scans and interpretative drawings of the seventh vertebra (A, B) in left lateral view and the eighth vertebra (C, D) in left dorsolateral view (ZIN PH 138/44 and ZIN PH 137/44, respectively) of *Azhdarcho lancicollis*. Dashed line indicates reconstructed regions.

The posterior cervical vertebrae of *Azhdarcho lancicollis* are less preserved than the others. The eighth vertebra (ZIN PH 137/44) has a short centrum and a neural arch

whose dorsal region is completely lost (Figure 3C). In addition to a fragmented centrum of reduced craniocaudal length, the ninth vertebra (ZIN PH 122/44) still has part of its vertically projected neural arch preserved, suggesting a tall neural spine. We thus interpret that the neural spines of both posterior cervical vertebrae of this pterosaur are taller than those of the mid-cervicals (Figure 3D). This morphology is similar to that of the dorsal vertebrae, and is also observed in the posterior cervical vertebrae of *Anhanguera piscator* and *Rhamphorhynchus muensteri* (Figure 4E, F).

The cervical vertebrae of the three analyzed pterosaurs are procoelous and exhibit an extremely convex condyle (Figure 4). The presence of synovial cartilage in the joints is suggested by the roughness, mainly on the margins, of the articular surfaces of the zygapophyses, cotyle and condyle of the pterosaurs (Figure 4). There is also a discreet dorsomedial fovea in the condyle, which is more robust in the posterior cervical vertebrae (Figure 4).

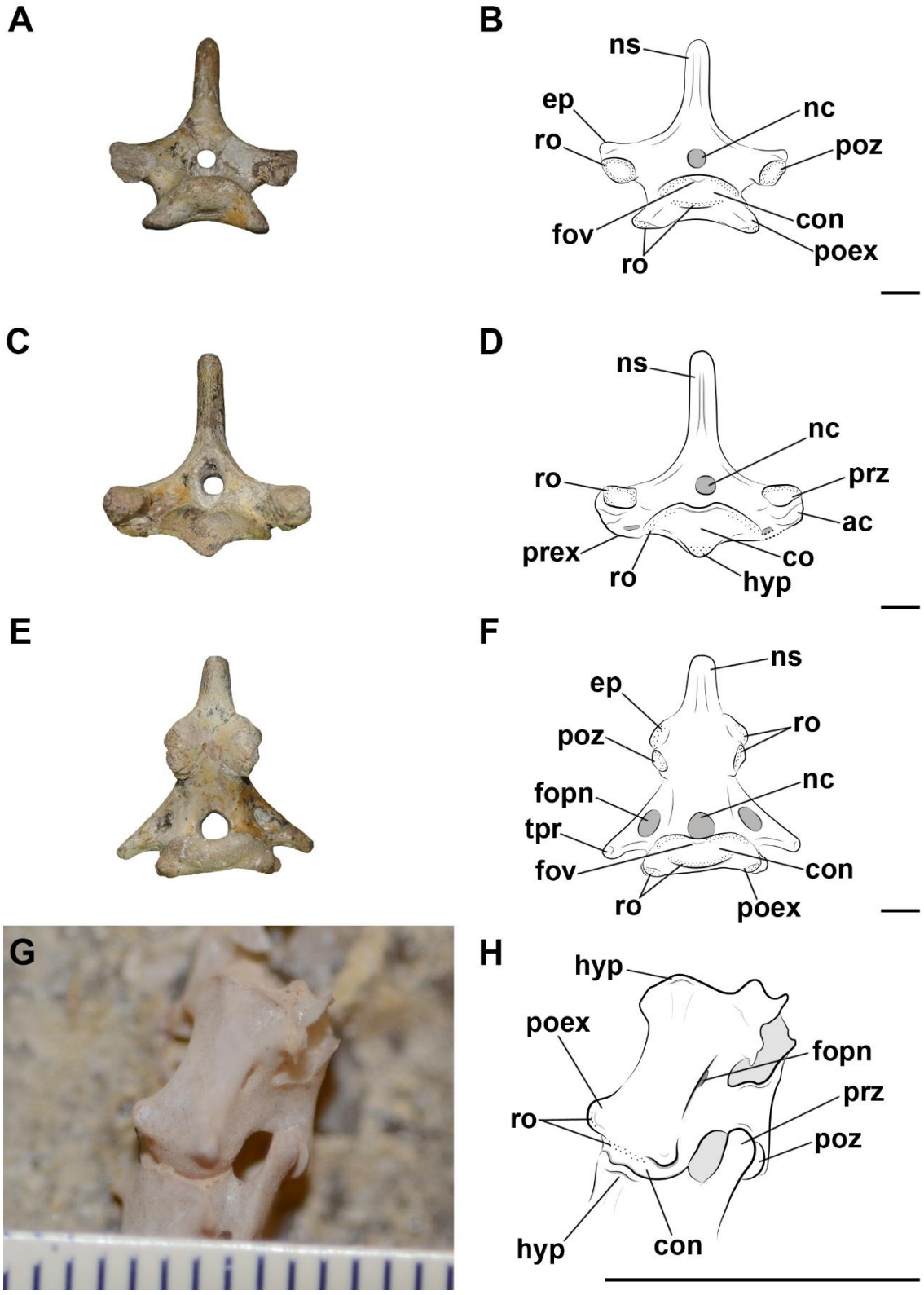

Figure 17. Photographs and interpretative drawings of the fourth vertebra (A, B) in caudal view, fifth vertebra (C, D) in cranial view and eighth vertebra (E, F) in caudal view of *Anhanguera piscator* (NSM-PV 19892) and the articulated seventh and eighth vertebrae (G, H) in ventrolateral view of *Rhamphorhynchus muensteri* (MGUH 1891.738). Dashed line indicates reconstructed regions. Dotted regions indicate greater surface roughness. Scale bar: 10 mm.

Although the atlas-axis and the third vertebra are still articulated in the *Anhanguera piscator* holotype, we cannot be sure that the angle and distance between them, as preserved, are similar to the position of the neck at rest.

The partial overlapping of the zygapophyses we calculated as approximately 50% for the joints between the axis and the mid-cervical vertebrae and approximately 75% for the joints in the posterior cervical vertebrae is similar to the arrangement observed for the position of the neck at rest in extant birds. This amount of overlapping of the zygapophyses and the anatomical differentiation of the pterosaur vertebrae allow inferences regarding the possible sinuosity of the neck. The short postzygapophyses and the less convex condyle of the third vertebra compared to the other mid-cervical vertebrae of pterosaurs indicate that this vertebra was articulated orienting itself more ventrally in relation to the axis, as is also the orientation of the fourth cervical in relation to the third vertebra (Table 2). This arrangement suggests a downward curvature in relation to the atlas and axis (Figure 5).

Table 8. Angles of inclination and distance (from the central and peripheral region) of the condyle and cotyle between a vertebra and its succeeding one on the neck of pterosaurs at rest. (+) above and (-) below the axis of succeeding vertebra. Abbreviations: ATAX, atlas and axis; CV, cervical vertebra; DV, dorsal vertebra. Roman algorisms indicate each vertebra's position.

	Angle	**Central distance (mm)**	**Peripheral distance (mm)**
Anhanguera piscator			
ATAX – CV **III**	-22°	2.02	2.47
CV **III –** CV **IV**	-6°	1.98	2.48
CV **IV –** CV **V**	+7°	2.15	2.22
CV **V –** CV **VI**	+6°	2.04	2.62
CV **VI –** CV **VII**	+19°	3.33	3.94
CV **VII –** CV **VIII**	+10°	3.67	4.62

CV **VIII** – CV **IX**	-6°	4.49	4.76
CV **IX** – DV **I**	-10°	5.24	5.64
Azhdarcho lancicollis			
ATAX – CV **III**	-46°	0.79	1.67
CV **III** – CV **IV**	-14°	0.95	1.28
CV **IV** – CV **V**	+12°	0.98	1.31
CV **V** – CV **VI**	+16°	1.04	1.25
CV **VI** – CV **VII**	+5°	1.33	1.78
CV **VII** – CV **VIII**	+7°	2.2	2.59
CV **VIII** – CV **IX**	+20°	2.46	2.62
CV **IX** – DV **I**	-19°	2.14	2.25
Rhamphorhynchus muensteri			
ATAX – CV **III**	-17°	0.11	0.13
CV **III** – CV **IV**	-2°	0.08	0.11
CV **IV** – CV **V**	+2°	0.10	0.11
CV **V** – CV **VI**	+6°	0.29	0.32
CV **VI** – CV **VII**	+12°	0.32	0.36
CV **VII** – CV **VIII**	-4°	0.38	0.48
CV **VIII** – CV **IX**	+3°	0.42	0.44
CV **IX** – DV **I**	+6°	0.43	0.49

The largest angle found was always in the most cranial joint of the neck of the analyzed pterosaurs. The more ventral orientation of the third vertebra relative to the axis

and of the fourth vertebra relative to the third indicates that this region was slightly ventrally arcuate up to the fourth vertebra (Table 2). The articulated series of the mid-cervical vertebrae (i.e., post-fourth vertebra) is arched in the opposite orientation to that observed between the axis and the fourth vertebra, which conferred sinuosity to the necks of the analyzed pterosaurs (Figure 4). In *Anhanguera piscator* and *Rhamphorhynchus muensteri*, the second largest angle between the neck joints is found between the sixth and seventh cervicals (Table 2). In *Azhdarcho lancicollis*, the largest angle between the mid-cervical vertebrae is seen more cranially, between the fifth and sixth vertebrae. The angle observed between the joints and lengths of the fourth to sixth vertebrae and those observed at the base of the neck of *Azhdarcho lancicollis* makes its neck more vertical than that of the analyzed others (Figure 5).

The cervical series is straighter in the posterior segment of the neck of all analyzed pterosaurs, based on the orientations of the joints between consecutive vertebrae (Table 2). The difference between the mid and posterior regions of the neck was also due to the longer prezygapophyses and the more convex condyle of the mid-cervical vertebrae compared to the posterior cervical vertebrae.

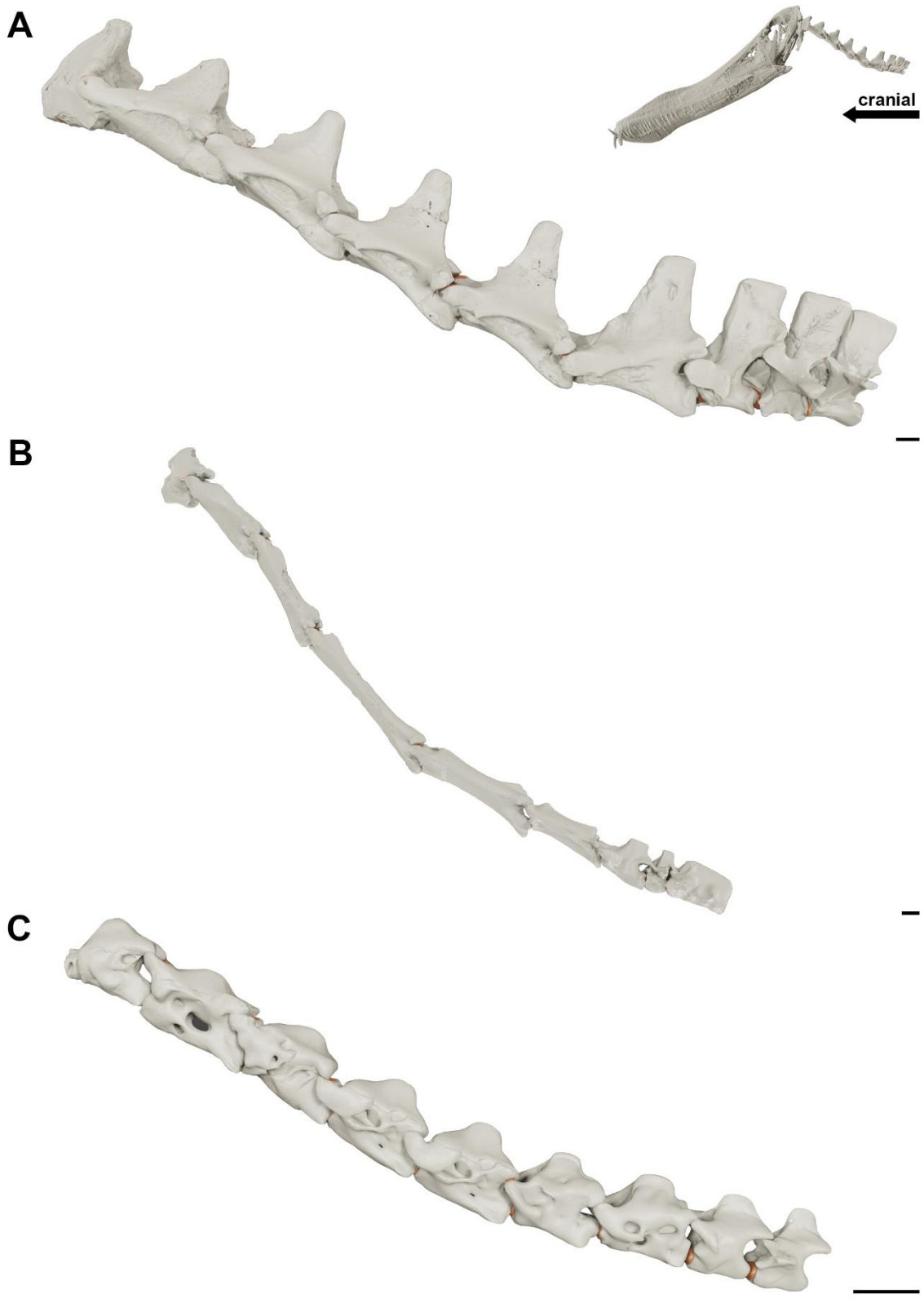

Figure 18. Reconstruction of the position at rest of the cervical vertebral column of *Anhanguera piscator* (A), *Azhdarcho lancicollis* (B) and *Rhamphorhynchus muensteri* (C) in left lateral view. Inset on the upper right corner shows a reconstructed *Anhanguera piscator* skull and neck. The intervertebral cartilage and cartilage of the zygapophyseal joints are shown in light brown. Scale bars: 10 mm.

In all analyzed pterosaurs, the prezygapophyses of the cervical vertebrae have their facets turned dorsally and slightly cranially, and oriented towards the medial side,

while the opposite is observed in the postzygapophyses, whose facets are pointed ventrally, slightly caudally and turned laterally to the vertebrae. This allows the zygapophyses, partially superimposed in rest position, to slide their cartilage on top of each other in all directions, though limited by an articular capsule, with friction reduced by the synovial fluid (Figure 6). The only exception to this orientation of the articular facets are the postzygapophyses of the axis, which are entirely turned ventrally, especially in *Azhdarcho lancicollis*, demonstrating that the movement in the articulation with the prezygapophyses of the third vertebra is possibly more horizontal, thus differing from the other cervicals, which are likely to slip slightly diagonally. Besides the orientation, we observed that the area of the facets of the zygapophyses seems to be larger in the middle portion of the neck. Considering the different species, the zygapophyses of *Azhdarcho lancicollis* are slightly wider, increasing in the craniocaudal distance they can slide over each other and possibly impacting the neck's range of motion.

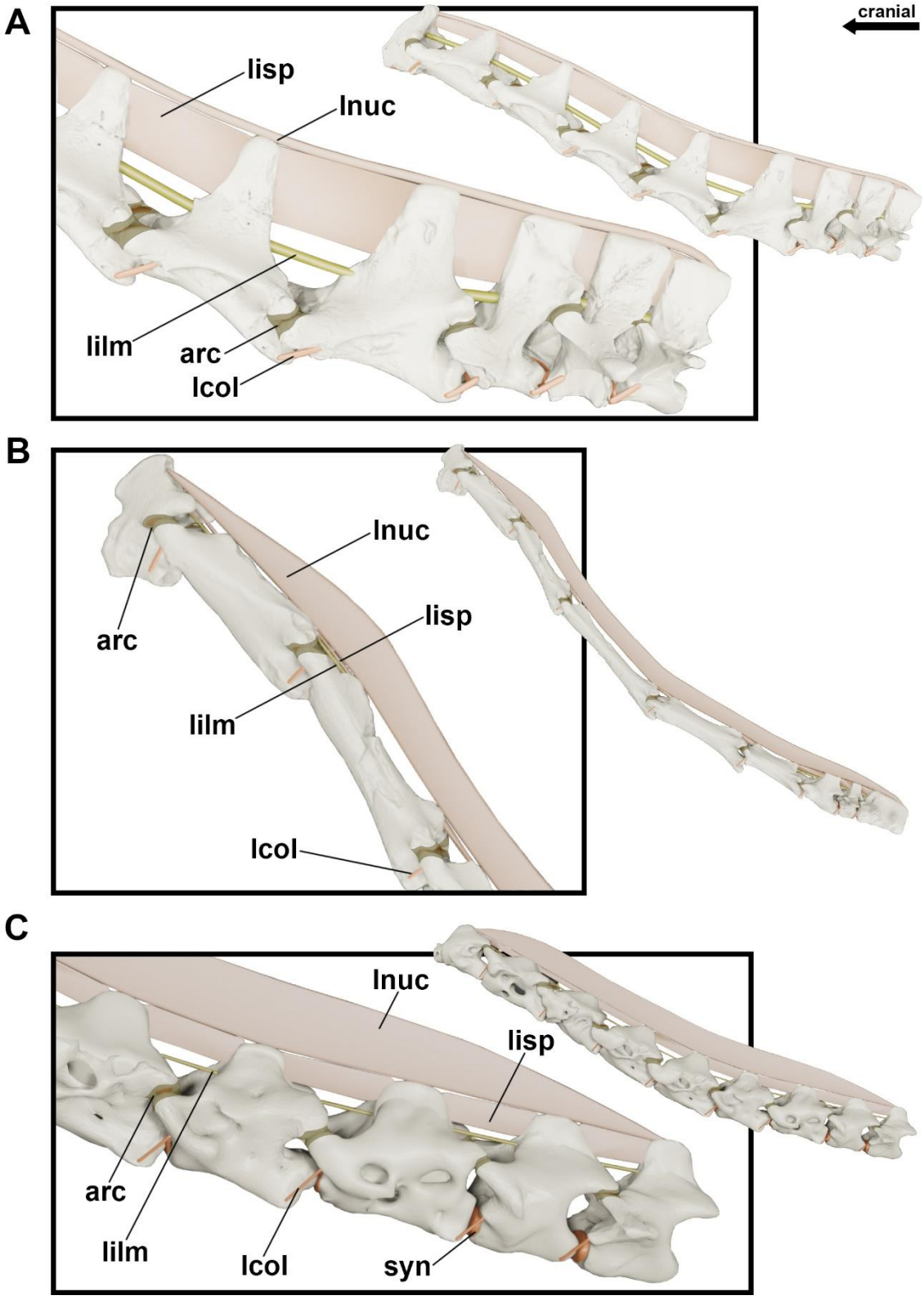

Figure 19. Detail of the reconstruction of the neck at rest position of *Anhanguera piscator* (A), *Azhdarcho lancicollis* (B) and *Rhamphorhynchus muensteri* (C), showing the reconstructed articular capsule and cervical ligaments.

As a result of the articulation of the cervical series with the partial overlap of the zygapophyses, the gaps presented between the vertebral condyles and the cotyles indicate

that the intervertebral cartilage corresponds to 2.1%–6.5% of the total neck length (Table 3).

Table 9. Proportion of total cartilage in the neck length. Abbreviations: CV, sum of the centrum lengths of the cervical vertebrae; TOTAL, total neck length; CART, percentage of synovial cartilage on the neck centra.

	CV (mm)	**TOTAL (mm)**	**CART (%)**
Anhanguera piscator	353.4	378.3	6.5
Azhdarcho lancicollis	539.6	551.4	2.1
Rhamphorhynchus muensteri	51.9	54.1	4.0

The shorter length of the pre- and postzygapophyses in the posterior cervicals indicates that the thickness of the cartilage present in the intervertebral joint in this region was greater than in the more cranial portions of the neck. In the latter, the prezygapophyses were elongate cranially and compensated the length of the condyle. The increase in cartilage thickness was gradual along the neck (Table 2; Figure 7). Due to the very convex condyle, the synovial cartilage in the peripheral part of the joint was probably thicker (Table 2). Although the ligamentous system of the pterosaur neck is difficult to understand, the presence of the *ligamentum collaterale* and *ligamentum elasticum* was highly likely. The *ligamentum collaterale* is suggested by the developed postexapophyses with rough surfaces along the entire cervical series in all analyzed pterosaurs (Figure 4), which would be points of insertion of this ligament. The preexapophyses present laterally to the cotyle indicate that this ligament possibly behaved as an extension of the articular capsule, which would contribute to joint stiffness throughout the neck (Figure 6).

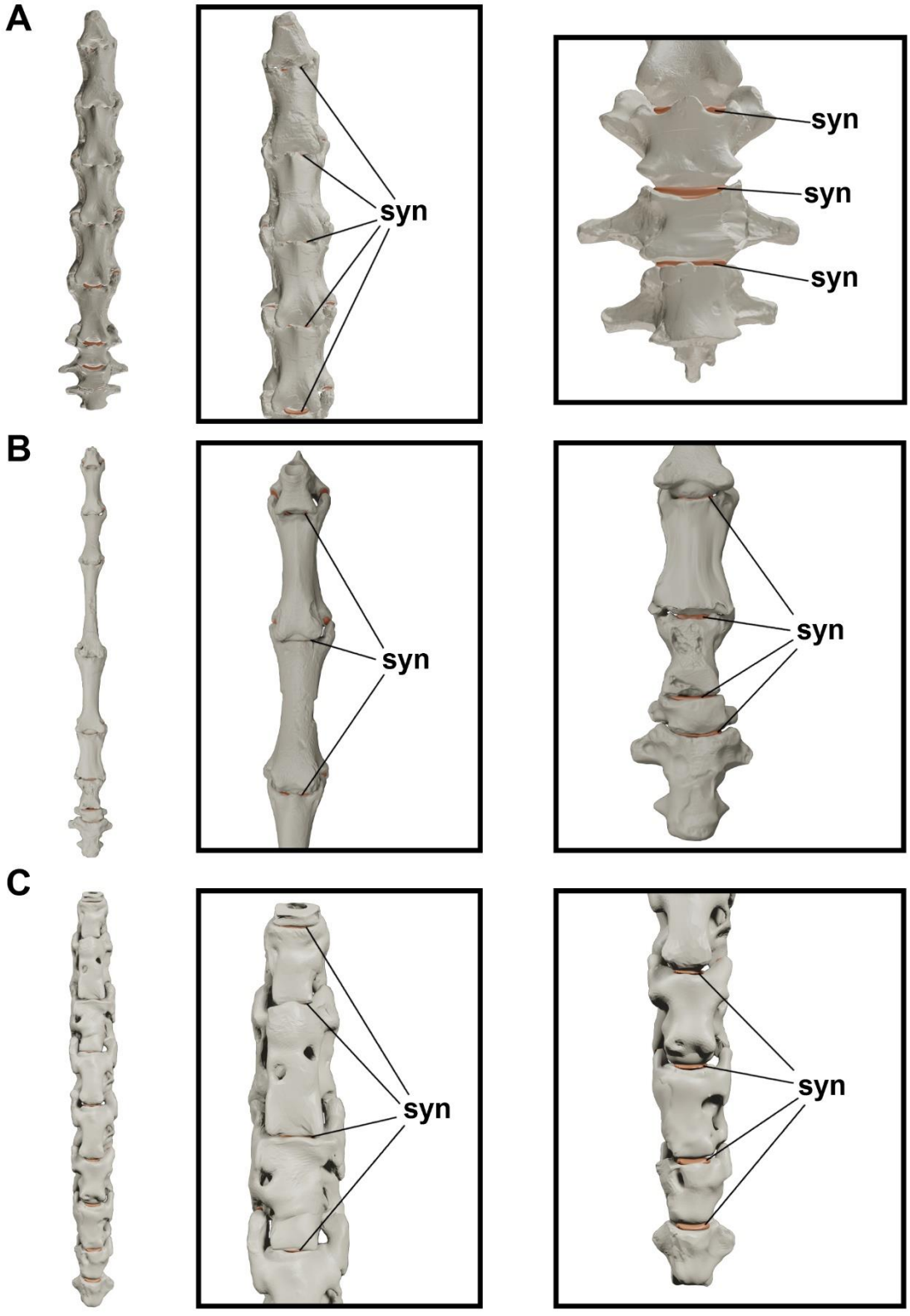

Figure 20. Reconstruction of the neck at rest position of *Anhanguera piscator* (A), *Azhdarcho lancicollis* (B) and *Rhamphorhynchus muensteri* (C) in ventral view, with the anterior and posterior portions of the neck in detail (middle and right-side columns, respectively).

The elevated head in relation to the neck, as observed in our reconstructions of the position at rest (Figure 5), hints the presence of elastic ligaments present dorsally to the

cervical vertebrae for stabilization (Figure 6). The presence of developed neural spines along the necks of *Anhanguera piscator* and *Rhamphorhynchus muensteri* supports the presence of the *ligamentum elasticum interlaminare*, which was possibly attached to the bases of the neural spines. The extremely reduced neural spines in the mid-cervical vertebrae of *Azhdarcho lancicollis* suggest a peculiar absence of this ligament in the middle portion of the neck (Figure 6).

Although the incomplete preservation of the top of the neural spines made it difficult to identify osteological correlates, we observed scars and roughness on the medial surface of the cranial and caudal portion of the neural spines of the cervical vertebrae, which we are interpreted as indicating the presence of the *ligamentum elasticum interspinale* (Figure 6). Scars and roughness are also present at the site on the dorsal vertebrae of *Anhanguera piscator* and *Rhamphorhynchus muensteri*, suggesting that the ligament is not limited to the neck.

The top of the neural spines of the cervical vertebrae also has a well-defined rough area along the entire neck. This could be interpreted as indicating the presence of the *ligamentum nuchae*, dorsally arranged and attached to each neural spine (Figure 6). Alternatively, the scar could also be from the insertions of the epaxial muscles in these same places. The constant increase in the width of the top of the neural spine from the mid-cervical to the posterior cervical vertebrae supports the hypothesis that this ligament was thinnest in the mid-portion of the neck and its thickness gradually increased to the base of the neck (Figure 8). In addition, such a ligament could present itself as an additional surface of muscle attachments when associated with vertebrae with low neural spines (Figure 6).

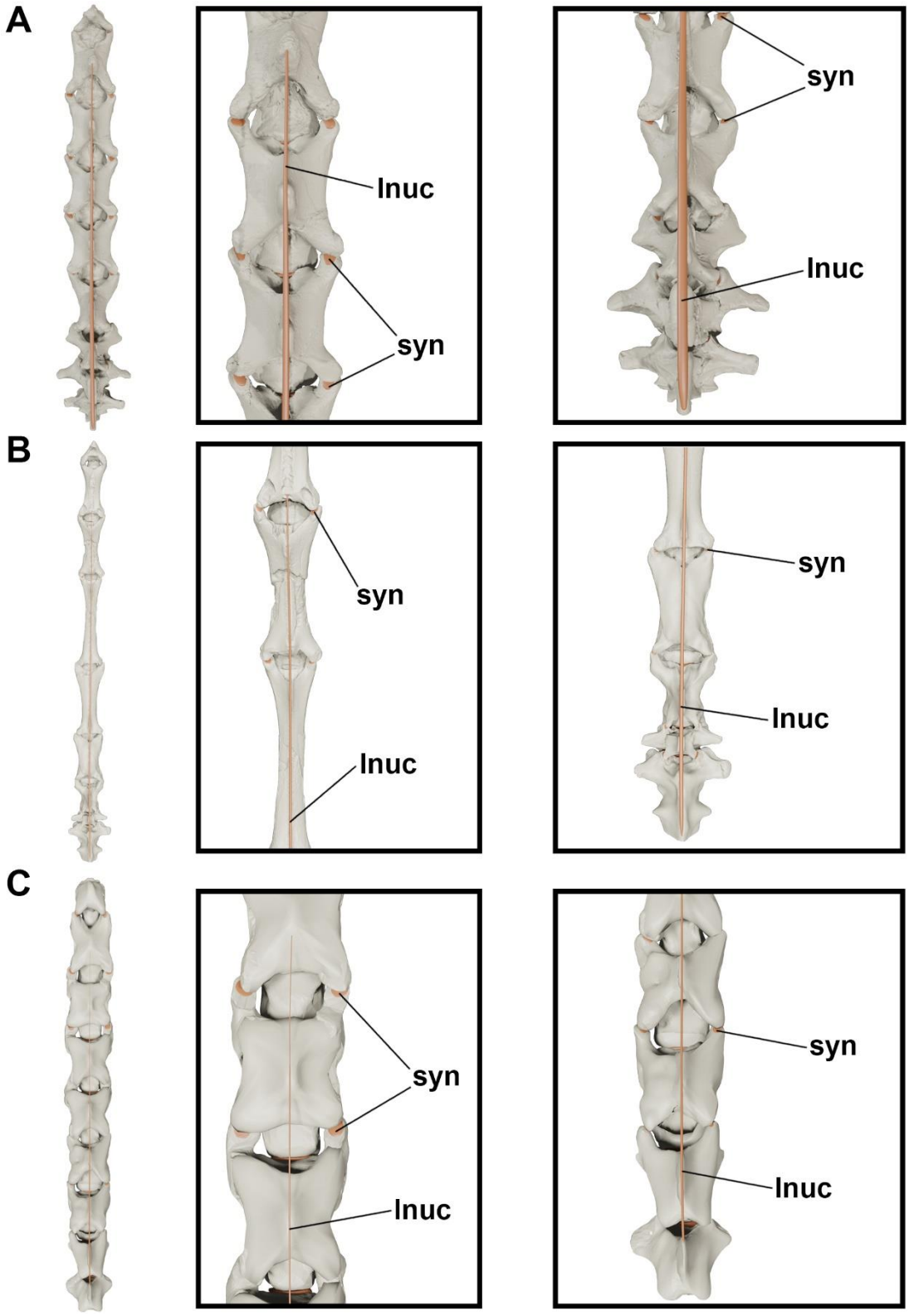

Figure 21. Reconstruction of the neck at rest position of *Anhanguera piscator* (A), *Azhdarcho lancicollis* (B) and *Rhamphorhynchus muensteri* (C) in dorsal view, with the anterior and posterior portions of the neck in detail (middle and right-side columns, respectively).

Discussion

Due to differences in vertebral morphologies from one neck region to the other, transitional vertebral morphologies are commonly present between them and between the cervical and dorsal vertebrae of archosarus (Bennett, 2001; Tambussi et al., 2012; Iijima & Kubo, 2019). For instance, the first set of vertebrae posterior to the neck of birds are commonly named *cervico-dorsales* (Baumel & Witmer, 1993).

The presence of a tall neural spine in posterior cervical vertebrae also seems appropriate as it has been recorded in azhdarchid and azhdarchoid pterosaurs (Pereda-Suberbiola et al., 2003; Aires et al., 2014, Vila Nova et al., 2015; Buchmann et al., 2018; Andres & Langston Jr., 2021).

In the analyzed pterosaurs, the morphology of the mid-cervical vertebrae ranged from extremely long with low neural spines to long with more developed neural spines, consistent with what is widely observed in Pterodactyloidea (Howse, 1986; Wellnhofer 1991; Kellner & Tomida, 2000; Bennett, 2001; Pereda-Suberbiola et al., 2003; Ösi et al., 2005; Averianov, 2010; Henderson & Peterson, 2006; Beccari et al., 2021; Andres & Langston Jr., 2021). In Rhamphorhynchidae, neural spines are apparently tall in all mid-cervical vertebrae, which are slightly longer than the posterior cervical vertebrae (Wellnhofer, 1975; Andres et al., 2010). The variation in the height of the neural spines in the mid-cervicals seen among pterosaurs imply differences in the locations of muscular adnexa and in the mobility of the neck. The tall neural spines of the mid-cervical vertebrae of *Anhanguera piscator* and *Rhamphorhynchus muensteri*, together with the long prezygapophyses, may indicate a certain level of restriction to the dorsal extension in this portion of the neck, suggesting that this region might not extend much beyond the position at rest (Witton & Naish, 2008; Molnar et al., 2015). The longer centra we observed mainly in mid-cervicals is the main mechanism of neck elongation in pterosaurs, as also seen in extant birds and in non-avian dinosaurs, although they also have more cervical vertebrae (Taylor & Wedel, 2013; Marek et al., 2021). The fewer number of vertebrae and the elongation of the mid-cervicals compared to extant birds may also have contributed to lesser overall neck flexibility in pterosaurs (Dzemski & Christian, 2007). However, this relative inflexibility likely strengthened the intervertebral joints, which are more stable in the presence of an intervertebral space (Witton & Naish, 2008; Vidal et al., 2020).

In all pterosaurs analyzed, the posterior cervical vertebrae have tall neural spines and lateral bone extensions with diapophyses, related to transverse processes, which may

be homologous to those observed in the dorsals in other archosaurs (Wellnhofer, 1975; Bennett, 2001; Souza, 2018). As in the mid-cervicals, the bigger length or height of these processes in the posterior cervical vertebrae may limit mobility in this region of the neck, even though those structures are compatible with osteological correlates for the origin of cervical muscles (Boas, 1929; Witton & Naish, 2008; Tambussi et al., 2012, Iijima & Kubo, 2019). The craniocaudally shorter centrum in posterior cervicals in relation to the other cervicals is also observed in extant birds and crocodylians (Iijima & Kubo, 2019; Terray et al., 2020).

The anatomical vertebral segments recognized here according to the cervical anatomy of pterosaurs are widely recognized in extant birds and crocodilians (Terray et al., 2020; Mook, 1921; Iijima & Kubo, 2019). The definition of such regions is important to recognize the possible attachment sites of muscle and/or ligament tissue in extinct archosaurs (Wedel & Sanders, 2002; Tsuihiji, 2004, 2005, 2007; Snively & Russell, 2007). Although the cervical osteological modules are not related to the functional segments of the neck (Kambic et al., 2017) in archosaurs, they are related to the muscles' anatomy and morphology, which in turn are associated to varied locomotor and foraging habits in extant species (Molnar et al., 2015; Marek et al 2021). Therefore, the morphological variation between cervical vertebrae in the analyzed pterosaurs, especially in the azhdarchid, may reflect differences in that animal's life habits (Averianov, 2013; Naish & Witton, 2017) in relation to the *Anhanguera* and *Rhamphorhynchus*.

The procoelous pterosaur cervicals differ from the heterocelic morphology of those in extant birds and resemble the morphology of the cervical vertebrae of extant crocodylians, in which they constitute joints that guarantee stiffness to the neck while maintaining a large range of motion (Baumel & Witmer, 1993; Molnar et al., 2015). The variation in convexity of the condyles and the length of the zygapophyses between the cervical modules probably causes the variation of movements along the neck in range of motion analyzes of extinct animals, since the bone intersection between these structures and adjacent vertebrae are the main factors that limit movement (Jones et al., 2021; Padian et al., 2021). However, disregarding the presence of soft tissue during manipulation of the vertebrae tends to reveal a range of motion that was not necessarily performed by the animal in life (Hutson & Hutson, 2012; Padian et al., 2021). The convex condyle of the cervical vertebrae of pterosaurs makes a precise fit to the cotyle of its neighboring vertebra, especially in the mid-cervicals, as observed in the measurements of the

intervertebral space (Table 2) and supports the hypothesis of a thin layer of cartilage covering this gap. Furthermore, the anatomical differences observed in the hypapophysis of pterosaurs when compared to those of crocodylians and the presence of preexapophyses and posexapophyses, which originate directly from the ventral portion of the cotyle and condyle, respectively, suggest that pterosaurs did not have a fibrous ring in the joint, or that, if present, it would be thinner than in extant crocodylians (Salisbury & Frey, 2001; Fronimos & Wilson, 2017).

Considering cartilage and ligaments allows for more assertive inferences regarding different levels range of motion throughout the neck, as demonstrated in extant birds (Boas, 1929; Zusi, 1962; Dzemski & Christian, 2007, Molnar et al., 2015). The presence of a dorsomedial fovea (*fovea condyli*) and of flattened ventral edges in relation to the central region of the condyle are consistent with osteological correlates for the presence of synovial cartilage in extant crocodylians and birds (Salisbury & Frey, 2001; Fronimos & Wilson, 2017; Chapter I). The vertebrae of the analyzed pterosaurs showed a certain roughness on several surfaces, which is also considered a correlate of the presence of synovial cartilage due to its presence in extant crocodylians (Fronimos & Wilson, 2017), although some roughness is also found in mammalian bones (McGowan, 1986). The rough edges of the zygapophyses, cotyle and condyle in the analyzed pterosaur vertebrae support inferences on the presence of a fibrous articular capsule connected to the synovial cartilage in these joints, also present in extant crocodylians (Schwarz et al., 2007; Fronimos & Wilson, 2017; Chapter I). Furthermore, the presence of the joint capsule in extant birds fixes the joint and can allow both facets to slide until the zygapophyses are nearly disarticulated (Taylor et al., 2009; Cobley at al., 2013; Kambic et al., 2017). Establishing the level of overlap of the zygapophysis is also important before submitting a 3D model to range of motion analysis, so that the level of disarticulation is measured from the neck position at rest (Jones et al., 2021).

Our estimates of intervertebral cartilage thickness are based on the intervertebral space that defines the length of synovial cartilage in extant animals (Vidal et al., 2020). This cartilage adds length to the neck, but that can vary according to the animal's ontogenetic stage, as there may be a reduction in the space throughout the animal's life (Vidal et al., 2020). The proportion of cartilage to the total neck length of the analyzed pterosaurs differs from that observed in extant mammals and crocodylians, which have more than 10% of the neck length composed of cartilage (Taylor & Wedel, 2013). Such

difference was expected due to the presence of intervertebral discs in the joints of extant mammals and some crocodylians, which are more robust than the likely thin synovial cartilages in the vertebrae of pterosaurs, according to the osteological correlates presented (Taylor & Wedel, 2013; Vidal et al., 2020). The proportion of cartilage we estimated for *Azhdarcho* and *Rhamphorhynchus* is similar to that observed in the Neognathae birds analyzed in the previous chapter. As in *Azhdarcho lancicollis*, extant birds with extremely long and dorsoventrally compact vertebrae, as *Ardea alba* and *Ixobrychus exilis*, also had less intervertebral cartilage in the neck (see previous chapter). The relatively thin intervertebral joint capsules proposed for *Azhdarcho lancicollis* corresponds to the intervertebral soft tissue thickness previously proposed for a range of motion analysis of the vertebral series of another azhdarchid pterosaur (Padian et al., 2021). The estimated 6.5% proportion of cartilage that makes up the length of the neck in *Anhanguera piscator* is similar to that observed in ostriches (6.3%), despite the presence of fibrous ring in ostrich joints, which increase the thickness of intervertebral space (Cobley et al., 2013). Studies with Sauropodomorpha vertebrae also indicated large differences in this proportion, but this may also occur due to ontogenetic factors (Taylor & Wedel, 2013). Although the proportion of cartilage obtained for pterosaurs reveals a smaller amount compared to extant mammals and crocodylians, we must consider that adding even small sums of cartilage impacts not only the length, but also the dorsoventral angulation and flexibility of the neck (Cobley et al., 2013; Taylor & Wedel, 2013). The presence of larger intervertebral spaces in the posterior region of the neck indicates that this region could have less dorsoventral flexion due to the greater volume of synovial cartilage between the vertebrae (Cobley et al., 2013; Molnar et al., 2014; Iijima & Kubo, 2019). The identification of variations in the thickness of the intervertebral synovial cartilage along the neck allows for more precise inferences of its range of motion, considering that the center of rotation is located in the intervertebral space (Haher et al., 1991; Selbie et al., 1993; Wintrich et al., 2019; Jones et al., 2021).

The position of the neck at rest we estimate here, with approximately 50% and 75% overlap of the zygapophyses in the mid-cervical and posterior cervical vertebrae, respectively, differs from the Osteological Neutral Pose (ONP), which establishes total overlap of the zygapophyses (Stevens & Parrish, 1999). Considering that partial overlap seems adequate to suggest the position of the animal's neck in life, these overlap levels will determine differences in terms of a more or less extended natural pose of the neck

(Taylor et al., 2009). The partial overlapping of the zygapophyses we attributed here contributes to show intervertebral flexibility in extinct archosaurs (Cobley et al., 2013; Iijima & Kubo, 2019) and that the variation in the overlapping level of the zygapophyses may indicate a restriction of mobility in the posterior segment of the pterosaur neck. Considering that movement requires sliding between the zygapophyses, the reduced overlap level could be limited to > 50%, as observed in extant archosaurs and mammals (Stevens & Parrish, 2005; Dzemski & Christian, 2007; Taylor et al., 2009). In addition, the presence of synovial cartilage ensures greater mobility in the sliding movement of the zygapophyses (Vidal et al., 1986), although a posture of full neck extension does not necessarily require a high sliding between the zygapophyses (Vidal et al., 2020).

The relative verticalization of the of the neck at rest position of *Azhdarcho lancicollis* is inferred by the angles observed in the mid and posterior segments of the neck, which were obtained by combining the partial overlap zygapophyses, intervertebral space thickness, and convexity of the condyles in vertebrae of both regions, and is also observed in extant amniotes (Taylor et al., 2009). This combination favored a larger angle with the axis of the third vertebra oriented more ventrally in relation to the second vertebra (axis), and in the mid-cervical vertebrae, smaller angles with the axes of the vertebrae always above their anterior vertebra. This result differs from the reconstruction of the neck in neutral posture for the same species proposed by Averianov (2013). A more vertical neck relative to the atlas and axis, which are arranged horizontally, is consistent with the neck posture of extant Amniota (Taylor et al., 2009). The reconstruction of the neck of *Quetzalcoatlus* by Padian et al. (2021) has a much more vertical neck in relation to the trunk in the normal position (as called by the authors), which was inferred based on the greater angles between the joints in the posterior portion of the mid-cervical series. We believe that the reconstruction of the cervical series of *Quetzalcoatlus* may differ due to using different levels of overlapping of the zygapophysis and spacing between the vertebrae in this region, but the authors do not indicate how they defined the values used in their work (Padian et al., 2021).

The verticalization of neck of the *Azhdarcho lancicollis* in relation to *Anhanguera* and *Rhamphorhynchus* observed here probably meant that it required less force to balance the neck and head, bringing both closer to the center of mass (Dzemski & Christian 2007; Marek et al., 2021). However, we consider that the neck of *Azhdarcho lancicollis* would only be as vertical as suggested for *Quetzalcoatlus* by Padian et al. (2021) during dorsal

extension. Unlike what we suggested for *Azhdarcho lancicollis*, the necks of the other pterosaurs we analyzed would probably be arranged more horizontally in relation to the trunk and may have suffered higher static pressure, especially at their bases (Dzemski & Christian, 2007; Taylor et al., 2009).

Scars are abundant in the analyzed pterosaur vertebrae, as expected in archosaur bones (McGowan, 1986). We interpreted many of them as muscular, although it is assumed that few muscles leave scars in extant archosaurs (Nicholls & Russell, 1985). Depressions on the base and roughness on the cranial and caudal surface of pterosaur neural spines are also observed in attachment sites of the *ligamentum elasticum interlaminare* and *ligamentum elasticum interspinale* in extant birds (Tsuihiji, 2004; Tambussi et al., 2012; see also the previous chapter). A depression on the cranial surface of the base of each neural spine of the mid-cervical and posterior cervical vertebrae demonstrates that the *ligamentum elasticum interlaminare* was discontinuous, as in extant birds (Tsuihiji, 2004; Tambussi et al., 2012). The presence of a *ligamentum elasticum interlaminare* restricted only to the cranial and caudal ends of the neck in *Azhdarcho lancicollis* is also observed in birds with extremely long necks, as in Rheiformes (Tsuihiji, 2004). Furthermore, the absence of the ligament in this region supports previous interpretations of inflexibility of the mid-cervical vertebrae of azhdarchid pterosaurs (Witton & Naish, 2008).

Tall neural spines with thick tops in the pterosaur posterior cervical vertebrae resemble those seen in extant birds, in which the *ligamentum nuchae* is also thicker in this region (Tambussi et al., 2012). The presence of the *ligamentum nuchae* dorsally to the cervical series in pterosaurs is supported by the presence of developed tuberosities on top of the neural spines of successive cervical vertebrae in extant birds (Tsuihiji, 2004). However, the thickness of the top of neural spines may also be associated with the presence of muscles from the developed *transversospinalis* group (Snively & Russell, 2007).

The above-mentioned ligaments could exert passive forces, stabilize the cervical series, and store energy (Dzemski & Christian, 2007). The long length and great strength and elasticity of the *ligamentum elasticum interlaminare* and *ligamentum elasticum interspinale* may have contributed to support the weight and helped to restore the neck to the rest position after ventral flexion (Gál, 1993; Tsuihiji, 2004; Witton & Naish, 2008;

Tambussi et al., 2012; Naish & Witton, 2017). The presence of the *ligamentum nuchae* above the cervical series could mean an additional surface for muscle attachments originating from the pectoral girdle (Dimery et al., 1985). Furthermore, the presence of a robust *ligamentum nuchae* would probably contribute to the stabilization of the skull above the height of the trunk in a position at rest (Dimery et al., 1985; Tsuihiji, 2004). The robustness of the *ligamentum collaterale* and intervertebral thickness of cartilages in the posterior segment probably contributes to the stability of this region, decreasing the range of motion and increasing stiffness between joints, which would also increase resistance to possible compression loads caused by dorsoventral flexion of the neck of these pterosaurs (Cobley et al., 2013; Molnar et al., 2014; Iijima & Kubo, 2019; Moore, 2020). Such resistance is probably further maximized in dsungaripteroids, including *Anhanguera* and *Azhdarcho*, by the formation of the notarium in osteologically mature individuals (Witton & Habib, 2010; Aires et al., 2021).

Conclusions

Pterosaur mid-cervical and posterior cervical vertebrae compose two distinct cervical anatomical modules, with longer mid-cervical vertebrae with more convex condyles and longer prezygapophyses, and shorter posterior cervicals with more developed vertebral processes. The presence of a fovea and extensive convex condyles, besides a rough area that borders all the articular surfaces of the vertebrae of the pterosaurs we analyzed, supports the presence of synovial cartilage in the vertebral joints, which are thicker near the base of the neck and probably affect the neck length and angulation at rest position.

The position of the neck at rest of the pterosaurs analyzed here indicates that they probably kept their heads above the level of the trunk and slightly flexed in a ventral direction. The verticalization of the neck in *Azhdarcho lancicollis* in rest position is inferred by the orientation of the vertebrae above the main axis of their subsequent vertebrae, from the fourth to the ninth cervicals.

The osteological correlates observed in the vertebrae of pterosaurs support the presence of the *ligamentum collaterale*, *ligamentum elasticum interspinale*, *ligamentum elasticam interlaminare* and *ligamentum nuchae*. Probably, most ligaments were present throughout the entire neck, except for the *ligamentum elasticum interlaminare*, which may have been absent in the middle section of the neck of *Azhdarcho lancicollis*, as

suggested by the lack of correlates. The scars and robustness of the neural spines indicate that the ligaments were probably more robust in the final segment of the neck. We discuss that the presence of these ligaments could probably stabilize the cervical series exert passive forces and store energy.

Acknowlegments

We thank Niels Bonde (Zoological Museum, Denmark), Maria Eduarda Castro Leal (Zoological Museum, Denmark), Alexander Averianov (Zoological Institute of the Russian Academy of Sciences, Russia), Takanobu Tsuihiji (National Museum of Nature and Science, Japan), Makoto Manabe (National Museum of Nature and Science, Japan) and Chisako Sakata (National Museum of Nature and Science, Japan), who CT-scanned the specimens and gently shared the data with us. We would like to thank Dr. Fabiana Costa and M.Sc. Rodrigo Pêgas for their valuable discussions on the topic and for their help in photographing the specimens. We are also grateful to the coordinators and staff of the Institute for the Research and Rehabilitation of Marine Animals (Instituto de Pesquisa e Reabilitação de Animais Marinhos - IPRAM) (Cariacica, Brazil), of the Caiman Project and Marcos Daniel Institute (Vitória, Brazil), and of the Universidade Federal do Espírito Santo's Veterinary Hospital (Alegre, Brazil). This study was partially funded by Coordenação de Aperfeiçoamento de Pessoal de Nível Superior – Brazil (CAPES) – Finance Code 001 (scholarship to RB) and by Conselho Nacional de Desenvolvimento Científico e Tecnológico (CNPq) (project grant #421412/2018-6 to TR). The funders had no role in study design, data collection and analysis, decision to publish, or preparation of the manuscript.

References

Aires ASS, Kellner AWA, Müller RT, Da Silva LR, Pacheco CP, Dias-da-Silva S. (2014). New postcranial elements of the Thalassodrominae (Pterodactyloidea, Tapejaridae) from the Romualdo Formation (Aptian–Albian), Santana Group, Araripe Basin, Brazil. Palaeontology 57 (2): 343–355.

Aires ASS, Reichert LM, Müller RT, Pinheiro FL, Andrade MB. (2021). Development and evolution of the notarium in Pterosauria. Journal of Anatomy 238: 400–415.

Andres B, Clark JM, Xing X. (2010). A new Rhamphorhynchid pterosaur from the upper Jurassic of Xinjiang, China, and the phylogenetic relationships of basal pterosaurs. Journal of Vertebrate Paleontology 30 (1): 163–187.

Andres B, Langston Jr W. (2021). Morphology and taxonomy of *Quetzalcoatlus* Lawson 1975 (Pterodactyloidea: Azhdarchoidea). Journal of Vertebrate Paleontology 41: 46–202.

Averianov AO. (2010). The osteology of *Azhdarcho lancicollis* (Nessov, 1984) (Pterosauria, Azhdarchidae) from the late Cretaceous of Uzbekistain. Proceedings of the Zoological Institute RAS 314: 264–317.

Averianov AO. (2013). Reconstruction of the neck of *Azhdarcho lancicollis* and lifestyle of azhdarchids (Pterosauria, Azhdarchidae). Paleontological Journal 47: 203–209.

Baumel JJ, Raikow RJ. (1993). Arthrologia. In: Baumel JJ, King AS, Breazile JC, Evans HE, Vanden Berge JC, editors. Handbook of avian anatomy: Nomina anatomica avium. Cambridge, MA: Nuttal Ornihtological Club. 133–187.

Baumel JJ, Witmer LM. (1993). Osteologia. In: Baumel JJ, King AS, Breazile JC, Evans HE, Vanden Berge JC, editors. Handbook of avian anatomy: *nomina anatomica avium*. Cambridge, MA: Nuttall Ornithological Club. 45–132.

Beccari V, Pinheiro FL, Nunes I, Anelli LE, Mateus O, Costa FR. (2021). Osteology of an exceptionally well-preserved tapejarid skeleton from Brazil: Revealing the anatomy of a curious pterodactyloid clade. Plos One 16 (8): e0254789.

Bennett SC. (2001). The osteology and functional morphology of the Late Cretaceous pterosaur *Pteranodon* Part I. General description of osteology. Palaeontographica Abteilung A 260: 1–112.

Blender Development Team. (2019). Blender (Version 2.91) [Computer software]. https://www.blender.org

Boas JEV. (1929). Biologisch-anatomische Studien über den Hals der Vögel. Kongl. Danske Vidensk. Selsk. Skrifter, Naturvidensk. Math (Ser. 9) 1, 105–222.

Bonde N, Christiansen P. (2003). The detailed anatomy of *Rhamphorhynchus*: axial pneumaticity and its implications. Geology Society Special Publications 217: 21–232.

Buchmann R, Rodrigues T, Polegario S & Kellner AWA. (2018). New information on the postcranial skeleton of the Thalassodrominae (Pterosauria, Pterodactyloidea, Tapejaridae). Historical Biology 30: 1139–1149.

Butler RJ, Barrett PM, Gower DJ. (2012). Reassessment of the evidence for postcranial skeletal pneumaticity in Triassic archosaurs, and the early evolution of the avian respiratory system. Plos One 7: e34094.

Cignoni P, Callieri M, Corsini M, Dellepiane M, Ganovelli F, Ranzuglia G. (2008). MeshLab: an open-source mesh processing tool. Sixth Eurographics Italian Chapter Conference: 129–136.

Cobley MJ, Rayfield EJ, Barrett PM. (2013). Inter-Vertebral Flexibility of the Ostrich Neck: Implications for Estimating Sauropod Neck Flexibility. Plos One 8 (8): e72187.

Dimery NJ, Alexander RM, Deyst KA. (1985) Mechanics of the ligamentum nuchae of some artiodactyls. Journal of Zoology 206 (3): 341–351.

Dzemski G, Christian A. (2007). Flexibility along the neck of the ostrich (*Struthio camelus*) and consequences for the reconstruction of dinosaurs with extreme neck length. Journal of Morphology 268: 701–714.

Fronimos JA, Wilson JA. (2017). Concavo-convex intercentral joints stabilize the vertebral column in sauropod dinosaurs and crocodylians. Ameghiniana 54 (2): 151–176.

Gál, J. (1993). Mammalian spinal biomechanics 2: intervertebral lesion experiments and mechanisms of bending resistance. Journal of Experimental Biology 174 (1): 281–297.

Howse SCB. (1986). On the cervical verteabrae of the Pterodactyloidea (Reptilia: Archosauria). Zoological Journal of the Linnaean Society 88: 307–328.

Hutson JD, Hutson KN. (2012). A test of the validity of range of motion studies of fossil archosaur elbow mobility using repeated-measures analysis and the extant phylogenetic bracket. Journal of Experimental Biology 215: 2030–2038.

Iijima M, Kubo T. (2019). Comparative morphology of presacral vertebrae in extant crocodylians: taxonomic, functional and ecological implications. Zoological Journal of the Linnean Society 186: 1006–1025.

Jones KE, Brocklehurst RJ, Pierce SE. (2021). AutoBend: An automated approach for estimating intervertebral joint function from bone-only digital models. Integrative Organismal Biology 3 (1): obab026

Kambic RE, Biewener AA, Pierce SE. (2017). Experimental determination of three-dimensional cervical joint mobility in the avian neck. Frontiers in Zoology 14: 37

Kellner AWA, Tomida Y. (2000). Description of a new species of Anhangueridae (Pterodactyloidea) with comments on the pterosaur fauna from the Santana Formation (Aptian-Albian), Northeastern Brazil. National Science Museum, Monographs, Tokyo, 17: 1–135.

Kellner AWA, Campos DA. (2002). The function of the cranial crest and jaw of a unique pterosaur from the Early Cretaceous of Brazil. Science 297: 389–392.

Lautenschlager S. (2017). Digital reconstruction of soft-tissue structures in fossils. The Paleontological Society Papers 22: 101–117.

Marek RD, Falkingham PL, Benson RBJ, Gardiner JD, Maddox TW, Bates KT. (2021). Evolutionary versatility of the avian neck. Proceedings Royale Society B 288: 20203150.

McGowan C. (1986). The wing musculature of the Weka (*Gallirallus australis*), a flightless rail endemic to New Zealand. Journal of Zoological Society of London 210: 305–346.

Molnar JL, Pierce SE, Hutchinson JR. (2014). An experimental and morphometric test of the relationship between vertebral morphology and joint stiffness in Nile crocodiles (*Crocodylus niloticus*). Journal of Experimental Biology 217: 758–768.

Molnar JL, Pierce SE, Bhullar BAS, Turner AH, Hutchinson JR. (2015). Morphological and functional changes in the vertebral column with increasing aquatic adaptation in crocodylomorphs. Royal Society Open Science 2: 150439.

Mook CC. 1921. Notes on the postcranial skeleton in the Crocodilia. Bulletin of the American Museum of Natural History 44: 67–100.

Moore AJ. (2020). Vertebral pneumaticity is correlated with serial variation in vertebral shape in storks. Journal of Anatomy 238: 615–625.

Naish D, Witton MP. (2017). Neck biomechanics indicate that giant Transylvanian azhdarchid pterosaurs were shirt-necked arch predators. PeerJ 5: e2908.

Nicholls EL, Russell AP. (1985). Structure and function of the pectoral girdle and forelimb of Struthiomimus altus (Theropoda: Ornithomimidae). Palaeontology 28: 643–677.

O'Connor PM. (2006). Postcranial pneumaticity: an evaluation of soft-tissue influences on the postcranial skeleton and the reconstruction of pulmonary anatomy in archosaurs. Journal of Morphology 267: 1199–1226.

Ösi A, Weishampel DB, Jianu CM. (2005). First evidence of azhdarchid pterosaurs from the Late Cretaceous of Hungary. Acta Palaeontologica Polonica 50 (4): 777–787.

Padian K, Cunningham JR, Langston Jr. W, Conway J. (2021). Functional morphology of *Quetzalcoatlus* Lawson 1975 (Pterdactyloidea: Azhdarchoidea). Journal of Vertebrate Paleontology 41: 218–251.

Pereda-Suberbiola X, Bardet N, Jouve S, Iarochène M, Bouya B, Amaghzaz M. (2003). A new azhdarchid pterosaur from the Late Cretaceous phosphates of Morocco. Geological Society, London, Special Publications 217: 79–90.

Pinheiro FL, Rodrigues T. (2017). *Anhanguera* taxonomy revisited: is our understanding of Santana Group pterosaur diversity biased by poor biological and stratigraphic control? PeerJ 5: e3285.

Rayfield EJ. (2007). Finite Element Analysis and understanding the biomechanics and evolution of living and fossil organisms. Annual Review of Earth and Planetary Sciences 35: 541–576.

Salisbury SW, Frey E. (2001). A biomechanical transformation model for the evolution of semi-spheroidal articulations between adjoining vertebral bodies in crocodilians. In: Grigg GC, Seebacher F, Franklin CE. Crocodilian biology and evolution. Surrey Beatty & Songs, Chipping Norton, p. 85–134.

Schneider CA, Rasband WS, Eliceiri KW. (2012). NIH Image to ImageJ: 25 years of image analysis. Nature Methods 9: 671–675.

Schwarz D, Frey E, Meyer CA. (2007). Pneumaticity and soft-tissue reconstructions in the neck of diplodocid and dicraeosaurid sauropods. Acta Palaentologica Polonica 52: 167–188.

Selbie WB, Thomson DB, Richmond FJR. (1993). Sagittal-plane mobility of the cat cervical spine. Journal of Biomechanics 26 (8): 917–927.

Snively E, Russell AP. (2007). Functional morphology of neck musculature in the Tyrannosauridae (Dinosauria, Theropoda) as determined via a hierarchical inferential approach. Zooloical Journal of the Linnean Society 151: 759–808.

Souza RG. (2018). Comments on the serial homology and homologues of vertebral lateral projections in Crocodylia (Eusuchia). The Anatomical Record 301: 1203–1215.

Stevens KA, Parrish JM. (1999). Neck posture and feeding habits of two Jurassic sauropod dinosaurs. Science 284: 798–800.

Stevens KA, Parrish JM. (2005). Digital reconstructions of sauropod dinosaurs and implications for feeding. *In*: K.A. Curry Rogers and J.A. Wilson (eds.), The Sauropods: Evolution and Paleobiology. University of California Press, Berkeley, California. 178–200.

Tambussi CP, de Mendoza R, Degrange FJ, Picasso MB. (2012). Flexibility along the Neck of the Neogene Terror Bird *Andalgalornis steulleti* (Aves Phorusrhacidae). Plos One 7 (5): e37701.

Taylor MP, Wedel MJ, Naish D. (2009). Head and neck posture in sauropod dinosaurs inferred from extant animals. Acta Palaeontologica Polonica 54 (2): 213–220.

Taylor MP, Wedel MJ. (2013). The Effect of Intervertebral Cartilage on Neutral Posture and Range of Motion in the Necks of Sauropod Dinosaurs. Plos One 8 (10): e78214.

Terray L, Plateau O, Abourachid A, Böhmer C, Delapré A, de la Bernardie X, Cornette, R. (2020). Modularity of the neck in birds (Aves). Evolutionary Biology. Doi: 10.1007/s11692-020-09495-w.

Tsuihiji T. (2004). The ligament system in the neck of *Rhea americana* and its implication for the bifurcated neural spines of sauropod dinosaurs. Journal of Vertebrate Paleontology 24 (1): 165–172.

Tsuihiji T. (2005). Homologies of the *transversospinalis* muscles in the anterior presacral region of Sauria (crown Diapsida). Journal of Morphology 263: 151–178.

Tsuihiji T. (2007). Homologies of the *longissimus*, *iliocostalis*, and hypaxial muscles in the anterior presacral region of extant diapsida. Journal of Morphology 268: 986–1020.

Vidal D, Mocho P, Páramo A, Sanz JL, Ortega F. (2020). Ontogenetic similarities between giraffe and sauropod neck osteological mobility. Plos One 15(1): e0227537.

Vidal PP, Graf W, Berthoz A. (1986). The orientation of the cervical vertebral column in unrestrained awake animals. Experimental Brain Research 61: 549–559.

Vila Nova BC, Sayão JM, Langer MC, Kellner AWA. (2015). Comments on the cervical vertebrae of the Tapejaridae (Pterosauria, Pterodactyloidea) with description of new specimens. Historical Biology 27 (6): 770–780.

Wedel MJ, Sanders RK. (2002). Osteological correlates of cervical musculature in Aves and Sauropoda (Dinosauria: Saurischia), with comments on the cervical ribs of Apatosaurus. PaleoBios 22 (3): 1–6.

Wellnhofer P. (1975). Die Rhamphorhynchoidea (Pterosauria) der Oberjura-Plattenkalke Süddeutschlands. Palaeontographica Abt. A 148: 1–33.

Wellnhofer P. (1991). Weitere Pterosaurierfunde aus der Santana-Formation (Apt) der Chapada do Araripe, Brasilien. Palaeontographica Abt. A 215: 43–101.

Wintrich T, Jonas R, Wilke HJ, Schmitz L, Sander PM. (2019). Neck mobility in the Jurassic plesiosaur *Cryptoclidus eurymerus*: finite element analysis as a new approach to understanding the cervical skeleton in fossil vertebrates. PeerJ 7: e7658.

Witmer LM. (1995). The Extant Phylogenetic Bracket and the importance of reconstructing soft tissues in fossils. In: Thomason JJ, editor. Functional morphology in vertebrate palaeontology. Cambridge: Cambridge University Press. 19–33.

Witton MP, Naish D. (2008). A reappraisal of azhdarchid pterosaur functional morphology and paleoecology. Plos One 3: e2271.

Witton MP, Habib MB. (2010). On the size and flight diversity of giant pterosaurs, the use of birds as pterosaur analogues comments on pterosaur flightlessness. Plos One 5: e13982.

Zusi RL. (1962). Structural adaptations of the head and neck in the Black Skimmer, *Rhynchops nigra* Linnaeus. Publications of the Nuttal Ornithological Club 3: 1–153.

Chapter III

Flesh and bone: The musculature and cervical movements of pterosaurs

Richard Buchmann[1], Taissa Rodrigues[1]

[1] Laboratório de Paleontologia, Departamento de Ciências Biológicas, Centro de Ciências Humanas e Naturais, Universidade Federal do Espírito Santo, Vitória, ES, 29075-910, Brazil.

Abstract

The cervical series of pterosaurs has vertebrae that vary in morphology along its length. Such osteological variations represent changes in the neck soft tissues, such as ligaments and muscles, and reflect on their efficiency. Here, we aim to identify the presence of osteological correlates in the cervical vertebrae and skull of pterosaurs to infer attachment sites for the cervical musculature. We also aim to determine the intensity capacity of each muscle, by examining their origin area and volume. Analyzes were performed on three-dimensionally preserved cervical series of *Anhanguera piscator* (NSM-PV 19892), *Azhdarcho lancicollis* (ZIN PH, several specimens) and *Rhamphorhynchus muensteri* (MGUH 1891.738), which were digitized for subsequent muscle reconstruction. Osteological correlates were identified from structures observed in vertebrae and skulls of extant archosaurs and supported by the criteria of the Extant Phylogenetic Bracket (EPB). The proportion of the muscle volume was defined based on observations of extant archosaurs, and corresponds to six times the value of the area of origin for muscles arranged dorsally and ventrally to the cervical series, and three times the value of the area of origin for the other muscles. The estimation of muscle capacity was calculated by multiplying the maximum muscle volume and the muscle stress value. According to the recognized osteological correlates, we inferred the presence of thirteen cervical muscles, of which only two do not correspond to a level I inference by the EPB. Six of the thirteen muscles had a limited length between the cranial end and the middle of the cervical series, which probably ensured an extremely mobile head. The muscles that perform dorsal extension and ventral flexion demonstrated greater robustness and, consequently, greater efficiency for the execution of movements. Dorsal extension could also be optimized by the action of epaxial ligaments. The muscles that showed extremely low potential serve a cervical stabilization function or represent only an additional activity for movements performed by more robust muscles. Most of the epaxial muscles were attached to the bones by aponeuroses, which is consistent with the stability near the base

of the neck, while the hypaxial muscles were attached by tendons, which may have contributed to the flexibility of the ventral movements.

Key words: cervical biomechanics, cervical vertebrae, cervical muscles, Pterosauria, Archosauria, neck.

Introduction

The pterosaur cervical vertebrae have unique specializations, varying morphologically between species and in different areas of the neck within the same individual (Wellnhofer, 1991; Kellner & Tomida, 2000; Bennett, 2001; Veldmeijer, 2009; Eck et al., 2011; Vila Nova et al., 2015, Buchmann et al., 2018; Andres & Langston Jr., 2021). Usually, their neck is anatomically segmented in the anterior cervical vertebrae (atlas and axis), the mid-cervical vertebrae (third to seventh), and posterior cervical vertebrae (eighth and ninth) (Bennett, 2001; Vila Nova et al., 2015). The anatomical complexities presented by these different segments reflect variations in the attachments of soft tissues, such as joints, ligaments, and muscles (Tambussi et al., 2012; Cobley et al., 2013). Muscle attachment sites in pterosaur vertebrae can be recognized through osteological correlates in extant archosaurs, and these inferences can be supported based on the Extant Phylogenetic Bracket criteria (Witmer, 1995).

Inferences regarding the presence of muscles of the *transversospinalis* and *longissimus* groups were previously made, mainly by the identification of insertion sites in correlates in the occipital region of the skull (Witmer et al., 2003; Habib & Godfrey, 2010, Naish & Witton, 2016). Dorsal muscles associated with the execution of appendicular movements that are arranged superficially at the base of the neck were also previously inferred (Bennett, 2003; Elgin & Frey, 2011). However, a complete analysis identifying possible osteological correlates in cervical vertebrae of different pterosaurs has not yet been performed.

Furthermore, inferences about pterosaur foraging habits and locomotion are often presented disregarding the activity of the cervical muscles (Nesov, 1984; Kellner & Langston Jr., 1996; Prieto, 1998; Kellner & Tomida, 2000; Kellner & Campos, 2002; Humphries, 2007; Averianov, 2013; Padian et al., 2021; Williams et al., 2021). The procoelous condyle of the cervical vertebrae indicates that the long necks of pterosaurs were mobile (Bennett, 2001; Fronimos & Wilson, 2017) but the convexity of the

condyles and the length of the vertebral processes, especially in Pteranodontoidea, indicate that the neck was not be sinuous and flexible like that of extant birds (Boas, 1929; Zusi, 1962; Kellner & Tomida, 2000; Bennett, 2001; Guinard et al., 2010; Eck et al., 2011; Cobley et a., 2013; Vila Nova et al., 2015, Fronimos & Wilson, 2017; Buchmann et al., 2018; Andres & Langston Jr., 2021). The identification of sites of insertion and inferences of muscle volume can more assertively demonstrate muscle efficiency and allow to extrapolate the cervical movements possibly performed by pterosaurs (Porro et al., 2012).

Here, we aim to identify osteological correlates of muscles in the cervical vertebrae and occipital region of pterosaurs, to establish the maximum potential of the force exerted by the musculature, and to relate these forces to cervical stability and mobility.

Material and methods

For soft tissue reconstruction, we used 3D digital models of the cervical vertebrae of the holotype of *Anhanguera piscator* (NSM-PV 19892), housed in the collection of the National Museum of Nature and Science, in Tsukuba, Japan (Kellner & Tomida, 2000); of several specimens of *Azhdarcho lancicollis*, housed in the Paleoherpetological collection of the Zoological Institute of the Russian Academy of Sciences (ZIN PH) and in the Chernyshev's Central Museum of Geological Exploration (CCMGE 1/11915), both in Saint Petersburg, Russia (Averianov, 2010); and of a specimen attributed to *Rhamphorhynchus muensteri* (MGUH 1891.738), housed in the Geological Museum/Natural History Museum of Denmark, Copenhagen, Denmark (Bonde & Christiansen, 2003). All cervical series were previously digitally reconstructed and articulated (see the previous chapter). The choice of these pterosaur specimens is justified by the excellent three-dimensional preservation of almost all vertebrae, which enables the recognition of osteological correlates.

The digital reconstruction of the muscles in the 3D models was done using Blender 3D software, version 2.91 (Blender Development Team, 2019). Anatomical nomenclature that had not yet been used for pterosaur vertebrae was established following the *Nomina Anatomica Avium* (Baumel et al. 1993). The recognition of the osteological correlates was carried out after avian vertebrae and that of a dissected alligator (*Caiman latirostris*) (see Chapter 1). The specimen of *Caiman latirostris* was euthanized by

veterinarians of the Caiman Project (Marcos Daniel Institute) (under the authorization SISBIO 92997549) and dissected at the University Federal do Espírito Santo.

The pterosaur soft tissue inference was supported by the criteria of the Extant Phylogenetic Bracket (EPB) (Witmer, 1995). We followed the hypothesis of homology between extant bird and crocodilian neck muscles established by Tsuihiji (2005; 2007). The names suggested for the musculature of pterosaurs were decided on the basis of the greatest similarity between the locations, amount, and shape of attachments of the muscles of extant birds or crocodilians.

The thickness of the belly of each flexor and extensor muscle arranged dorsally and ventrally to the cervical series was calculated as six times the muscle's origin area, as we observed in extant birds in Chapter I. The thickness of each thin muscle arranged laterally to the cervical series was defined as three times the muscle's origin area, after to the same reasoning.

The maximum possible force production ($F_{pmax)}$ of the muscles was obtained by multiplying the cross-sectional area of each muscle by the isometric muscle stress value, as previously established in extant crocodilians (Porro et al., 2011). We considered the isometric muscle stress value to be equivalent to 25 N/cm^2 (Herzog, 2007).

Anatomical abbreviations

ac, *ansa costotransversaria*; arc, articular capsule; bo, basioccipital; ca, *capitulum*; caat, *capitulum* of the atlas; caax, *capitulum* of the axis; ceat, centrum of the atlas; ceax, centrum of the axis; cnt, *crista nuchalis transversa*; com, *complexus*; con, condyle; ep, epipophyses; flx, *flexor colli*; fm, foramen magnum; fov, fovea; ftr, *foramen transversarium*; hyp, hypapophysis; incr, *intercristales*; insp, *interspinales*; intr, *intertransversarii*; lcas, *longissimus capitis superficialis*; lcap, *longissimus capitis profundus*; loc, *longus colli*; mus, muscle scar; nc, neural canal; ns, neural spine; oc, occipital condyle; pa, parapophysis; poex, postexapophysis; preex, preexapophysis; po, paraoccipital; poz, postzygapophysis; prz, prezygapophysis; rcl, *rectus capitis lateralis*; rcv, *rectus capitis ventralis*; soccr, supraoccipital crest; spca, *splenius capitis*; tat, atlas tubercle; tax, axis tubercle; td, *torus dorsalis*; toc, transverse oblique crest; tpr, transverse process; trca, *transversospinalis capitis*; trce, *transversospinalis cervicis*; tub, tubercle

Identification of osteological correlates

Due to the state of preservation, it was not possible to identify osteological correlates in the neural arch of the atlas and axis of MGUH 1891.738 (*Rhamphorhynchus muensteri*). The centrum of the atlas of *Anhanguera piscator* and *Azhdarcho lancicollis* presents the cotyle expanded in the medial portion, thinning ventrally, forming a process located on the cranioventral surface similar to a short hypapophysis (Figure 1). The atlas of both these pterosaurs has bulges laterally that resemble muscle attachment sites in avian vertebrae (Figure 1). Craniolaterally, in the *ansa costotransversaria* of the axis of all analyzed pterosaurs, tubercle and *capitulum* are observed, which are more developed in *Azhdarcho lancicollis* (Figure 1). The epipophysis of the axis is well developed in *Anhanguera piscator* and *Azhdarcho lancicollis*, resembling the *torus dorsalis* of extant birds (Figure 1). The axis' neural spine is tall and its cranial face has a well-defined muscular scar in both Pterodactyloidea pterosaurs, resembling that seen in extant birds (Figure 1).

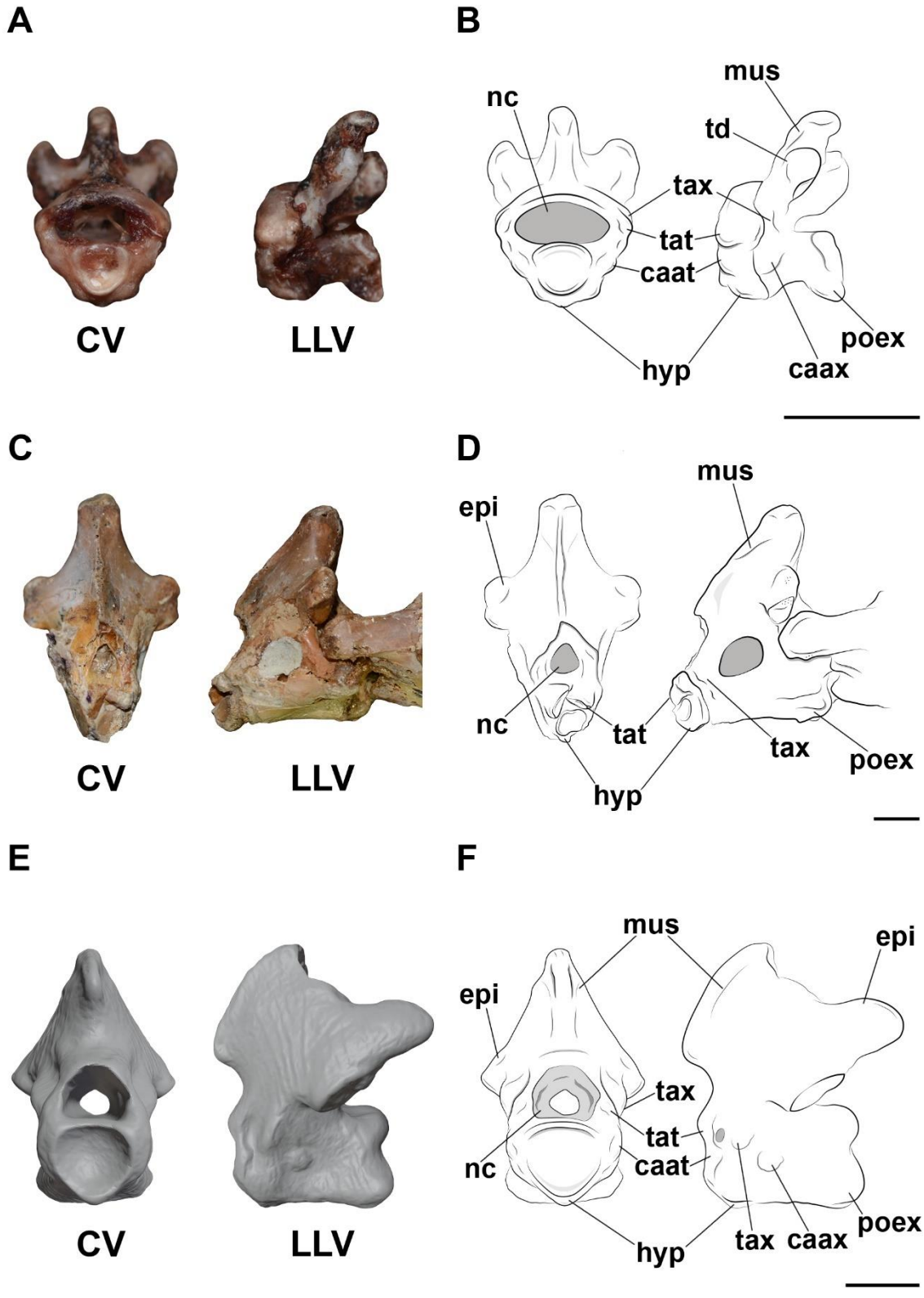

Figure 22. Photographs/3D models and interpretative drawings of the atlas and axis of *Procellaria aequinoctiallis* (A, B), *Anhanguera piscator* (C, D) and *Azhdarcho lancicollis* (E, F) in cranial (CV) and left lateral view (LLF). Dotted regions indicate greater surface roughness. Scale bar: 10 mm.

In the rest of the vertebrae, the hypapophyses of all analyzed pterosaurs are well developed ventrocranially, as in extant birds, and are longer in the mid-cervical vertebrae.

The hypapophysis of the eighth vertebra of pterosaurs is pronounced and extends cranioventrally, and it is wider than the hypapophyses present in the mid-cervical vertebrae (Figure 2). The preexapophyses are located laterally to the hypapophysis of each vertebra in *Anhanguera piscator* and *Azhdarcho lancicollis*, as seen in extant birds ventrally to the *ansa costotransversaria* (Figure 2). These pterosaurs have the preexapophyses of the eighth vertebra longer than those in ninth vertebra, but the hypapophysis and preexapophyses of the posterior cervicals are not as developed as in the mid-cervicals (Figure 2). We observed the presence of a *capitulum* in the entire cervical series of *Rhamphorhynchus muensteri*, in the same region where preexapophyses are present in the other pterosaurs analyzed, indicating the presence of articulation surfaces for the cervical ribs (Figure 2). The *ansa costotransversaria* of pterosaurs is not developed as in extant birds (Figure 2). Short bony structures that extend ventrolaterally to the *ansa costotransversaria* are defined here as tubercles in all pterosaurs analyzed, after the developed *tuberculum ansae* in extant birds (Figure 2). *Anhanguera piscator* and *Azhdarcho lancicollis* have transverse processes longer than tubercles in the posterior cervical vertebrae, as in more posterior cervicals of extant birds (Figure 2).

Robust epipophyses are present on the dorsal surface of the postzygapophyses of *Anhanguera piscator* e *Azhdarcho lancicollis*, as seen on the *torus dorsalis* in extant birds (Figure 2). The epipophyses of the eighth vertebra are the most developed of all in the cervical series, while in the ninth vertebra they are more discrete (Figure 2). Transverse-oblique crests are seen in *Anhanguera piscator* and *Azhdarcho lancicollis* and are shorter and more concave than in extant birds. The posterior cervical vertebrae of *Azhdarcho lancicollis* do not present the region of the transverse-oblique crests preserved, however, in *Anhanguera piscator* the crests are reduced in the eighth vertebra and absent in the ninth. The neural spines are tall throughout the cervical series in *Anhanguera piscator* and *Rhamphorhynchus muensteri*, which are observed in the counter slab in the latter. The cervical vertebrae of *Azhdarcho lancicollis* have reduced or absent neural spines in the mid-cervical vertebrae. In *Anhanguera piscator*, the posterior cervical vertebrae have tall neural spines with a blade-like shape, differing from the shape commonly presented in mid-cervical vertebrae, which are sharp-like (Figure 2), while the shape of the neural spines of *Rhamphorhynchus muensteri* does not vary along the neck, and the analyzed material of *Azhdarcho lancicollis* does not present this structure preserved in posterior vertebrae.

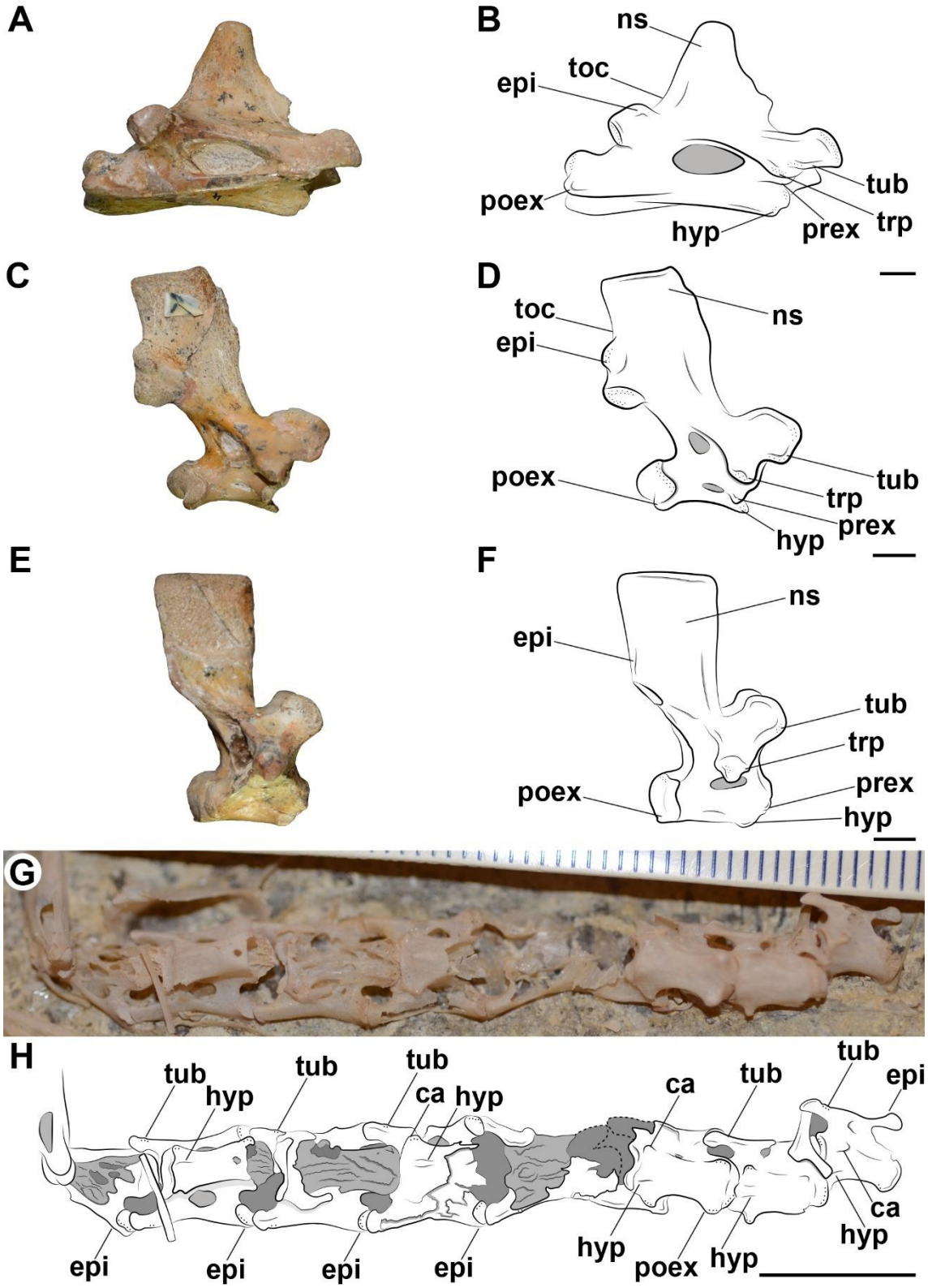

Figure 23. Photographs and interpretative drawings of the fifth (A, B), eighth (C, D) and ninth (E, F) cervical vertebrae of *Anhanguera piscator* in right lateral view and the articulated cervical series of *Rhamphorhynchus muensteri* in ventral view. Dotted regions indicate greater surface roughness. Scale bar: 10 mm.

Cervical musculature reconstruction

Epaxial muscles

Transversospinalis group

Transversospinalis capitis

This muscle is probably the most dorsal in the neck (Figure 3). Its insertion was probably on the dorsal portion of the supraoccipital crest of the skull, which is wide in *Anhanguera piscator* (Figure 4). It would probably be attached on the broad surfaces of the top of the neural spines of mid-cervical vertebrae, including on the reduced neural spines of the mid-cervical vertebrae of *Azhdarcho lancicollis* (Figure 5). The elongated top of the neural spine of the first dorsal (or notarial) vertebra and posterior cervical vertebrae indicates that the origins of the muscle were attached to them, as is observed in extant birds and crocodilians (Figure 5). Its wide areas of origin indicate robustness near the posterior cervical vertebrae, due to the width of the top of the neural spines (Table 1). We consider its presence to be supported as a level I inference by the EPB, being homologous to the *biventer cervicis* and *transversospinalis capitis* of extant birds and crocodilians, respectively.

Complexus

The muscle probably had a superficial position and was located craniolaterally in the neck (Figure 3). The *crista nuchalis transversa* bordering both lateral surfaces of the occipital region of the skull of *Anhanguera piscator* provides a wide area for its attachment (Figure 4). The muscle probably attached to the tubercles and epipophyses from the axis to the fourth vertebra, as is seen in extant birds and crocodilians (Figure 5). Its origin was probably on the tubercles developed laterally to the *ansa costotransversaria* of the fifth and sixth vertebrae and on the prominent epipophyses in the fourth and fifth vertebrae, which indicates that it extended along only the cranial half of the neck (Figure 5). The developed osteological correlates indicate a robust muscle, which may have presented its thickest portion between the third, fourth and fifth vertebrae (Table 1). According to the similarities of the osteological correlates, the muscle was probably homologous to the *complexus* and *transversospinalis capitis* of extant birds and crocodilians, respectively, representing a level I inference by the EPB.

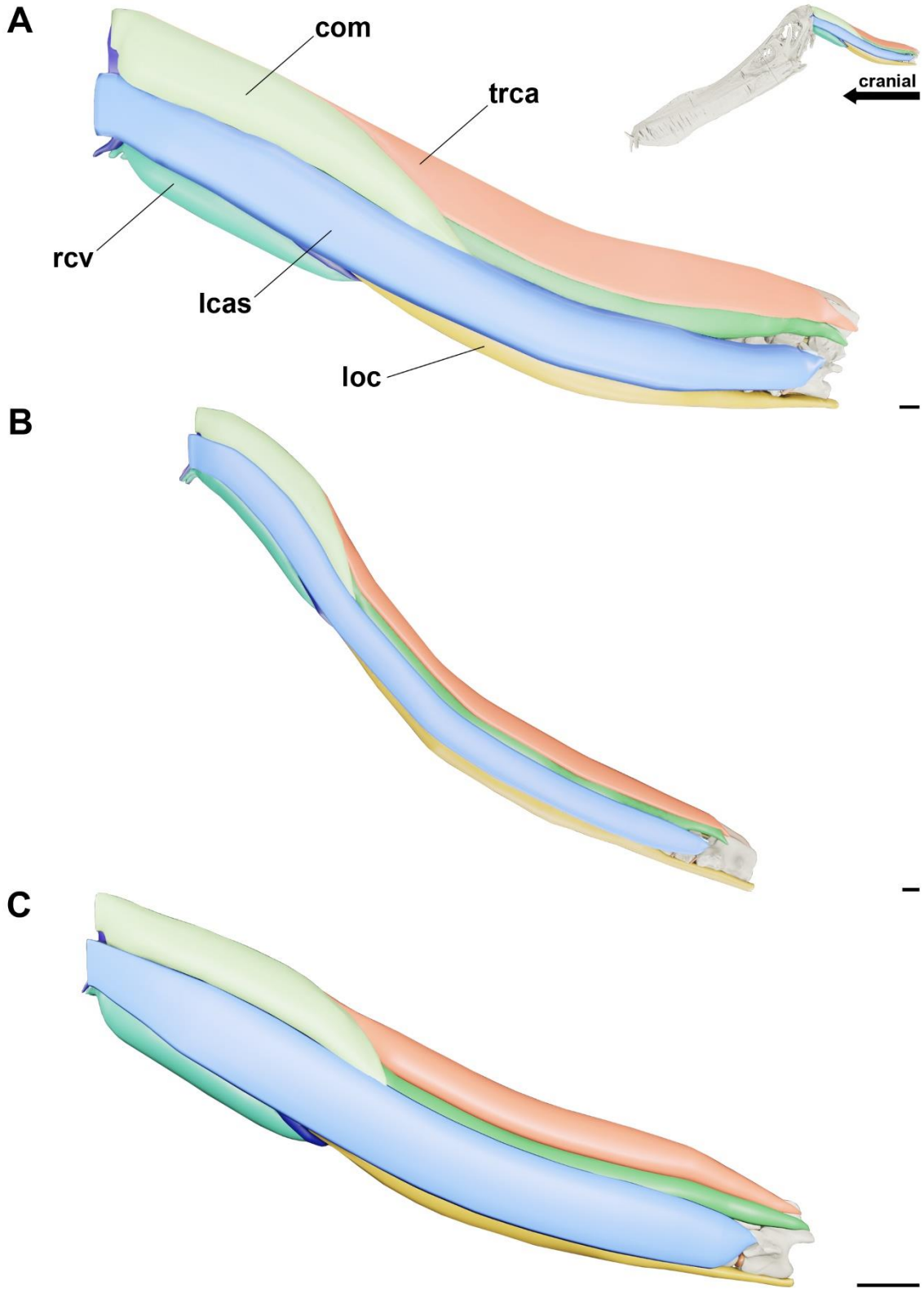

Figure 24. Cervical muscle reconstruction showing the superficial musculature of *Anhanguera piscator* (A), *Azhdarcho lancicollis* (B) and *Rhamphorynchus muensteri* (C) in left lateral view. Scale bar: 10 mm.

Transversospinalis cervicis

It was probably the deepest of the *transversospinalis* group, being overlapped by the *complexus*, *transversospinalis capitis*, and *longissimus capitis superficialis* (Figure 6). The presence of well-developed epipophyses in all cervical vertebrae of *Anhanguera piscator* and *Azhdarcho lancicollis* supports the presence of attachments of this muscle in each vertebra from the axis onwards, as in extant birds and crocodilians. Its origin was likely attached to the robust epipophyses of the seventh and eighth vertebrae and at the mid-height of the posterior edge of the neural spine of the ninth cervical or first dorsal (or notarial) vertebra, as seen in extant birds and crocodilians (Figure 5). Although the preservation of MGUH 1891.738 makes it difficult to visualize its correlates on the mid-cervical vertebrae, we observed the presence of developed epipophyses in the seventh, eighth and ninth vertebrae, confirming the presence of the origins of this muscle (Figure 2). According to the osteological correlates, this may have been the thickest cervical muscle in pterosaurs, based on the broad dorsolateral regions of the neural arch, mainly of the sixth and seventh vertebrae. Correlates support that it was likely homologous to the *longus colli dorsalis*, *pars. cranialis* and *caudalis*, in extant birds, and *transversospinalis cervicis*, in extant crocodilians, which indicates a level I inference by the EPB.

Splenius capitis

This muscle was single, arranged dorsomedially and superimposed by the cranial portions of the *complexus* and *transversospinalis capitis* (Figure 7). The depression surrounding the edge of the *crista nuchalis transversa* in the occipital region of the skull of *Anhanguera piscator* indicates that its insertions were probably completely overlapped by those of the *complexus* up to the most dorsal portion of the paraoccipitals. The muscle scar present on the cranial surface of the neural arch of the axis probably corresponds to the most cranial origin of this muscle. The slender shape of the cranial surface of the neural spine of the third vertebra suggests that the more caudal origin of *splenius capitis* attaches to this vertebra, as in extant birds (Figure 5). The presence of a muscle scar on the broad cranial surface of the axis neural arch suggests that the muscle was robust, but we must consider that this is the only muscle we infer for the neck that is not bilaterally arranged (Table 1). According to the osteological correlates identified, it would probably be homologous to the *splenius capitis* of extant birds, and to the *epistropheo-capitis* and *atloïdo-capitis* of extant crocodilians, which we consider a level I inference by the EPB.

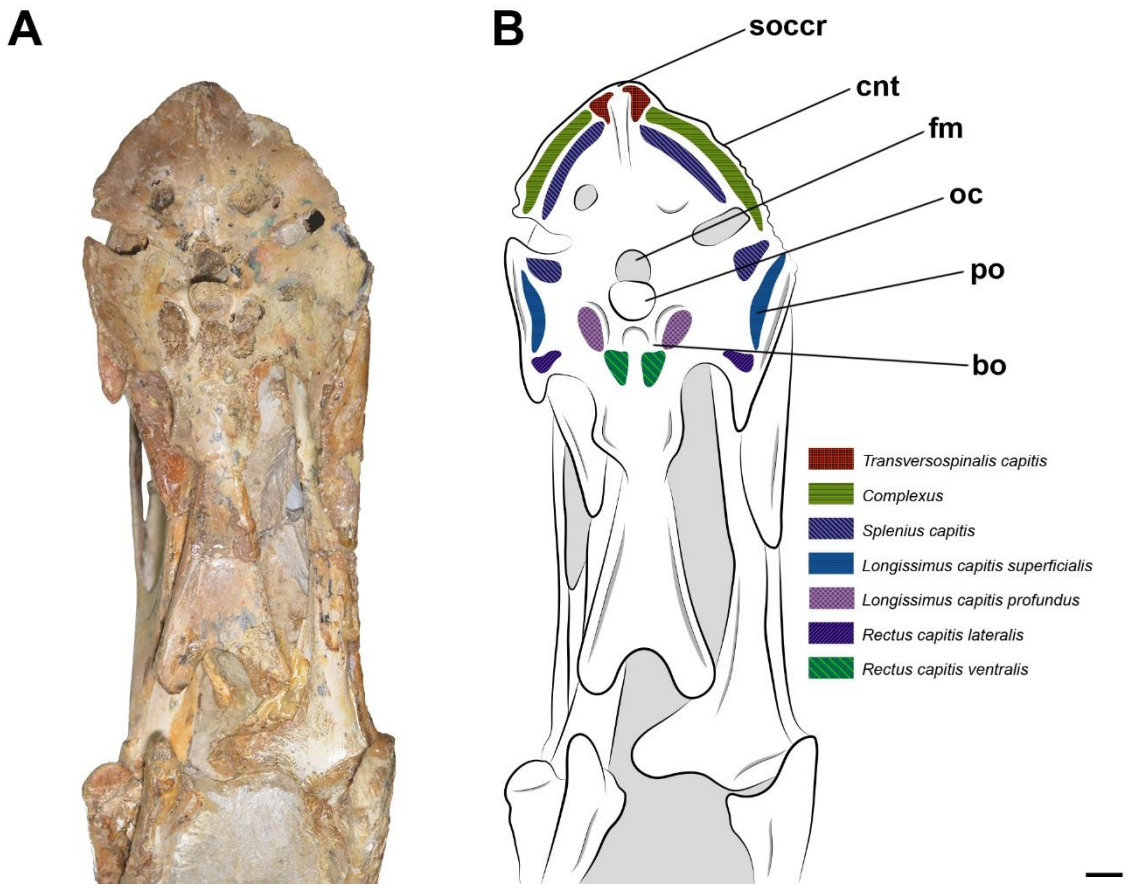

Figure 25. Photography (A) and interpretative drawing with locations of muscular attachments (B) of the occipital region of the skull of *Anhanguera piscator*. Scale bar: 10 mm.

Intercristales

These muscles probably extended deeply throughout the cervical series, arranged laterally to the base of the neural spines and superimposed by the *transversospinalis cervicis* (Figure 7). The prominent transverse oblique crest presented caudolaterally to the bases of the neural spines of *Anhanguera piscator* and *Azhdarcho lancicolis* indicates that their attachments were present from their insertion on the axis to their origins in the seventh and eighth vertebra, in which the transverse oblique crest is more concave due to the morphology of the epipophyses (Figure 5). Due to the mode of preservation of MGUH 1891.738, we can observe these structures only at the origins of the muscles in the posterior cervical vertebrae; however, it was likely present in the rest of the cervical series of *Rhamphorhynchus muensteri*. Shallow osteological correlates indicate that these muscles were extremely thin (Table 1). They were likely homologous to the *intercristales* and *interarticulares* of extant birds and crocodilians, respectively, representing a level I inference by the EPB.

Interspinales

These muscles are arranged in segments between the neural spines of the cervical vertebrae, probably bordering the *ligamentum elasticum insterspinale* (Figure 7). The cranial and caudal ends of the neural spines of the cervical vertebrae are thick and have a slight concavity at their margin, indicating attachments of a pair of thin muscles from the neural spine of the axis to that of the dorsal vertebrae (Figure 5). These muscles are homologous to the *interspinales* present in extant birds and crocodilians, which supports their presence as a level I inference by the EPB.

Longissimus and *Iliocostalis* group

Longissimus capitis superficialis

It is probably the most superficial muscle of this group (Figure 6). The lateral margins of the paraoccipitals in the skull of *Anhanguera piscator* provide a wide area of insertion, as in extant crocodilians (Figure 6). The transverse processes gradually increase in length from the fifth to the posterior cervical vertebrae, supporting the hypothesis that this muscle was attached to each vertebra from the half to the end of the cervical series (Figure 5). Although the preservation of MGUH 1891.738 attached to a slab makes analysis difficult, we observed that more developed transverse processes are also present from the fifth vertebra onwards. The origin of the muscle was probably associated with the broad transverse processes of the ninth cervical and first dorsal vertebrae, as is also seen in extant crocodilians. The broad surfaces of the transverse processes suggest that the *longissimus capitis superficialis* was the most robust muscle disposed laterally to the cervical series. Apparently, there is no homologue in extant birds, which is consistent with a level II inference by the EPB in this case.

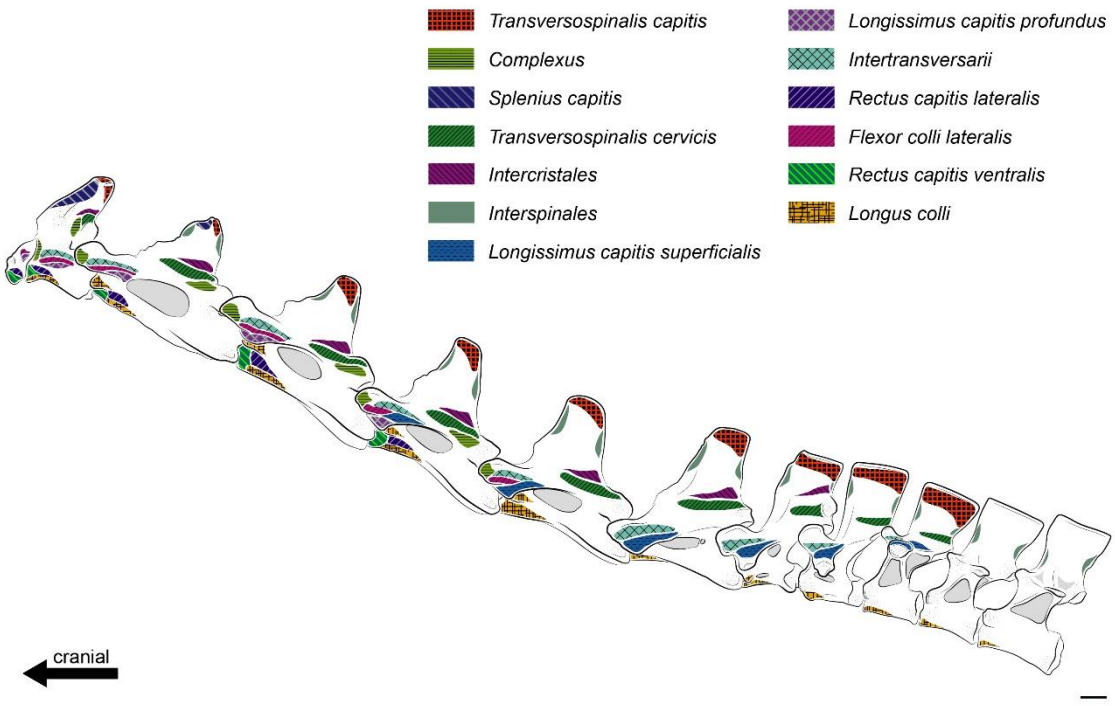

Figure 26. Locations of muscular attachments in the cervical vertebral column of *Anhanguera piscator*. Scale bar: 10 mm.

Longissimus capitis profundus

This muscle would be superimposed by the *longus capitis superficialis* (Figure 6). Probably, the depressions on the basioccipital bones of *Anhanguera piscator* are its insertion sites, as in extant birds and crocodilians (Figure 4). It attached to the short transverse processes of the first half of the neck of pterosaurs, as also seen in extant crocodilian vertebrae (Figure 5). In extant birds its attachments occur on the costal processes, which are absent in pterosaur vertebrae. In extant crocodilians, the origin of the *longissimus capitis profundus* is also anterior to the muscular attachments of the *longissimus capitis superficialis*. The origin of the *longissimus capitis profundus* in pterosaurs was possibly on the fifth vertebra, which supports the inference of a thin muscle arranged laterally to the cervical series (Table 1). It would probably be homologous to the *rectus capitis dorsalis* and *longissimus capitis profundus* of extant birds and crocodilians, respectively. We thus consider a level I inference for the presence and position of the muscle insertion and level II for the rest of the muscle attachments.

Table 10. Established area of muscle origins and maximum suggested thickness of each inferred cervical muscle. This table disregards the bilateral arrangement.

	Area of muscle origin (cm^2)	Muscle thickness (cm^2)
Anhanguera piscator		
Transversospinalis capitis	0.8088	4.853
Complexus	1.0961	6.577
Transversospinalis cervcicis	1.9211	11.527
Splenius capitis	1.5710	9.426
Intercristales	0.1720	0.516
Interspinales	0.1183	0.355
Longissimus capitis superficialis	0.8003	2.401
Longissimus capitis profundus	0.1806	0.542
Flexor colli	0.1036	0.311
Intertransversarii	0.2990	0.897
Longus colli	1.2503	7.502
Rectus capitis ventralis	0.6238	3.743
Rectus capitis lateralis	0.3983	1.195
Azhdarcho lancicollis		
Transversospinalis capitis	0.2995	1.377
Complexus	0.3925	2.355
Transversospinalis cervicis	0.4135	2.481
Splenius capitis	0.5861	3.517
Intercristales	0.0190	0.057
Interspinales	0.0060	0.018

Longissimus capitis superficialis	0.2783	0.835
Longissimus capitis profundus	0.0580	0.174
Flexor colli	0.0706	0.212
Intertransversarii	0.0846	0.254
Longus colli	0.5278	3.167
Rectus capitis ventralis	0.3921	2.353
Rectus capitis lateralis	0.2070	0.621
Rhamphorhynchus muensteri		
Transversospinalis capitis	0.0378	0.227
Complexus	0.0541	0.325
Transversospinalis cervicis	0.0806	0.484
Splenius capitis	0.0801	0.481
Intercristales	0.0043	0.013
Interspinales	0.0016	0.005
Longissimus capitis superficialis	0.0330	0.099
Longissimus capitis profundus	0.0213	0.064
Flexor colli	0.0110	0.033
Intertransversarii	0.0243	0.073
Longus colli	0.072	0.433
Rectus capitis ventralis	0.0350	0.210
Rectus capitis lateralis	0.0226	0.068

Flexor colli

It was probably superimposed by the *longissimus capitis superficialis* and extended laterally to the neural arch of the cranial half of the cervical series (Figure 6). The most cranial insertions of this muscle would attach to the osteological correlates present laterally to the centrum and intercentrum of the axis and atlas, respectively, probably next to the attachments of the *longissimus capitis profundus* (Figure 5). The presence of tubercles laterally on the *ansa costotransversaria* in the third, fourth and fifth vertebrae in the analyzed pterosaurs indicates the presence of muscular attachments along the cervical series, as in extant birds and crocodilians (Figure 5). We consider that its origin was on the tubercles of the sixth vertebra, which are more developed than in the more cranial vertebrae of *Azhdarcho lancicollis* and *Rhamphorhynchus muensteri*, although they still suggest a thin muscle (Table 1). It was probably homologous to the *flexor colli lateralis*, in extant birds, and portions of the *longissimus cervicis* and *iliocostalis cervicis*, in extant crocodilians. The attachment sites of both muscles in extant crocodilians are found near the prezygapophyses and on the cervical ribs, differing from the position and anatomy of the osteological correlates present in the vertebrae of *Anhanguera piscator*. Therefore, we suggest the presence of only one *flexor colli* muscle disposed laterally, as observed in extant birds, representing an EPB II inference for the position of the insertions.

Intertransversarii

We suggest the presence of this muscle laterally to the neural arch of the cervical series and superimposed by the *flexor colli* and *longissimus capitis profundus*, in the first half of the neck, and by the *longissimus capitis superficialis*, along its entire length (Figure 7). The muscle was attached to the concavity that borders the lateral tubercles of vertebrae from its insertion on the axis to its origin in the ninth cervical and first dorsal vertebra (Figure 5). The small areas of origin indicate that this was the thinnest long muscle of the pterosaur neck (Table 1). It is present with the same nomenclature in both extant taxa, but in birds it is superficial and in crocodilians, deeper (as we suggest here for pterosaurs). As the characteristics of the osteological correlates of the attachment sites are similar in both extant taxa, we establish them as an EPB inference level I.

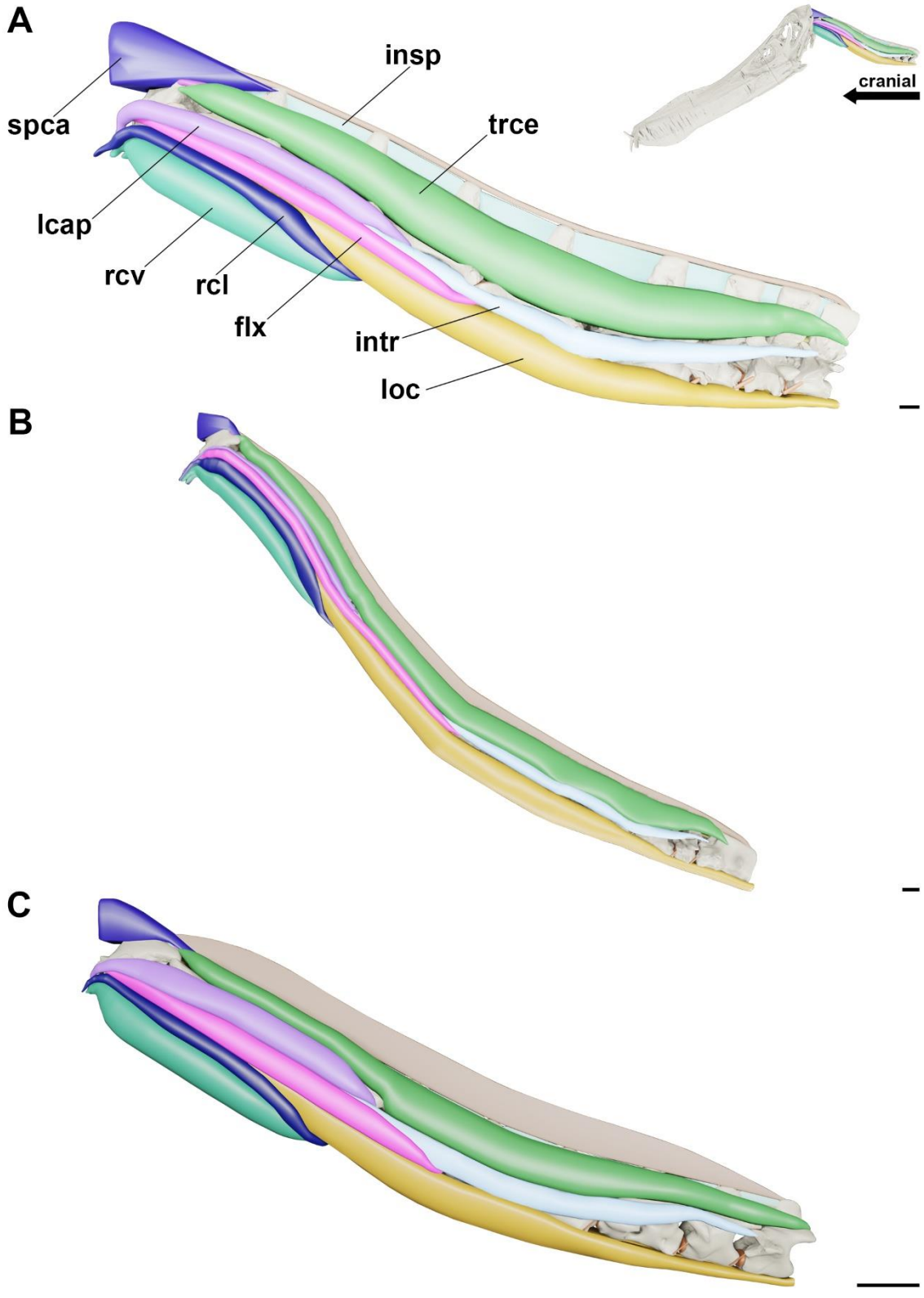

Figure 27. Muscular reconstruction of the neck of *Anhanguera piscator* (A), *Azhdarcho lancicollis* (B) and *Rhamphorynchus muensteri* (C), without the *transversospinalis capitis*, *complexus* and *longissimus capitis superficialis*, in left lateral view. Scale bar: 10 mm.

Hypaxial muscles

Longus colli

We suggest that this muscle was positioned ventrally to the cervical vertebrae, being superimposed by the *rectus capitis ventralis* in the first half of the neck and superficial in the other half (Figure 7). The prominence present in ventral view of the centrum of the axis of *Anhanguera piscator* and *Rhamphorhynchus muensteri* and on the first third of the length of the atlas-axis of *Azhdarcho lancicollis* is possibly associated with its insertion (Figure 5). The well-developed hypapophyses and preexapophyses in all mid-cervical vertebrae suggests that the muscle was attached along the entire neck (Figure 5). The cervical ribs of *Rhamphorhynchus muensteri* probably also had attachment sites, as in extant crocodilians (Figure 5). Its origin is restricted to the attachment on the hypapophyses of the eighth cervical to the third dorsal vertebrae (Figure 5). The wide areas of origin on the posterior cervical and first dorsal vertebrae support the presence of a robust muscle, mainly in the caudal half of the neck (Table 1). It is probably homologous to the *longus colli ventralis* in extant birds and to portions of the *longus colli* in extant crocodilians. In extant archosaurs, the origin is on the ventral surface of the centrum and the hypapophyses of the posterior cervical and free thoracic vertebrae, indicating that the muscle could also be as long in pterosaurs. In *Anhanguera piscator* and *Azhdarcho lancicollis*, additional attachments could be established in the preexapophyses, due to the scars and roughness of this structure, as in the carotid processes of extant birds. The attachments suggested represent an inference level I for the hypapophyses and ventral surfaces of the centrum. However, an inference level III is considered for attachments in preexapophyses.

Rectus capitis ventralis

This muscle was superficial and located ventrally (Figure 6). It probably inserted into the depressions observed on the ventrolateral surface of the basioccipital of the skull of *Anhanguera piscator* (Figure 4). We suggest that it was attached to vertebrae that had well-developed hypapophyses, which would indicate its origin on the fifth vertebra and further attachments from the intercentrum of the atlas to the fourth vertebra in all analyzed pterosaurs (Figure 5). An origin on the highly developed hypapophyses allows the inference of a robust muscle limited in length, from the head to the half of the neck (Table 1). It was homologous to the *rectus capitis ventralis*, which attaches to the hypapophyses of the vertebrae of extant birds, and to the *rectus capitis anticus major*, which attaches to the ventral processes of the vertebrae of extant crocodilians. The insertion in both extant taxa is concentrated on each side of the ventral portion of the basioccipital, as we suggest

in *Anhanguera piscator*. Therefore, the muscle insertions described here can be considered an EPB inference level I.

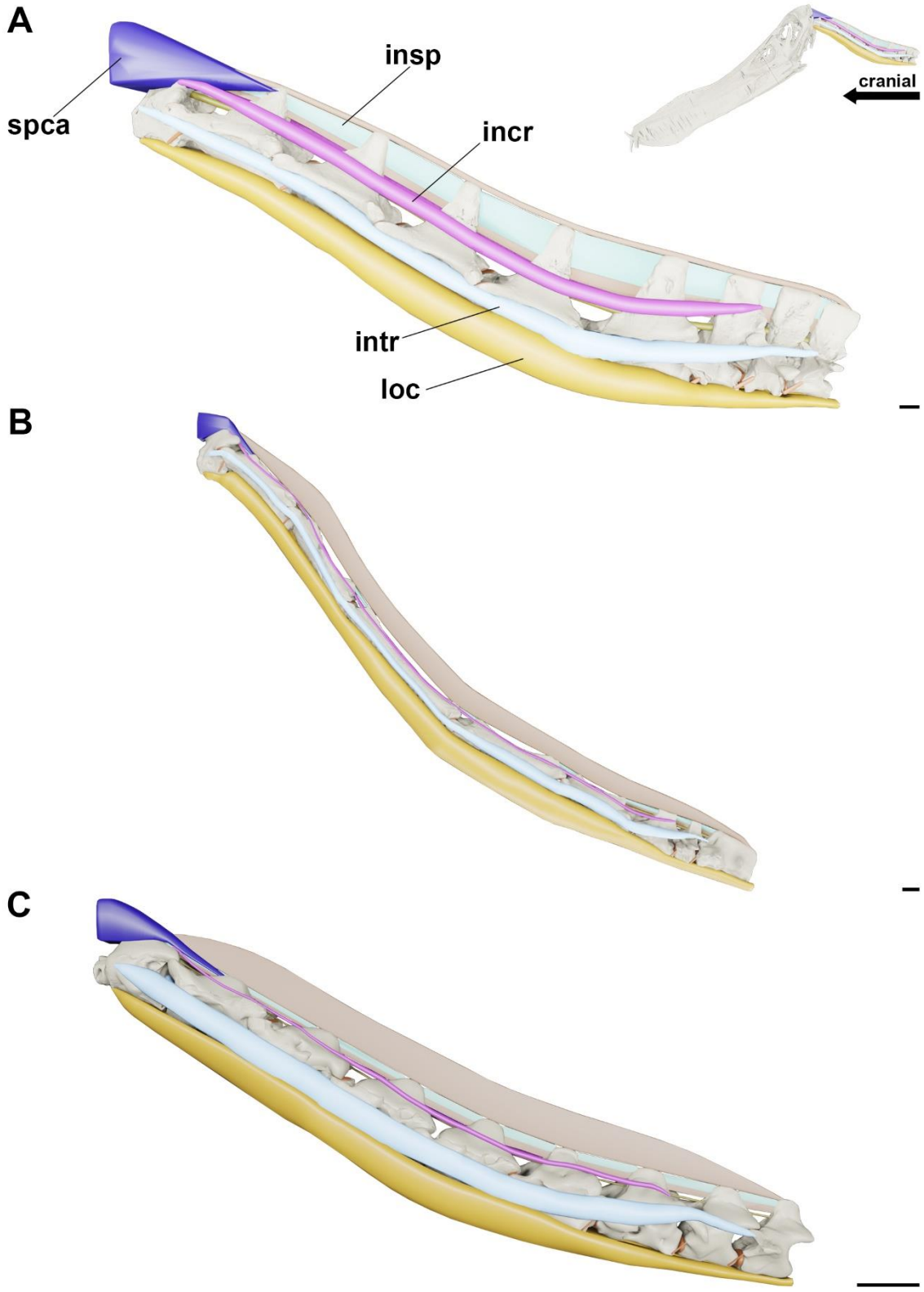

Figure 28. Muscular reconstruction of the neck of *Anhanguera piscator* (A), *Azhdarcho lancicollis* (B) and *Rhamphorynchus muensteri* (C) without the *transversospinalis capitis*, *complexus*, *transversospinalis*

cervicis, *longissimus capitis superficialis*, *longissimus capitis profundus*, *flexor colli*, *rectus capitis ventralis* and *rectus capitis lateralis* in left lateral view. Scale bar: 10 mm.

Rectus capitis lateralis

It was probably superimposed by the *longissimus capitis superficialis* (Figure 6). The pronounced ventral margins of the paraoccipital processes in the skull of*Anhanguera piscator* support the inference of its insertion (Figure 4). The atlas and axis attachments would likely be on the ventrolateral surface of the centrum and intercentrum, respectively (Figure 5). In *Rhamphorhynchus muensteri*, this muscle was probably attached to the ventral surfaces of the capitulum of the vertebrae of the cranial half of the neck. The origin would probably also be on the developed hypapophyses of the fourth and fifth vertebrae, but on the lateral surfaces. According to the attachment surfaces of the origins, this muscle was the thinnest of the hypaxial muscles and extended from the head to the half of the neck (Table 1). It was likely homologous to the *rectus capitis lateralis* and to a portion of the *iliocostalis capitis* of extant birds and crocodilians, respectively. The attachment sites in the capitulum of the vertebrae of *Rhamphorhynchus muensteri* are similar to those seen in extant crocodilians. The attachments on the hypapophyses is similar to that observed in extant birds, which present these prominent structures in the anterior segment of the neck, as discussed in Chapter I. Therefore, we assume an EPB inference I for the muscle attachments.

Maximum possible force production ($F_{pmax)}$ by the cervical muscles

According to our reconstruction, the cervical muscle arrangement was the same size in width and height and its shape was circular in cross-sectional view anywhere in the neck (Figure 8). The area filled by epaxial muscles in any region of the neck is larger than the area containing hypaxial muscles, being approximately double in *Anhanguera piscator* and *Rhamphorhynchus muensteri*. The larger epaxial area is due to the thickness of the *transversospinalis* muscles, the number of epaxial muscles, and their dorsal and lateral arrangements. Laterally to the cervical vertebrae, the sum of the width of musculature on both sides corresponds to approximately one third of the total width at the widest point of any cross-section of the neck. This same value also represents 50% of the width of the vertebra (Figure 8). The sum of the width of both sides of the lateral cervical musculature varies between species and is proportionately thinner in *Azhdarcho lancicollis*, representing 32 to 34% of the total width of the neck transverse sections, while

Anhanguera piscator and *Rhamphorhynchus muensteri* present 35 to 36.5% and 33.5 to 34%, respectively.

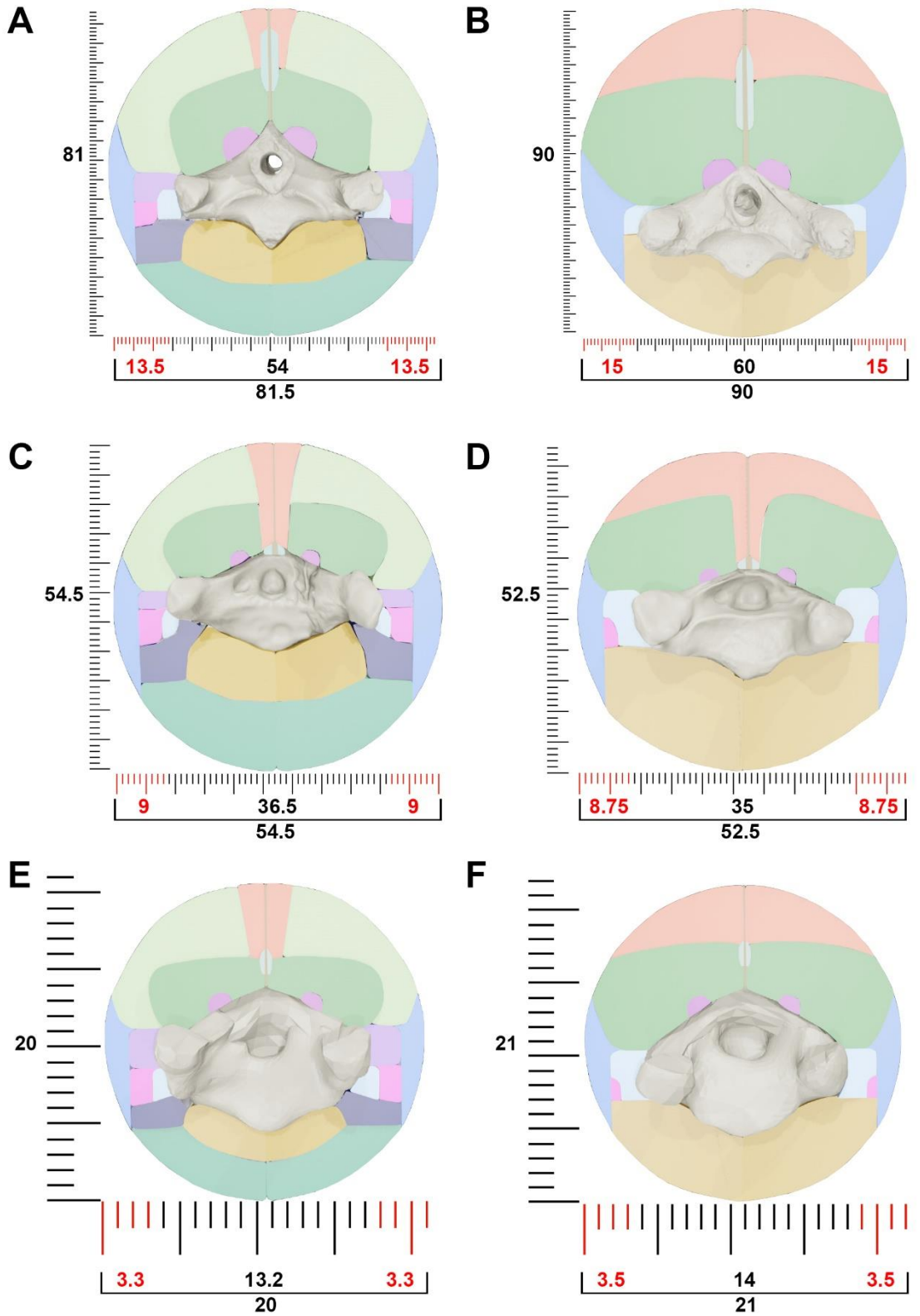

Figure 29. Cross-section showing the fourth (A) and seventh (B) cervical vertebra of *Anhanguera piscator*, the fourth (C) and sixth (D) cervical vertebra of *Azhdarcho lancicollis* and the fourth (E) and sixth (F) cervical vertebra of *Rhamphorhynchus muensteri* in cranial view. The ruler on the left and below each cross-section shows the height and the width of the neck, respectively. The red marks on the ruler below

the cross-section indicate that the width of the lateral musculature, which together represents approximately one third of the total width of the neck and 50% of the width of the vertebra. Ruler measurements shown in millimeters.

The most robust muscles of the neck were those whose thickness corresponded to six times their area of origin (Table1). According to our estimates, the longer and more superficial musculature has a greater potential than the deep muscles and/or than the musculature limited to the first segment of the neck (Table 2). The F_{pmax} calculated for the *transversospinalis capitis* and *transversospinalis cervicis*, and for the *longus colli* and *rectus capitis ventralis* muscles, indicate an optimal potential for neck extension and flexion, respectively (Table 2) (Snively & Russell, 2007). The great potential of the *longissimus capitis superficialis*, together with the *transversospinalis capitis*, probably ensured vast lateral incursions of the neck and skull (Table 2) (Snively & Russell, 2007).

Table 11. Area established for the locations of maximum thickness of each inferred cervical muscle and Maximum possible force production (F_{pmax}) of each muscle. The cross-sectional areas were multiplied by two for muscles arranged bilaterally.

	Cross-sectional area (cm^2)	**F_{pmax} (N)**
Anhanguera piscator		
Transversospinalis capitis	9.706	242.65
Complexus	13.154	328.85
Transversospinalis cervicis	23.054	576.35
Splenius capitis	9.426	235.65
Intercristales	1.032	25.80
Interspinales	0.710	17.75
Longissimus capitis superficialis	4.802	120.05
Longissimus capitis profundus	1.084	27.10
Flexor colli	0.622	15.55
Intertransversarii	1.794	44.85

Longus colli	15.004	375.10
Rectus capitis ventralis	7.486	187.15
Rectus capitis lateralis	2.390	59.75
Azhdarcho lancicollis		
Transversospinalis capitis	2.754	68.85
Complexus	4.710	117.75
Transversospinalis cervicis	4.962	124.05
Splenius capitis	3.517	87.925
Intercristales	0.114	2.85
Interspinales	0.036	0.90
Longissimus capitis superficialis	1.670	41.75
Longissimus capitis profundus	0.348	8.70
Flexor colli	0.424	10.60
Intertransversarii	0.508	12.70
Longus colli	6.334	158.35
Rectus capitis ventralis	4.706	117.65
Rectus capitis lateralis	1.242	31.05
Rhamphorhynchus muensteri		
Transversospinalis capitis	0.454	11.35
Complexus	0.650	16.25
Transversospinalis cervicis	0.968	24.20
Splenius capitis	0.481	12.02

Intercristales	0.026	0.65
Interspinales	0.010	0.25
Longissimus capitis superficialis	0.198	4.95
Longissimus capitis profundus	0.128	3.20
Flexor colli	0.066	1.65
Intertransversarii	0.146	3.65
Longus colli	0.866	21.65
Rectus capitis ventralis	0.420	10.50
Rectus capitis lateralis	0.136	3.40

The *splenius capitis* also has great potential for lateral movements in the cranial segment of the neck, along with the *rectus capitis lateralis* which performs this function in the same region (Snively & Russell, 2007). The reconstructed height of the *longissimus capitis superficialis* and the potential of the *splenius capitis* and *rectus capitis lateralis* are consistent with the ability to perform twisting movements of the skull and the neck (Snively & Russell, 2007).

The low potentials recovered for the *flexor colli* and *longissimus capitis profundus* are explained by the presence of muscles such as *rectus capitis ventralis* and *longissimus capitis superficialis*, which are more robust and perform the flexion and torsion function, respectively (Snively & Russell, 2007). The low potential of the *intercristales* and *interspinales* indicate that they were probably related to the stabilization of the cervical series (Snively & Russell, 2007; Carlson, 1978).

Discussion

Of the thirteen pterosaur muscles we reconstructed here, only the *longissimus capitis superficialis* and *flexor colli* had not a EPB level I inference because we could not recognize the correlate of the muscle attachment site present in one of the extant archosaurs (Tsuihiji, 2005; 2007; Snively & Russell, 2007). Nevertheless, we consider

that the tubercles representing vestiges of transverse processes in *Anhanguera piscator* and *Azhdarcho lancicollis* indicate an attachment site for the *longissimus capitis superficialis* and the *flexor colli* (Naish & Witton, 2017).

The proportion of height and width of all cross-sections of the cervical muscles is equivalent to that observed in extant birds (Figure 8) (Chapter I). The lateral musculature corresponding to one third of the width at the widest point of any cross-section of the neck is also observed in extant birds and supports our inferences on the thickness of muscles disposed laterally to the cervical series in pterosaurs (Chapter I). This proportion also agrees with the measurements presented by the neck muscles of the dissected alligator.

Our inference of the *transversospinalis capitis* with a more medial insertion on the supraoccipital crest of *Anhanguera piscator* differs from the hypothesis of a dorsolateral insertion on the occipital region of the skull of the azhdarchid *Hatzegopteryx*, which would indicate an attachment on the edges of the nuchal crest (Naish & Witton, 2017). Here, we assume that the nuchal crest anchored the insertion of the *complexus*, as in extant birds, because besides their role in extension, the muscles attached to the broad *crista nuchalis transversa* would contribute greatly to the lateral movement of the skull (Burton, 1974; Snively & Russell, 2007). Our inference of the insertion of the *longissimus capitis superficialis* on the wide paraoccipitals of *Anhanguera piscator* agrees with the hypothesis that a robust muscle would attach to this surface in *Hatzegopteryx* (Naish & Witton, 2017), although Naish and Witton (2017) inferred it to be the *spino-capitis posticus*. In any case, either the *longissimus capitis superficialis* or the *spino-capitis posticus* would dorsally extend and/or laterally flex the neck, due to the position of the insertion and other muscle attachments of both of them, as observed along the cervical series in extant crocodilians (Cleuren & De Vree, 2000; Tsuihiji, 2005; 2007; Snively & Russell, 2007). Besides the *transversospinalis capitis* and *longissimus capitis superficialis* presenting great F_{pmax}, they probably extended to the base of the neck and would insert on large surfaces of the dorsal and lateral portions of the occipital region of the skull, which would confer mechanical advantage for dorsal extension and lateral movements of the head and neck (Seidel, 1978; Frey, 1988; Cleuren & De Vree, 2000; Snively & Russell, 2007; Naish & Witton, 2017).

The sturdiness and strength we suggest for the muscles limited to the cranial half of the pterosaur neck is consistent with the wide and developed insertion sites present on the occipital region of *Anhanguera piscator* (Witmer et al., 2003; Habib & Godfrey, 2010). The insertion of the *longissimus capitis profundus* and *rectus capitis ventralis* on the wide concavities of the basioccipitals of *Anhanguera piscator* would provide a great mechanical advantage for ventral neck flexion (Cleuren & De Vree, 2000; Naish & Witton, 2017). Our identification of osteological correlates that indicate the insertion and origin of the *splenius capitis* on the skull and third vertebra, respectively, was similar to that observed in *Hatzegopteryx*, although in that pterosaur the muscle was named as the homologous *epistropheo-capitis* (Naish & Witton, 2017).

The atlas and axis of *Anhanguera piscator* and *Azhdarcho lancicollis* are morphologically similar to those of extant birds and crocodilians, but the pterosaur axis has more osteological correlates in common with extant birds (Mook, 1921). The anatomy of both vertebrae is consistent with the great potential for torsion and ventral flexion that the *splenius capitis*, *longissimus capitis profundus* and *rectus capitis* muscles could exert on them (Cleuren & De Vree, 2000; Dzemski & Christian, 2007; Witton & Naish, 2008, Taylor et al., 2009; Guinard et al., 2010). The reduced neural spines in azhdarchids and the evolutionary change of transverse processes into tubercles in all pterosaurs analyzed are consistent with slightly thinner muscles associated with the mid-cervical vertebrae when compared to those at the base of the neck (Naish & Witton, 2017). However, muscle scars may be less prominent in the middle of the neck, as they may not be associated with an insertion nor origin, which are usually more expressive attachments to ensure mechanical advantage (Naish & Witton, 2017).

Attachments to the neural spines of the mid-cervical vertebrae demonstrate that the *transversospinalis capitis* is thick along the cranial half of the neck in pterosaurs, differing from the thin *biventer cervicis* of extant birds, as seen in Chapter I. Despite the reduced neural spines in the mid-cervical vertebrae of *Azhdarcho lancicollis*, the presence of the *transversospinalis capitis* in azhdarchid pterosaurs has been proposed previously based on the height of the neural spines at the cranial and caudal ends of the neck (Witton & Naish, 2008). Furthermore, our estimates of muscle thickness indicate a slightly thick musculature dorsally, as also observed in avian vertebrae, which have a reduced neural spine (Chapter I). This demonstrates that the size of a correlate should not be the only indication of muscle thickness (Naish & Witton, 2017).

Our reconstruction of a *transversospinalis cervicis* attached to the epipophyses agrees with previous inferences about extensor muscles being attached to zygapophyses in azhdarchid vertebrae (Herrel & De Vree, 1999; Tsuihiji, 2005; Snively & Russell, 2007). Our inferred length for the *transversospinalis cervicis* along the neck of *Rhamphorhynchus muensteri* is also supported by the presence of epipophyses in mid-cervical vertebrae (Wellnhofer, 1975). Despite the developed extensor muscles, neck extension in *Anhanguera piscator* and *Rhamphorhynchus muensteri* probably did not allow for an extremely sinuous neck, due to limitations imposed by the tall neural spines and elongate prezygapophyses (Witton & Naish, 2008; Molnar et al., 2015).

The developed hypapophyses provide an area for the attachment of the *longus colli* in all mid-cervical vertebrae of the analyzed pterosaurs, differing from extant archosaurs, which frequently present this pronounced structure only near the base of the neck (Chamero et al., 2014; Iijima & Kubo, 2019; Chapter I), but whose developed cervical ribs provide additional attachment sites in the first segment of the neck (Cleuren & De Vree, 2000; Tsuihiji, 2007; Snively & Russell, 2007). Furthermore, the presence of hypapophyses prevents the opening of the *sulcus caroticus* and, thus, the presence of carotid processes, which are attachment sites for the *longus colli ventralis* in the second neck segment in extant birds (Tsuihiji, 2007; Snively & Russell, 2007). The large hypapophyses and postexapophyses limit ventral flexion less than the neural spines limit extension (Witton & Naish, 2008). The convex condyles of the mid-cervical vertebrae and the robustness of the *transversospinalis capitis* and *cervicis* and of the *longus colli* indicate ample dorsoventral flexion in the mid-neck (Burton, 1974; Frey, 1988; Tsuihiji, 2004; Dzemski & Christian, 2007; Snively & Russell, 2007; Fronimos & Wilson, 2017; Iijima & Kubo, 2019).

We suggest attachments of the *longissimus capitis superficialis* from the fifth to the ninth vertebrae in *Anhanguera piscator* due to the similarity of the osteological correlates present in the specimen AMNH 22555, identified as *Anhanguera* sp., which has the sixth and cranial portions of the seventh vertebrae preserved (Wellnhofer, 1991; Pinheiro & Rodrigues, 2017). The *longissimus capitis superficialis* was probably less thick in the cranial half of the neck, indicating that it exerted lateral incursions with greater intensity in the caudal cervical portion (Cleuren & De Vree, 2000). However, the presence of the *complexus*, *splenius capitis* and *rectus capitis lateralis*, which also move the skull laterally, would contribute to the complexity of these movements (Burton, 1974,

Snively & Russell, 2007). The mid-portion of the neck of *Azhdarcho lancicollis* has the thinnest lateral musculature of the analyzed pterosaurs, which may be due to its elongate vertebrae, but yet it is only slightly thinner than in *Anhanguera piscator* and *Rhamphorhynchus muensteri*, supporting the hypothesis that azhdarchids also have strong lateral musculature (Naish & Witton, 2017).

Our reconstruction of the *complexus*, *longissimus capitis profundus*, *flexor colli*, *rectus capitis ventralis* and *rectus capitis lateralis* muscles extending from the skull to the fifth or sixth vertebra in pterosaurs is similar to that observed in Aequorlitornithes, as discussed in Chapter I. However, in pterosaurs this length reaches approximately half the neck, while in extant birds it does not exceed the first cervical segment (Chapter I). We named the muscle "*flexor colli*" here without specifying its lateral or medial arrangement, as we did not find evidence to support the presence of another flexor muscle belonging to the *iliocostalis* group, as seen in extant birds (Tsuihiji, 2007). The absence of the sixth vertebra and of the cranial portion of the seventh vertebra also made it difficult to infer the origin of the *complexus*, *longissimus capitis profundus*, *flexor colli*, *rectus capitis ventralis* and *rectus capitis lateralis* muscles in *Anhanguera piscator* (Kellner & Tomida, 2000). However, the presence of developed tubercles and short hypapophyses in the sixth and seventh vertebrae in AMNH 22555 (Wellnhofer, 1991) support our inferences as postcranial elements are very similar within the genus (Kellner & Tomida, 2000).

The length of six muscles (*complexus*, *splenius capitis*, *longissimus capitis profundus*, *flexor colli*, *rectus capitis ventralis* and *rectus capitis lateralis*) being limited to about half of the neck indicates that the cranial cervical portion could be subject to great stress (Dzemski & Christian, 2007). The F_{pmax} of the *complexus* and *rectus capitis ventralis* is higher than that of the *transversospinalis cervicis* and *longus colli* in the cranial portion of the neck, suggesting that both were the ones mainly responsible for the dorsoventral and lateral movements of the skull (Table 2) (Burton, 1974; Cleuren & De Vree, 2000; Snively & Russell, 2007). Furthermore, although the *longissimus capitis profundus*, *flexor colli*, and *rectus capitis lateralis* have considerably lower F_{pmax}, they probably contributed additional force to extension, flexion, and lateral movements of the skull, respectively (Cleuren & De Vree, 2000; Snively & Russell, 2007). The absence or reduction of transverse processes, tubercles and cervical ribs in the most cranial mid-cervical vertebrae indicate that lateral movements performed mainly by *transversospinalis*, *splenius capitis* and *rectus capitis lateralis* muscles could be wider

close to the skull (Burton, 1974; Cleuren & De Vree, 2000; Dzemski & Christian, 2007; Snively & Russell, 2007; Witton & Naish, 2008; Molnar et al., 2015).

We suggest that in pterosaurs the *intercristales* muscles attach to the developed transverse oblique crests in the mid-cervical vertebrae, differing from that seen in extant crocodilians, although the muscle attachments occur anatomically at the same location (Tsuihiji, 2005; Snively & Russell, 2007; Chamero et al., 2014; Iijima & Kubo, 2019). The F_{pmax} of the *intercristales* was the lowest compared to the other long muscles, but was constant throughout its length, probably conferring stability and contributing to intervertebral dorsoventral flexion in the mid-cervical series (Table 2) (Snively & Russell, 2007).

The posterior cervical vertebrae of all analyzed pterosaurs have more developed osteological correlates than the mid-cervical vertebrae, due to the attachment of muscular origins being more robust than others along the cervical series (Kellner & Tomida, 2000; Averianov, 2013, Naish & Witton, 2017). The cranio-caudal increase in height, length and thickness of the top of the neural spines of the cervical vertebrae of *Anhanguera piscator* and *Rhamphorhynchus muensteri* is also present in extant crocodilians and indicates a more robust *transversospinalis capitis* in the caudal half of the neck (Chamero et al., 2014; Iijima & Kubo, 2019). Such robustness would optimize the F_{pmax} for executing the movement in this cervical region (Table 2), agreeing with the hypothesis of a great mechanical advantage for neck extension (Seidel, 1978; Frey, 1988; Snively & Russell, 2007; Naish & Witton, 2017).

Our interpretation of the *tranversospinalis cervicis* and *longus colli* being thicker between the end of the mid-cervical vertebrae and the beginning of the posterior cervical vertebrae is consistent with the developed epipophyses and hypapophyses, which were, respectively, probable attachment sites for each muscle in this region of the neck in pterosaurs (Wellnhofer, 1975; Wellnhofer, 1991; Averianov, 2010). The great F_{pmax} of both muscles is consistent with the execution of ventral flexion, dorsal extension and lateral incursions of a slightly sinuous neck in this region, considering the raising of the head in an alert position or lowering it to the ground for foraging (Seidel, 1978; Frey, 1988; Cleuren & De Vree, 2000; Snively & Russell, 2007). Cervical dorsal extension performed by the *transversospinalis* muscles would also be optimized by robust epaxial ligaments mainly in the caudal half of the neck, which contributed to support the skull

and maintain the neck position at rest, as discussed in the previous chapter (Gál, 1993; Dzemski & Christian, 2007, Witton & Habib, 2010).

The wide transverse processes of the posterior cervical vertebrae provide attachment areas for the *longissimus capitis superficialis* and are compatible with its greater thickness near the base of the neck in pterosaurs, as present in extant archosaurs and discussed in Chapter I. A thicker *longissimus capitis superficialis* in the posterior segment of the neck probably optimized the dorsal extension, torsion and lateral movements, though the width of the transverse processes indicate less amplitude in this area (Cleuren & De Vree, 2000; Boas, 1929; Witton & Naish, 2008; Tambussi et al., 2012).

The robustness of the muscles, ligaments and synovial cartilages in the caudal portion of the neck provides flexibility and intensity to a rigid, less pneumatized, and stable region (Witton & Habib, 2010; Averianov, 2013; Gutzwiller et al., 2013; Iijima & Kubo, 2019; Buchmann at al., 2021; Chapters I and II). In all analyzed pterosaurs, the larger cranial surface of the neural spines of the posterior cervical vertebrae probably contributes to more robust and stronger *interspinales* muscles, which provide more stability to this neck sector (Carlson, 1978).

We suggest attachments of the *complexus*, *longissimus capitis profundus*, and *intertransversarii* muscles along the neck to rough surfaces of the *ansa costotransversaria* of pterosaur vertebrae. In extant birds and crocodilians, they attach to the vertebrae by aponeuroses (Snively & Russell, 2007; Chapter I). This is also observed for the *flexor colli lateralis* in extant birds and for the *longissimus colli superficialis* in extant crocodilians (Snively & Russell, 2007; Chapter I). The *transversospinalis cervicis* is the only muscle we inferred whose respective homologues have aponeurotic attachments to smooth bony surfaces in extant birds and crocodilians (Snively & Russell, 2007; Chapter I). Therefore, we assumed the aforementioned muscles could be also be aponeurotic in pterosaurs, which would ensure more stability and strength for their muscle fibers (McGowan, 1979; 1986; Bryant & Seymour, 1990; Snively & Russell, 2007). The fibers of the *complexus*, which we suggest attach to epipophyses, and of the *longus colli*, *rectus capitis ventralis* and *rectus capitis lateralis* muscles, which we propose attach to hypapophyses, probably do so by tendons, as seen in extant archosaurs (Snively & Russell, 2007; Chapter I), that if so would confer greater mobility and

flexibility to them (McGowan, 1979; 1986; Bryant & Seymour, 1990; Snively & Russell, 2007).

Conclusion

Based on the osteological correlates present in the cervical vertebrae of the analyzed pterosaurs, we infer the presence of thirteen cervical muscles, of which only two didn't have an inference level I by the EPB criteria. Six of them probably had limited length from the head to about the middle of the cervical series, enabling complex movements and a mobile head, but likely subjected the cranial cervical region to more stress.

We estimate that the area filled by the epaxial muscles was greater than that of the hypaxial muscles and that the sum of the widths of both lateral muscles represents one third of the total width in all cross-sections. The height and width of the neck had the same proportion in all regions, as in extant archosaurs.

The *interspinales* and *intercristales* muscles have low strength potential, which indicates that both had a limited role in cervical stabilization. The *longissimus capitis profundus* and *flexor colli* also showed low potential, but that may be related to the existence of stronger muscles that are also responsible for rotating and flexing the neck, restricting the function of both muscles to additional force movements and flexibility.

The hypaxial muscles were attached by tendons, while the epaxial muscles were more often attached by aponeuroses, which could have provided more stability for the latter, especially in origins near the base of the neck, and more flexibility for the hypaxial flexors.

The robust neck musculature we inferred for pterosaurs would ensure mobility and strength for a long neck, which also supports a relatively long skull. The muscles with the greatest potential for force production were the neck extensors and flexors, which probably provided intensity for the execution of dorsoventral movements. Their robustness in approximately the middle of the neck and the complexity of the vertebral anatomy also indicates that these dorsoventral movements may have been performed with greater amplitude and intensity in that region. However, estimates of cervical motion should be inferred with caution, as many of the properties that influence mechanics can be difficult to observe in fossils. Other factors must also be considered for the execution

of the movements we discuss, such as vertebral bone resistance to loads and tensions generated by soft tissues.

Acknowlegments

We thank Niels Bonde (Zoological Museum, Denmark), Maria Eduarda Castro Leal (Zoological Museum, Denmark), Alexander Averianov (Zoological Institute of the Russian Academy of Sciences, Russia), Takanobu Tsuihiji (National Museum of Nature and Science, Japan), Makoto Manabe (National Museum of Nature and Science, Japan) and Chisako Sakata (National Museum of Nature and Science, Japan), who CT-scanned the specimens and gently shared the data with us. We would like to thank Dr. Fabiana Costa and M.Sc. Rodrigo Pêgas for their help in photographing the specimens. We thank Dr. Felipe Montefeltro for the valuable discussions about archosaur musculature. We are also grateful to the coordinators and staff of the Institute for the Research and Rehabilitation of Marine Animals (Instituto de Pesquisa e Reabilitação de Animais Marinhos - IPRAM) (Cariacica, Brazil), of the Caiman Project (Vitória, Brazil), and of the Universidade Federal do Espírito Santo Veterinary Hospital (Alegre, Brazil). This study was partially funded by Coordenação de Aperfeiçoamento de Pessoal de Nível Superior – Brazil (CAPES) – Finance Code 001 (scholarship to RB) and by Conselho Nacional de Desenvolvimento Científico e Tecnológico (CNPq) (project grant #421412/2018-6 to TR). The funders had no role in study design, data collection and analysis, decision to publish, or preparation of the manuscript.

References

Andres B, Langston Jr W. 2021. Morphology and taxonomy of *Quetzalcoatlus* Lawson 1975 (Pterodactyloidea: Azhdarchoidea). Journal of Vertebrate Paleontology 41: 46–202.

Averianov AO. 2010. The osteology of *Azhdarcho lancicollis* (Nessov, 1984) (Pterosauria, Azhdarchidae) from the late Cretaceous of Uzbekistain. Proceedings of the Zoological Institute RAS 314: 264–317.

Averianov AO. 2013. Reconstruction of the neck of *Azhdarcho lancicollis* and lifestyle of azhdarchids (Pterosauria, Azhdarchidae). Paleontological Journal 47: 203–209.

Baumel JJ, Raikow RJ. 1993. Arthrologia. In: Baumel JJ, King AS, Breazile JC, Evans HE, Vanden Berge JC, editors. Handbook of avian anatomy: Nomina anatomica avium. Cambridge, MA: Nuttal Ornihtological Club. 133–187.

Bennett SC. 2001. The osteology and functional morphology of the Late Cretaceous pterosaur *Pteranodon* Part I. General description of osteology. Palaeontographica Abteilung A 260: 1–112.

Bennett SC. 2003. Morphological evolution of the pectoral girdle of pterosaurs: myology and function. Geology Society Special Publications 217: 191–125.

Blender Development Team. (2019). Blender (Version 2.91) [Computer software]. https://www.blender.org

Boas JEV. 1929. Biologisch-anatomische Studien über den Hals der Vögel. Kongl. Danske Vidensk. Selsk. Skrifter, Naturvidensk. Math (Ser. 9) 1: 105–222.

Bonde N, Christiansen P. 2003. The detailed anatomy of *Rhamphorhynchus*: axial pneumaticity and its implications. Geology Society Special Publications 217: 21–232.

Bryant HN, Seymour KL. 1990. Observations and comments on the reliability of muscle reconstruction in fossil vertebrates. Journal of Morphology 206: 109–117.

Buchmann R, Rodrigues T, Polegario S & Kellner AWA. 2018. New information on the postcranial skeleton of the Thalassodrominae (Pterosauria, Pterodactyloidea, Tapejaridae). Historical Biology 30: 1139–1149.

Buchmann R, Holgado B, Sobral G, Avilla LS, Rodrigues T. 2021. Quantitative assessment of the vertebral pneumaticity in an anhanguerid pterosaur using micro-CT scanning. Scientific Reports 11:18718.

Burton PJK. 1974. Feeding and the feeding apparatus in waders: a study of anatomy and adaptations in the Charadrii. London, England: British Museum Press 719.

Carlson H. 1978. Morphology and contraction properties of cat lumbar back muscles. Acta Physiologica Scandinavica 103: 180–197.

Chamero B, Buscalioni AD, Marugán-Lobón J, Sarris I. 2014. 3D geometry and quantitative variation of the cervico-thoracic region in Crocodylia. The Anatomical Record 297: 1278–1291.

Cleuren J, De Vree F. 2000. Feeding in crocodilioans. In: Schwenk K, editor. Feeding: form, function, and evolution in tetrapod vertebrates. San Diego, CA: Academic Press. 337–358.

Cobley MJ, Rayfield EJ, Barrett PM. 2013. Inter-Vertebral Flexibility of the Ostrich Neck: Implications for Estimating Sauropod Neck Flexibility. Plos One 8 (8): e72187.

Dzemski G, Christian A. 2007. Flexibility along the neck of the ostrich (*Struthio camelus*) and consequences for the reconstruction of dinosaurs with extreme neck length. Journal of Morphology 268: 701–714.

Eck K, Elgin RA, Frey E. 2011. On the osteology of *Tapejara wellnhoferi* KELLNER 1989 and the first occurrence of a multiple specimen assemblage from the Santana Formation, Araripe Basin, NE-Brazil. Swiss Journal of Palaeontology 130: 277-296.

Elgin RA, Frey E. 2011. A new azhdarchoid pterosaur from Cenomanian (Late Cretaceous) of Lebanon. Swiss Journal of Geosciences 104: 21–33.

Frey E. 1988. Anatomie des Korperstammes von Alligator mississippiensis Daudin. Stuttgarter Beitrage zur Naturkunde 424: 1–106.

Fronimos JA, Wilson JA. 2017. Concavo-convex intercentral joints stabilize the vertebral column in sauropod dinosaurs and crocodylians. Ameghiniana 54 (2): 151–176.

Gál JM. 1993. Mammalian spinal biomechanics 2: intervertebral lesion experiments and mechanisms of bending resistance. Journal of Experimental Biology, 174, 281–297.

Guinard G, Marchand D, Courant F, Gauthier-Clerc M, Le Bohec C. 2010 Morphology, ontogenesis and mechanics of cervical vertebrae in four species of penguins (Aves: Sphenicidae). Polar Biology, 33: 807–822.

Gutzwiller SC, Su A, O'Connor PM. 2013. Postcranial pneumaticity and bone structure in two clades of neognath birds. The Anatomical Record 296: 867–876.

Habib M, Godfrey S. 2010. On the hypertrophied opisthotic processes in *Dsungaripterus weii* Young (Pterodactyloidea, Pterosauria). Acta Geocientica Sinica 31: 26.

Herrel A, De Vree F. 1999. The cervical musculature in helodermatid lizards. Belgian Journal of Zoology 129: 175–186.

Herzog W. 2007. Muscle. In: Nigg BM, Herzog W, editors. Biomechanics of the musculoskeletal system. Chinchester, England: 3rd ed. John Wiley & Sons. 337–358.

Humphries S, Bosner RHC, Witton MP, Martill, DM. 2007. Did pterosaurs feed by skimming? Physical modelling and anatomical evaluation of an unsual feeding method. Plos Biology, 5, 1647–1655.

Iijima M, Kubo T. 2019. Comparative morphology of presacral vertebrae in extant crocodylians: taxonomic, functional and ecological implications. Zoological Journal of the Linnean Society 186: 1006–1025.

Kellner AWA, Tomida Y. 2000. Description of a new species of Anhangueridae (Pterodactyloidea) with comments on the pterosaur fauna from the Santana Formation (Aptian-Albian), Northeastern, Brazil. National Science Museum, Monographs, Tokyo, 17: 1–135.

Kellner AWA, Langston Jr. W. 1996. Cranial remains of *Quetzalcoatlus* (Pterosauria, Azhdarchidae) from Late Cretaceous sediments of Big Bend National Park, Texas. Journal of Vertebrate Paleontology 16: 222–231.

Kellner AWA, Campos DA. 2002. The function of the cranial crest and jaw of a unique pterosaur from the Early Cretaceous of Brazil. Science 297: 389–392.

McGowan, C. 1979. The hind limb musculature of the Brown kiwi, *Apteryx australis mantelli*. Journal of Morphology, 160, 33–74.

McGowan, C. 1986. The wing musculature of the Weka (*Gallirallus australis*), a flightless rail endemic to New Zealand. Journal of Zoological Society of London, 210, 305–346.

Molnar JL, Pierce SE, Hutchinson JR. 2014. An experimental and morphometric test of the relationship between vertebral morphology and joint stiffness in Nile crocodiles (*Crocodylus niloticus*). Journal of Experimental Biology 217: 758–768.

Molnar JL, Pierce SE, Bhullar BAS, Turner AH, Hutchinson JR. 2015. Morphological and functional changes in the vertebral column with increasing aquatic adaptation in crocodylomorphs. Royal Society Open Science 2: 150439.

Mook CC. 1921. Notes on the postcranial skeleton in the Crocodilia. Bulletin of the American Museum of Natural History 44: 67–100.

Naish D, Witton MP. 2016. Neck biomechanics indicate that giant Transylvanian azhdarchid pterosaurs were shirt-necked arch predators. PeerJ 5: e2908.

Nesov LA. 1984. Pterosaurs and birds of the Late Cretaceous of Central Asia. Palaontologische Zeitschrift 1: 47–57.

Padian K, Cunningham JR, Langston Jr. W, Conway J. 2021. Functional morphology of *Quetzalcoatlus* Lawson 1975 (Pterdactyloidea: Azhdarchoidea). Journal of Vertebrate Paleontology 41: 218–251.

Pinheiro FL, Rodrigues T. 2017. *Anhanguera* taxonomy revisited: is our understanding of Santana Group pterosaur diversity biased by poor biological and stratigraphic control? PeerJ 5: e3285.

Porro LB, Holliday CM, Anapol F, Ontiveros LC, Ontiveros LT, Ross CF. 2011. 2011. Free body analysis, beam mechanics, and finite elements modeling of the mandible of *Alligator mississippiensis*. Journal of Morphology 272: 910–937.

Prieto IR. 1998. Morfología funcional y hábitos alimentarios de Quetzalcoatlus (Pterosauria). Coloquios de Paleontologia 49: 129–144.

Salisbury SW, Frey E. 2001. A biomechanical transformation model for the evolution of semi-spheroidal articulations between adjoining vertebral bodies in crocodilians. In: Grigg GC, Seebacher F, Franklin CE. Crocodilian biology and evolution. Surrey Beatty & Songs, Chipping Norton, p. 85–134.

Schneider CA, Rasband WS, Eliceiri KW. 2012. NIH Image to ImageJ: 25 years of image analysis. Nature Methods 9: 671–675.

Schwarz D, Frey E, Meyer CA. 2007. Pneumaticity and soft-tissue reconstructions in the neck of diplodocid and dicraeosaurid sauropods. Acta Palaentologica Polonica 52: 167–188.

Seidel R. 1978. The somatic musculature of the cervical and occipital regions of Alligator mississippiensis. PhD dissertation, City University of New York.

Snively E, Russell AP. 2007. Functional morphology of neck musculature in the Tyrannosauridae (Dinosauria, Theropoda) as determined via a hierarchical inferential approach. Zooloical Journal of the Linnean Society 151: 759–808.

Tambussi CP, de Mendoza R, Degrange FJ, Picasso MB. 2012. Flexibility along the Neck of the Neogene Terror Bird *Andalgalornis steulleti* (Aves Phorusrhacidae). Plos One 7 (5): e37701.

Taylor MP, Wedel MJ, Naish D. 2009. Head and neck posture in sauropod dinosaurs inferred from extant animals. Acta Palaeontologica Polonica 54 (2): 213–220.

Tsuihiji T. 2004. The ligament system in the neck of *Rhea americana* and its implication for the bifurcated neural spines of sauropod dinosaurs. Journal of Vertebrate Paleontology 24 (1): 165–172.

Tsuihiji T. 2005. Homologies of the *transversospinalis* muscles in the anterior presacral region of Sauria (crown Diapsida). Journal of Morphology 263: 151–178.

Tsuihiji T. 2007. Homologies of the *longissimus*, *iliocostalis*, and hypaxial muscles in the anterior presacral region of extant diapsida. Journal of Morphology 268: 986–1020.

Veldmeijer AJ, Meijer HJM, Signore M. 2009. Description of pterosaurian (Pterodactyloidea: Anhangueridae, *Brasileodactylus*) remains from the Lower Cretaceous of Brazil. Deinsea 13: 9–40.

Vila Nova BC, Sayão JM, Langer MC, Kellner AWA. Comments on the cervical vertebrae of the Tapejaridae (Pterosauria, Pterodactyloidea) with description of new specimens. Historical Biology 27: 770–780.

Wellnhofer P. 1975. Die Rhamphorhynchoidea (Pterosauria) der Oberjura-Plattenkalke Süddeutschlands. Palaeontographica Abt. A 148: 1–33.

Wellnhofer P. 1991. Weitere Pterosaurierfunde aus der Santana-Formation (Apt) der Chapada do Araripe, Brasilien. Palaeontographica Abt. A 215: 43–101.

Witmer LM. 1995. The Extant Phylogenetic Bracket and the importance of reconstructing soft tissues in fossils. In: Thomason JJ, editor. Functional morphology in vertebrate palaeontology. Cambridge: Cambridge University Press. 19–33.

Witmer LM, Chatterjee S, Franzosa J, Rowe, T. 2003. Neuroanatomy of flying reptiles and implications for flight, posture and behavior. Nature 425: 950–953.

Witton MP, Naish D. 2008. A reappraisal of azhdarchid pterosaur functional morphology and paleoecology. Plos One 3: e2271.

Witton MP, Habib MB. 2010. On the size and flight diversity of giant pterosaurs, the use of birds as pterosaur analogues comments on pterosaur flightlessness. Plos One 5: e13982.

Zusi RL. 1962. Structural adaptations of the head and neck in the Black Skimmer, *Rhynchops nigra* Linnaeus. Publications of the Nuttal Ornithological Club 3: 1–153.

Final Conclusions

The cervical vertebrae of extant birds vary anatomically in different segments of the neck, which reflect on the morphology of the associated soft tissues and consequently on the flexibility of the different cervical sectors. Pelecaniformes was the group that most differed among the Aequorlitornithes, due to the level of overlap of the zygapophyses, sites of muscle attachments and the thickness of the intervertebral spaces and muscles. The thin synovial cartilage and the level of overlap of zygapophyses did not significantly increase cervical length in Aequorlitornithes birds, as is the case of vertebrate necks that have intervertebral discs. However, the presence of synovial cartilage influences the angulation between the vertebrae in the neck position at rest, considering that the center of rotation would be located in the intervertebral space. The intervertebral spaces, ligaments and muscles of the Aequorlitornithes are thickest in the third segment of the neck, which we hypothesize is a response to biomechanical requirements. Aequorlitornithes showed roughness and scars on the vertebrae related to their soft tissue attachments, which facilitate the recognition of osteological correlates in fossil species.

The osteological correlates indicate that the intervertebral space of the pterosaur neck was likely filled with thin synovial cartilage, as in extant birds. The pterosaur neck position at rest differs from a vertical neck and from the division into three mobile segments as in extant birds. However, the analyzed pterosaurs had a slight cervical sinuosity, which is more pronounced in *Azhdarcho lancicollis* due to the high angulation present between their posterior cervical vertebrae.

Four ligaments were identified associated with rough surfaces and/or scars in avian vertebrae that were also recognized in correlates present in pterosaurs. These ligaments would confer joint stiffness, cervical stabilization, and the execution of passive forces in pterosaurs, such as restoring the neutral position of the neck without energy expenditure, as occurs in extant birds.

We identified thirteen cervical muscles according to osteological correlates in pterosaur vertebrae, from sixteen cervical muscles associated with scarring and/or roughness on the vertebral surface we recognized in birds. Most aponeurotic muscle attachments were associated with rough surfaces in extant birds. Tendon attachments were common for hypaxial muscles with ventral neck flexion function in birds. We inferred the same types of attachments for each muscle in pterosaurs due to the similarity

of the correlates, which probably contributed to greater cervical stabilization for epaxial muscles and flexibility for hypaxial muscles.

The maximum thickness of the cervical muscles responsible for dorsoventral flexion in extant birds was approximately six times their area of origin. The other muscles had their maximum thickness equivalent to three times the area of origin. This proportion proved to be reliable to reconstruct the neck of pterosaurs, due to the similarity of the muscular origins and vertebral morphology. Besides, musculature arranged laterally to the cervical series represented approximately one third of the width of the vertebrae, and the height and width of the neck cross-section were the same size in all regions. This allowed us to confirm that the inferred volumes of the pterosaur muscles were adequate for the complete cervical arrangement.

The cervical muscles that were potentially the strongest were those with dorsoventral flexion function, which possibly provided intensity to this movement. The low potential of the *interspinales* and *intercristales* muscles is probably due to the limitation of the stability and joint flexion function of both. The low force potential obtained for some muscles with limited length between the head and the middle of the neck may mean that they are mostly synergistic, exerting only additional forces and/or contributing to the flexibility of complex movements.

The presence of thicker vertebral spaces and more developed osteological correlates in the vertebrae from the middle to the base of the neck of pterosaurs support the hypothesis that the synovial cartilage, ligaments, and muscles would be thicker in the caudal half of the neck, as is also observed in the extant birds. This probably contributed to a wider angulation between the vertebrae, more resistance to the ligaments, and more robustness for the execution of muscle movement in this region, which we hypothesize is a response to the biomechanical demands at the base of the neck.

References

Aires ASS, Reichert LM, Müller RT, Pinheiro FL, Andrade MB. 2021. Development and evolution of the notarium in Pterosauria. Journal of Anatomy 238: 400–415.

Alvarenga HMF, Höfling E. 2003. Systematic revision of the Phorusrhacidae (Aves: Ralliformes). Papéis Avulsos de Zoologia, Museu de Zoologia da Universidade de São Paulo 43 (4): 55–91.

Anchundia DJ, Anderson JF, Anderson DJ. 2017. Overland flight by seabirds at Isla Isabela, Galápagos. Marine Ornithology 45: 139–141.

Andres B, Clark JM, Xing X. 2010. A new Rhamphorhynchid pterosaur from the upper Jurassic of Xinjiang, China, and the phylogenetic relationships of basal pterosaurs. Journal of Vertebrate Paleontology 30 (1): 163–187.

Andres B, Langston Jr W. 2021. Morphology and taxonomy of *Quetzalcoatlus* Lawson 1975 (Pterodactyloidea: Azhdarchoidea). Journal of Vertebrate Paleontology 41: 46–202.

Averianov AO. 2010. The osteology of *Azhdarcho lancicollis* (Nessov, 1984) (Pterosauria, Azhdarchidae) from the late Cretaceous of Uzbekistain. Proceedings of the Zoological Institute RAS 314: 264–317.

Averianov AO. 2013. Reconstruction of the neck of *Azhdarcho lancicollis* and lifestyle of azhdarchids (Pterosauria, Azhdarchidae). Paleontological Journal 47: 203–209.

Barbraud C, Johnson AR, Bertault G. 2003. Phenotypic correlates of post-fledging dispersal in a population of greater flamingos: the importance of body condition. Journal of Animal Ecology 72: 246–257.

Baumel JJ, Raikow RJ. 1993. Arthrologia. In: Baumel JJ, King AS, Breazile JC, Evans HE, Vanden Berge JC, editors. Handbook of avian anatomy: Nomina anatomica avium. Cambridge, MA: Cambridge University Press. 133–187.

Baumel JJ, Witmer LM. 1993. Osteologia. In: Baumel JJ, King AS, Breazile JC, Evans HE, Vanden-Berge JC, editors. Handbook of avian anatomy: nomina anatomica avium. Cambridge, MA: Cambridge University Press. 45–132.

Beccari V, Pinheiro FL, Nunes I, Anelli LE, Mateus O, Costa FR. 2021. Osteology of an exceptionally well-preserved tapejarid skeleton from Brazil: Revealing the anatomy of a curious pterodactyloid clade. Plos One 16 (8): e0254789.

Bennett SC. 2001. The osteology and functional morphology of the Late Cretaceous pterosaur *Pteranodon* Part I. General description of osteology. Palaeontographica Abteilung A 260: 1–112.

Bennett SC. 2003. Morphological evolution of the pectoral girdle of pterosaurs: myology and function. Geology Society Special Publications 217: 191–125.

Boas JEV. 1929. Biologisch-anatomische Studien über den Hals der Vögel. Kongl. Danske Vidensk. Selsk. Skrifter, Naturvidensk. Math (Ser. 9) 1: 105–222.

Bonde N, Christiansen P. 2003. The detailed anatomy of *Rhamphorhynchus*: axial pneumaticity and its implications. Geology Society Special Publications 217: 21–232.

Bryant HN, Seymour KL. 1990. Observations and comments on the reliability of muscle reconstruction in fossil vertebrates. Journal of Morphology 206: 109–117.

Buchmann R, Rodrigues T, Polegario S & Kellner AWA. 2018. New information on the postcranial skeleton of the Thalassodrominae (Pterosauria, Pterodactyloidea, Tapejaridae). Historical Biology 30: 1139–1149.

Buchmann R, Rodrigues T. 2019 The evolution of pneumatic foramina in pterosaur vertebrae. Anais da Academia Brasileira de Ciências 91: e20180782.

Buchmann R, Avilla LS, Rodrigues T. 2019. Comparative analysis of the vertebral pneumatization in pterosaurs (Reptilia: Pterosauria) and extant birds (Avialae: Neornithes). Plos One 14 (10): e0224165.

Buchmann R, Holgado B, Sobral G, Avilla LS, Rodrigues T. 2021. Quantitative assessment of the vertebral pneumaticity in an anhanguerid pterosaur using micro-CT scanning. Scientific Reports 11:18718.

Burton PJK. 1974. Feeding and the feeding apparatus in waders: a study of anatomy and adaptations in the Charadrii. London, England: British Museum Press 719.

Butler RJ., Barrett PM., Gower DJ. 2012. Reassessment of the evidence for postcranial skeletal pneumaticity in Triassic archosaurs, and the early evolution of the avian respiratory system. Plos One 7: e34094.

Carlson H. 1978. Morphology and contraction properties of cat lumbar back muscles. Acta Physiologica Scandinavica 103: 180–197.

Chamero B, Buscalioni AD, Marugán-Lobón J, Sarris I. 2014. 3D geometry and quantitative variation of the cervico-thoracic region in Crocodylia. The Anatomical Record 297: 1278–1291.

Cleuren J, De Vree F. 2000. Feeding in crocodilioans. In: Schwenk K, editor. Feeding: form, function, and evolution in tetrapod vertebrates. San Diego, CA: Academic Press. 337–358.

Cobley MJ, Rayfield EJ, Barrett PM. 2013. Inter-Vertebral Flexibility of the Ostrich Neck: Implications for Estimating Sauropod Neck Flexibility. Plos One 8 (8): e72187.

Dimery NJ, Alexander RM, Deyst KA. 1985. Mechanics of the ligamentum nuchae of some artiodactyls. Journal of Zoology 206 (3): 341–351.

Dzemski G, Christian A. 2007. Flexibility along the neck of the ostrich (*Struthio camelus*) and consequences for the reconstruction of dinosaurs with extreme neck length. Journal of Morphology 268: 701–714.

Eck K, Elgin RA, Frey E. 2011. On the osteology of *Tapejara wellnhoferi* KELLNER 1989 and the first occurrence of a multiple specimen assemblage from the Santana Formation, Araripe Basin, NE-Brazil. Swiss Journal of Palaeontology 130: 277-296.

Elgin RA, Frey E. 2011. A new azhdarchoid pterosaur from Cenomanian (Late Cretaceous) of Lebanon. Swiss Journal of Geosciences 104: 21–33.

Fasquelle B, Furet M, Chevallereau C, Wenger P. 2019. Dynamic modeling and control of a tensegrity manipulator mimicking a bird neck. Mechanisms and Machine Science 73: 2087–2097.

Frey E. 1988. Anatomie des Korperstammes von Alligator mississippiensis Daudin. Stuttgarter Beitrage zur Naturkunde 424: 1–106.

Fronimos JA, Wilson JA. 2017. Concavo-convex intercentral joints stabilize the vertebral column in sauropod dinosaurs and crocodylians. Ameghiniana 54 (2): 151–176.

Furet M, Van Riesen A, Chevallereau C, Wenger P. 2018. Optimal design of tensegrity mechanisms used in a bird neck model. Mechanisms and Machine Science 59: 365–375.

Gál JM. 1993. Mammalian spinal biomechanics 2: intervertebral lesion experiments and mechanisms of bending resistance. Journal of Experimental Biology, 174, 281–297.

Guinard G, Marchand D, Courant F, Gauthier-Clerc M, Le Bohec C. 2010 Morphology, ontogenesis and mechanics of cervical vertebrae in four species of penguins (Aves: Sphenicidae). Polar Biology, 33: 807–822.

Gutzwiller SC, Su A, O'Connor PM. 2013. Postcranial pneumaticity and bone structure in two clades of neognath birds. The Anatomical Record 296: 867–876.

Habib M, Godfrey S. 2010. On the hypertrophied opisthotic processes in *Dsungaripterus weii* Young (Pterodactyloidea, Pterosauria). Acta Geocientica Sinica 31: 26.

Herrel A, De Vree F. 1999. The cervical musculature in helodermatid lizards. Belgian Journal of Zoology 129: 175–186.

Herzog W. 2007. Muscle. In: Nigg BM, Herzog W, editors. Biomechanics of the musculoskeletal system. Chinchester, England: 3rd ed. John Wiley & Sons. 337–358.

Howse SCB. 1986. On the cervical verteabrae of the Pterodactyloidea (Reptilia: Archosauria). Zoological Journal of the Linnaean Society 88: 307–328.

Humphries S, Bosner RHC, Witton MP, Martill, DM. 2007. Did pterosaurs feed by skimming? Physical modelling and anatomical evaluation of an unsual feeding method. Plos Biology, 5, 1647–1655.

Hutson JD, Hutson KN. 2012. A test of the validity of range of motion studies of fossil archosaur elbow mobility using repeated-measures analysis and the extant phylogenetic bracket. Journal of Experimental Biology 215: 2030–2038.

Iijima M, Kubo T. 2019. Comparative morphology of presacral vertebrae in extant crocodylians: taxonomic, functional and ecological implications. Zoological Journal of the Linnean Society 186: 1006–1025.

Jones KE, Brocklehurst RJ, Pierce SE. 2021. AutoBend: An automated approach for estimating intervertebral joint function from bone-only digital models. Integrative Organismal Biology 3: obab026.

Kambic RE, Biewener AA, Pierce SE. 2017. Experimental determination of three-dimensional cervical joint mobility in the avian neck. Frontiers in Zoology 14: 37

Kellner AWA, Tomida Y. 2000. Description of a new species of Anhangueridae (Pterodactyloidea) with comments on the pterosaur fauna from the Santana Formation (Aptian-Albian), Northeastern, Brazil. National Science Museum, Monographs, Tokyo, 17: 1–135.

Kellner AWA, Langston Jr. W. 1996. Cranial remains of *Quetzalcoatlus* (Pterosauria, Azhdarchidae) from Late Cretaceous sediments of Big Bend National Park, Texas. Journal of Vertebrate Paleontology 16: 222–231.

Kellner AWA, Campos DA. 2002. The function of the cranial crest and jaw of a unique pterosaur from the Early Cretaceous of Brazil. Science 297: 389–392.

Kuroda N. 1962. On the cervical muscles of birds. Journal of the Yamashina Institute for Ornithology 3: 189–211.

Landolt R, Zweers GA. 1984. Anatomy of the muscle-bone apparatus of the cervical system in the Mallard (*Anas platyrhynchus* L.). Netherlands Journal of Zoology 35: 611–670.

Lautenschlager S. 2017. Digital reconstruction of soft-tissue structures in fossils. The Paleontological Society Papers 22: 101–117.

Liu T, El-Rich M. 2020. Effects of nucleus pulposus location on spinal loads and joint centers of rotation and reaction during forward flexion: a combined finite element and musculoskeletal study. Journal of Biomechanics 104: 109740.

Marek RD, Falkingham PL, Benson RBJ, Gardiner JD, Maddox TW, Bates KT. 2021. Evolutionary versatility of the avian neck. Proceedings Royale Society B 288: 20203150.

McGowan, C. 1979. The hind limb musculature of the Brown kiwi, *Apteryx australis mantelli*. Journal of Morphology, 160, 33–74.

McGowan, C. 1986. The wing musculature of the Weka (*Gallirallus australis*), a flightless rail endemic to New Zealand. Journal of Zoological Society of London, 210, 305–346.

Molnar JL, Pierce SE, Hutchinson JR. 2014. An experimental and morphometric test of the relationship between vertebral morphology and joint stiffness in Nile crocodiles (*Crocodylus niloticus*). Journal of Experimental Biology 217: 758–768.

Molnar JL, Pierce SE, Bhullar BAS, Turner AH, Hutchinson JR. 2015. Morphological and functional changes in the vertebral column with increasing aquatic adaptation in crocodylomorphs. Royal Society Open Science 2: 150439.

Mook CC. 1921. Notes on the postcranial skeleton in the Crocodilia. Bulletin of the American Museum of Natural History 44: 67–100.

Muller J, Scheyer TM, Head JJ, Barrett PM, Werneburg I, Ericson PG, Pol D, Sánchez-Villagra MR. 2010. Homeotic effects, somitogenesis and the evolution of vertebral numbers in recent and fossil amniotes. Proceedings of the National Academy of Sciences 107 (5): 2118–2123.

Moore AJ. 2020. Vertebral pneumaticity is correlated with serial variation in vertebral shape in storks. Journal of Anatomy 238: 615–625.

Naish D, Witton MP. 2017. Neck biomechanics indicate that giant Transylvanian azhdarchid pterosaurs were shirt-necked arch predators. PeerJ 5: e2908.

Nesov LA. 1984. Pterosaurs and birds of the Late Cretaceous of Central Asia. Palaontologische Zeitschrift 1: 47–57.

Nesbitt SJ. 2011. The early evolution of archosaurs: relationships and the origins of major clades. Bulletin of the American Museum of Natural History 352: 1–292.

Nicholls EL, Russell AP. 1985. Structure and function of the pectoral girdle and forelimb of Struthiomimus altus (Theropoda: Ornithomimidae). Palaeontology 28: 643–677.

O'Connor PM. 2006. Postcranial pneumaticity: an evaluation of soft-tissue influences on the postcranial skeleton and the reconstruction of pulmonary anatomy in archosaurs. Journal of Morphology 267: 1199–1226.

Ősi A, Weishampel DB, Jianu CM. 2005. First evidence of azhdarchid pterosaurs from the Late Cretaceous of Hungary. Acta Palaeontologica Polonica 50 (4): 777–787.

Padian K, Cunningham JR, Langston Jr. W, Conway J. 2021. Functional morphology of *Quetzalcoatlus* Lawson 1975 (Pterdactyloidea: Azhdarchoidea). Journal of Vertebrate Paleontology 41: 218–251.

Pereda-Suberbiola X, Bardet N, Jouve S, Iarochène M, Bouya B, Amaghzaz M. 2003. A new azhdarchid pterosaur from the Late Cretaceous phosphates of Morocco. Geological Society, London, Special Publications 217: 79–90.

Pinheiro FL, Rodrigues T. 2017. *Anhanguera* taxonomy revisited: is our understanding of Santana Group pterosaur diversity biased by poor biological and stratigraphic control? PeerJ 5: e3285.

Porro LB, Holliday CM, Anapol F, Ontiveros LC, Ontiveros LT, Ross CF. 2011. 2011. Free body analysis, beam mechanics, and finite elements modeling of the mandible of *Alligator mississippiensis*. Journal of Morphology 272: 910–937.

Prieto IR. 1998. Morfología funcional y hábitos alimentarios de Quetzalcoatlus (Pterosauria). Coloquios de Paleontologia 49: 129–144.

Prince PA, Wood AG, Barton T, Croxall JP. 1992. Satellite tracking of wandering albatrosses (Diomedea exulans) in the South Atlantic. Antarctic Science 4 (1): 31–36.

Prum RO, Berv JS, Dornburg A, Field DJ, Townsend JP, Lemmon EM, Lemmon AR. (2015) A comprehensive phylogeny of birds (Aves) using targeted next-generation DNA sequencing. Nature 526: 569–573.

Rayfield EJ. 2007. Finite Element Analysis and understanding the biomechanics and evolution of living and fossil organisms. Annual Review of Earth and Planetary Sciences 35: 541–576.

Salisbury SW, Frey E. 2001. A biomechanical transformation model for the evolution of semi-spheroidal articulations between adjoining vertebral bodies in crocodilians. In: Grigg GC, Seebacher F, Franklin CE. Crocodilian biology and evolution. Surrey Beatty & Songs, Chipping Norton, p. 85–134.

Schneider CA, Rasband WS, Eliceiri KW. 2012. NIH Image to ImageJ: 25 years of image analysis. Nature Methods 9: 671–675.

Schreiber EA, Burger J. 2001. Biology of Marine Birds. Boca Raton, FL: CRC Press. 722 pp.

Schwarz D, Frey E, Meyer CA. 2007. Pneumaticity and soft-tissue reconstructions in the neck of diplodocid and dicraeosaurid sauropods. Acta Palaentologica Polonica 52: 167–188.

Seidel R. 1978. The somatic musculature of the cervical and occipital regions of Alligator mississippiensis. PhD dissertation, City University of New York.

Selbie WB, Thomson DB, Richmond FJR. 1993. Sagittal-plane mobility of the cat cervical spine. Journal of Biomechanics 26 (8): 917–927.

Sick H, Pacheco JF. 1997. Ornitologia Brasileira vol 1. Rio de janeiro, RJ: Editora Nova Fronteira.

Snively E, Russell AP. 2007. Functional morphology of neck musculature in the Tyrannosauridae (Dinosauria, Theropoda) as determined via a hierarchical inferential approach. Zooloical Journal of the Linnean Society 151: 759–808.

Snively E, Cotton JR, Ridgely R, Witmer, LM. 2013. Multibody dynamics model of head and neck function in Allosaurus (Dinosauria, Theropoda). Palaeontologia Electronica 16 (2): 11A29p

Souza RG. 2018. Comments on the serial homology and homologues of vertebral lateral projections in Crocodylia (Eusuchia). The Anatomical Record 301: 1203–1215.

Stevens KA, Parrish JM. 1999. Neck posture and feeding habits of two Jurassic sauropod dinosaurs. Science 284: 798–800.

Stevens KA, Parrish JM. 2005. Digital reconstructions of sauropod dinosaurs and implications for feeding. In: Curry Rogers KA, Wilson JA, editors. The Sauropods: Evolution and Paleobiology. Berkeley, CA: University of California Press: 178–200.

Tambussi CP, de Mendoza R, Degrange FJ, Picasso MB. 2012. Flexibility along the Neck of the Neogene Terror Bird *Andalgalornis steulleti* (Aves Phorusrhacidae). Plos One 7 (5): e37701.

Taylor MP, Wedel MJ, Naish D. 2009. Head and neck posture in sauropod dinosaurs inferred from extant animals. Acta Palaeontologica Polonica 54 (2): 213–220.

Taylor MP, Wedel MJ. 2013. The Effect of Intervertebral Cartilage on Neutral Posture and Range of Motion in the Necks of Sauropod Dinosaurs. Plos One 8 (10): e78214.

Terray L, Plateau O, Abourachid A, Böhmer C, Delapré A, de la Bernardie X, Cornette R. 2020. Modularity of the neck in birds (Aves). Evolutionary Biology: Doi: 10.1007/s11692-020-09495-w.

Tsuihiji T. 2004. The ligament system in the neck of *Rhea americana* and its implication for the bifurcated neural spines of sauropod dinosaurs. Journal of Vertebrate Paleontology 24 (1): 165–172.

Tsuihiji T. 2005. Homologies of the *transversospinalis* muscles in the anterior presacral region of Sauria (crown Diapsida). Journal of Morphology 263: 151–178.

Tsuihiji T. 2007. Homologies of the *longissimus, iliocostalis*, and hypaxial muscles in the anterior presacral region of extant diapsida. Journal of Morphology 268: 986–1020.

Vanden-Berge JC, Zweers GA. 1993. Myologia In: Baumel JJ, King AS, Breazile JC, Evans HE, Vanden Berge JC, editors. Handbook of avian anatomy: Nomina anatomica avium. Cambridge, MA: Cambridge University Press. 189–247.

Veldmeijer AJ, Meijer HJM, Signore M. 2009. Description of pterosaurian (Pterodactyloidea: Anhangueridae, *Brasileodactylus*) remains from the Lower Cretaceous of Brazil. Deinsea 13: 9–40.

Vidal D, Mocho P, Páramo A, Sanz JL, Ortega F. 2020. Ontogenetic similarities between giraffe and sauropod neck osteological mobility. Plos One 15 (1): e0227537.

Vidal PP, Graf W, Berthoz A. 1986. The orientation of the cervical vertebral column in unrestrained awake animals. Experimental Brain Research 61: 549–559.

Vila Nova BC, Sayão JM, Langer MC, Kellner AWA. Comments on the cervical vertebrae of the Tapejaridae (Pterosauria, Pterodactyloidea) with description of new specimens. Historical Biology 27: 770–780.

Wedel MJ, Sanders RK. 2002. Osteological correlates of cervical musculature in Aves and Sauropoda (Dinosauria: Saurischia), with comments on the cervical ribs of Apatosaurus. PaleoBios 22 (3): 1–6.

Wellnhofer P. 1975. Die Rhamphorhynchoidea (Pterosauria) der Oberjura-Plattenkalke Süddeutschlands. Palaeontographica Abt. A 148: 1–33.

Wellnhofer P. 1991. Weitere Pterosaurierfunde aus der Santana-Formation (Apt) der Chapada do Araripe, Brasilien. Palaeontographica Abt. A 215: 43–101.

Wendeln H, Becker PH. 1996. Body mass change in breeding common terns *Sterna hirundo*. Bird Study 43: 85–95.

Wintrich T, Jonas R, Wilke HJ, Schmitz L, Sander PM. 2019. Neck mobility in the Jurassic plesiosaur *Cryptoclidus eurymerus*: finite element analysis as a new approach to understanding the cervical skeleton in fossil vertebrates. PeerJ 7: e7658.

Witmer LM. 1995. The Extant Phylogenetic Bracket and the importance of reconstructing soft tissues in fossils. In: Thomason JJ, editor. Functional morphology in vertebrate palaeontology. Cambridge: Cambridge University Press. 19–33.

Witmer LM, Chatterjee S, Franzosa J, Rowe, T. 2003. Neuroanatomy of flying reptiles and implications for flight, posture and behavior. Nature 425: 950–953.

Witton MP, Naish D. 2008. A reappraisal of azhdarchid pterosaur functional morphology and paleoecology. Plos One 3: e2271.

Witton MP, Habib MB. 2010. On the size and flight diversity of giant pterosaurs, the use of birds as pterosaur analogues comments on pterosaur flightlessness. Plos One 5: e13982.

Yuri T, Kimball RT, Harshman J, Bowie RCK., Braun MJ, Chojnowski JL, Han KL, Hackett SJ, Huddleston CJ, Moore WS, Reddy S, Sheldon FH, Steadman DW, Witt CC, Braun EL. 2013. Parsimony and model-based analyses of indels in avian nuclear genes reveal congruent and incongruent phylogenetic signals. Biology 2: 419–444.

Zusi RL. 1962. Structural adaptations of the head and neck in the Black Skimmer, *Rhynchops nigra* Linnaeus. Publications of the Nuttal Ornithological Club 3: 1–153.

Zusi RL, Bentz GD. 1984. Myology of the purple-throated carib (*Eulampis jugularis*) and other hummingbirds (Aves: Trochilidae). Smithsonian Contributions to Zoology 385: 1–70.

Zusi RL, Storer RW. 1969. Osteology and myology of the head and neck of the pied-billed grebes (*Podilymbus*). In: Publications of the Museum of Zoology vol 139: University of Michigan. 49 pp.

Zweers GA, Vanden-Berge JC, Koppendraier R. 1987. Avian cranio-cervical systems. Part I: Anatomy of the cervical column in the chicken (*Gallus gallus* L.). Acta Morphologica Neerlando-scandinavica 25: 131–155.

Zweers GA, Bout R, Heidweiller J. 1994. Motor organization of avian head-neck system. In: David M, Green P, editors. Perception and motor control in birds. Berlin: Springer-Verlag. 201–221.